THE EFFECT OF HYPOSMOTIC SHOCK ON MOTILITY AND CALCIUM SIGNALLING OF HUMAN SPERMATOZOA

by

RUBÉN DARÍO PERALTA ARIAS

A thesis submitted to
The University of Birmingham
For the degree of
DOCTOR OF PHILOSOPHY

College of Life and Environmental Sciences
School of Biosciences
The University of Birmingham
September 2011

ABSTRACT

Chloride (Cl^-) channels are thought to be implicated in volume regulation of human spermatozoa, a process vital for diverse cell functions. The Cl^- channel blockers DIDS, NPPB and niflumic acid were utilized to evaluate the influence of Cl^- channels on motility, morphology and $[Ca^{2+}]_i$ signaling of human spermatozoa exposed to hyposmotic shock (295, 270 and 200 mOsm, equivalent to the osmotic conditions of cervical mucus, fallopian tubes, and non physiological respectively). At 295 and 270 mOsm, 50 and 100 µM DIDS inhibited motility whereas 400 µM abolished it. 400 µM DIDS augmented the percentage of sperm with coiled tails. Conversely, 100 µM NPPB and 200 µM niflumic acid did not affect motility or the number of coiled sperm. Immunodetection studies showed that DIDS inhibited serine/threonine phosphorylation of proteins in sperm cells, suggesting that DIDS (50, 100 and 400 µM) inhibits the production of cAMP.

When sperm cells were exposed to hyposmotic shock there was a substantial increase in $[Ca^{2+}]_i$ that exhibited a biphasic behaviour, with a transient peak of fluorescence immediately followed by a plateau with levels that remain more elevated than those observed during the control period, suggesting an important role for Ca^{2+} stores in volume regulation of human sperm. This increase in $[Ca^{2+}]_i$ was independent of extracellular Ca^{2+}. All the Cl^- channel blockers caused a significant rise in $[Ca^{2+}]_i$ on their own, but only DIDS and niflumic acid attenuated the increase in $[Ca^{2+}]_i$ caused by osmotic stress. Thus, though Cl- channel blockers have profound effects on motility and cause flagellar angulation in human sperm, their effects on $[Ca^{2+}]_i$ signaling are such that conclusions on the role of Cl- channels in RVD of human sperm, based upon use of Cl^--channel blockers, must be interpreted cautiously. In addition, DIDS may be affecting the HCO_3^- / Cl^- exchanger, preventing HCO_3^- entry into the cells,

reducing activity of soluble adenylate cyclase and suppressing phosphorylation of proteins essential for sperm motility and volume regulation.

DEDICATION

To my father Rubén Darío Peralta, who passed away within a few months of my arrival to Birmingham. He was a man from a very modest background that believed in the power of education, and I wish that he was here enjoying the completion of my studies.

To my daughter Marthina, the best present that Anne and I could ever have from the United Kingdom.

ACKNOWLEDGMENTS

First, I want to express my gratitude towards my supervisor Dr. Stephen Publicover, who gave me the opportunity to come to the United Kingdom to undertake PhD studies in an excellent laboratory, part of a world class higher education institution such as the University of Birmingham. I was privileged to work and learn here. Steve was very supportive during the difficult times and I always thank him for all his help, critical advice, scientific thinking and actions that were fundamental for completing my doctoral degree successfully.

I also want to say thanks to the staff of the Assisted Conception Unit at the Birmingham Women's Hospital, for providing donors during big part of the project. Thanks to the people of the Medical School, Dr.Yuchun Gu and Dr. Prem Kumar, who help me during the initial steps. I will miss those funny moments with Matthew, Selina, Su, Fei and the rest of the guys in the PhDs office of the yellow wing.

Thanks to the staff of the School of Biosciences, especially to my friends and lab colleagues Aduén Morales García, Sarah Costello, Gisela Machado de Oliveira, Katherine Nash, Jennifer Morris, and Dr. Linda Lefièvre. All of them excellent scientists and better persons, that create a great work environment with plenty of laughs and good conversations. Thank you for teach me all those protocols and techniques guys. I also must express my gratitude to Antonio Alvau, from the University of Florence, who visited the laboratory as part of his Master's project and worked hard with me in the experiments of motility and Ca^{2+}.

This PhD is basically product of two women. One is my mother Nancy Arias, who made incredible efforts to support me during my first year. My mother has worked very hard during

her life to give us the best education possible, and there are no words that can express my gratitude to her.

The other woman, and at the same time the most important acknowledgement, is my wife Annelisse Theuerkauf, who sacrificed many things to come along with me in this adventure. She has been so patient, so caring, so brave and so supportive during the difficult times that I am completely sure that without her love I wouldn't be able to overcome all the challenges that I encountered during this journey. I want to say that this thesis and the degree certificate should have your name printed above mine!

I want to thank my family in Venezuela, my brothers, and friends at Birmingham. Thanks to the United Kingdom, an extraordinary country that has changed my life. Last but not least, I express my gratitude to the Fondo Nacional de Ciencia y Tecnología de Venezuela (FONACIT) for the financial support throughout my PhD research.

TABLE OF CONTENTS

LIST OF FIGURES

LIST OF TABLES

LIST OF ABBREVIATIONS

AKAP - A-Kinase anchor protein
ADP - Adenosine diphosphate
ADAM - a disintegrin and a metelloprotease domain
ALH - Amplitude of lateral head displacement
ART - Assisted reproductive techniques
ATP - Adenosine triphosphate
BCF - Beat cross frequency
BSA - Bovine serum albumin
Ca^{2+} - Calcium ions
$[Ca^{2+}]_i$ - Intracellular calcium concentration
$[Ca^{2+}]_o$ - Extracellular calcium concentration
CaM - Calmodulin
cAMP - Cyclic adenosine monophosphate
CASA - Computer-assisted semen analysis
CFTR - Cystic fibrosis transient receptor
cGMP - Cyclic guanosine monophosphate
Cl^- - Chloride ions
CNG - Cyclic nucleotide-gated
CRISP - Cystein-rich secretory protein
DIDS - 4,4′-Diisothiocyanatostilbene-2,2′-disulfonic acid disodium salt hydrate
DMSO - Dimethyl sulfoxide
DTT - Dithiothreitol
EBSS - Earle's balanced salt solution
EDTA - Ethylenediaminetetraacetic acid
EGTA - Ethylene glycol-bis (β-amino-ethylether)-N,N,N'N'-tetraacetic acid
EnaCs - Epithelial sodium channels
ESHRE - European Society of Human Reproduction and Embryology
FSH - Follicle stimulating hormone
$GABA_A$ - Gamma-aminobutyric acid type A
GAPDS - Glyceraldehyde 3-phosphate dehydrogenase-S
GlyR - Glycine receptor/chloride channel
H^+ - Hydrogen ions
HCO_3^- - Bicarbonate ions
Hepes - 4-(2-hydroxyethyl)-1-piperazineethanesulfonic acid
HFEA - Human Fertilisation and Embriology Authority
HOS - hyposmotic swelling test
IP_3 - Inositol-1,4,5-triphosphate
I^- - Iodine
IVF - *in vitro* fertilization
IVR - Isovolumetric regulation
K^+ - Potassium ions
KCl - Potassium chloride
LH - Luteinizing hormone
LIN - Linearity
mAC - Membrane-associated adenylate cyclase
Mg^{2+} - Magnesium ions

Mn^{2+} - Manganese ions
$MgCl_2$ - Magnesium chloride
$MgSO_4$ - Magnesium sulphate
Na^+ - Sodium ions
$NaHCO_3$ - Sodium bicarbonate
NADPH - Nicotinamide adenine dinucleotide phosphate
NCX – Sodium/calcium exchanger
NPPB - 5-Nitro-2-(3-phenylpropylamino) benzoic acid
NO - Nitric oxide
NO_3^- - Nitrate
OGB-1AM - Oregon green 488 BAPTA 1-acetoxymethyl
PBS - Phosphate buffered saline
PDL - Poly-D-lysine
PGK2 - phosphoglycerate kinase 2
PKA - Protein kinase A
PKC - Protein kinase C
PTK - Protein tyrosin kinase
PLC - Phospholipase C
PP1 – Phophatase 1
PMCA - Plasma membrane Ca^{2+} -ATPase
RVD - Regulatory volume decrease
RVI - Regulatory volume increase
RyR - Ryanodine receptor
sAC - Soluble adenylate cyclase
SDS – Sodium dodecyl sulphate
SDS-PAGE - Sodium dodecyl sulphate polyacrylamide gel electrophoresis
sEBSS - Supplemented Earle's balanced salt solution
SERCA - Sarcoplasmic-endoplasmic Ca^{2+} -ATPase
SNARE - Soluble N-ethylmaleimide-sensitive factor-attachment protein receptor
SOC - Store-operated Ca^{2+} channel
SPCA - Secretory pathway Ca^{2+} -ATPase
TTBS - Tween-20 Tris buffer saline
TRP - Transient receptor potential
TRPC - Transient receptor potential-canonical
VAP - Mean path velocity
VOCCs - Voltage-operated Ca^{2+} channels
VSL - Straight-line velocity
WHO - World Health Organization
ZP3 - Zona pellucida protein 3

CHAPTER ONE

PHYSIOLOGY OFTHE HUMAN SPERMATOZOON

Foreword to Chapter One

The following pages have been designed to provide information about the biogenesis, structure, and physiology of the human spermatozoon as background for this research project. Emphasis is put in Ca^{2+} signalling, volume regulation, and Cl^- channels.

1.1 The Importance of Studying the Human Spermatozoon

The human spermatozoon is a specialized and complex cell responsible for the safe transport of paternal DNA to the oocyte in order to achieve fertilization. The term spermatozoon is derived from the Greek words *sperma* (σπέρμα) "seed" and *zoon* (ζῷον) "living being", and was first observed by Johan Ham, a young medical student of Anthony van Leeuwenhoek in 1677 (Gonzalès, 2006). Ham informed van Leeuwenhoek about the existence of "*living animalcules that possess a tail"* while studying a sample of a man affected by gonorrhoea. Van Leeuwenhoek confirmed this found himself in the semen of a healthy man (Gonzalès, 2006). The importance of studying spermatozoa arises from the statistics of infertility worldwide, which show a prevalence of about 16% of all couples in reproductive age (Juul et al., 1999, Oakley et al., 2008). According to the last report published by the European Society of Human Reproduction and Embryology (ESHRE), the number of treatments by 2006 involving Assisted Reproductive Techniques (ART) across Europe were 458,759; 40,648 more than 2005 (+ 9.7%) (de Mouzon et al., 2010). A total of 44,000 corresponded to the United Kingdom (de Mouzon et al., 2010). In addition, the Human Fertilisation and Embryology Authority (HFEA) reports that by 2006, in the United Kingdom almost 45,000 cycles of ART treatments were performed in 35,000 patients (HFEA, 2008), being expected that this trend will increase in the coming years. As male factors for infertility are found in half of involuntary childless couples, it must be assumed that about 8% of all men are going to confront a problem associated with infertility during their lives. This means that the prevalence of male infertility would exceed that of diabetes mellitus, which was estimated to be 2.8% in 2000 and 4.4% in 2030 according to the WHO (Wild et al., 2004), and is considered almost epidemic.

The reasons aforementioned have stimulated extensive research on male fertility, and more specifically, on sperm function, in order to understand the complex physiological processes that the cell experiences (capacitation, localization of the oocyte, acrosome reaction, fusion, etc). All these processes must be precisely controlled and must occur at the right time and in the right order to achieve fertilization successfully.

1.2 Spermatogenesis

The human testes are two organs of the shape of rotation ellipsoids with diameters of 2.5 × 4 cm engulfed by a capsule (tunica albuginea) of strong connective tissue (Holstein et al., 2003). Thin septa divide the parenchyma of the testis in about 370 conical lobules. The lobules consist of the seminiferous tubules and interstitial tissue, containing groups of endocrine Leydig cells and additional cellular elements such as macrophages, microvasculature, nerve fibres, fibroblasts, lymph vessels, and connective tissue (Holstein et al., 2003). The seminiferous tubules are coiled loops that end up open into the spaces of the rete testis (Roosen-Runge and Holstein, 1978). The fluid secreted by the seminiferous tubules is collected in the rete testis and delivered to the ductal system of the epididymis, where they are stored until the ejaculation.

The term spermatogenesis describes and includes all the processes involved in the production of the male gamete (spermatozoon) within the testis. The spermatogenesis takes place in the tubular compartment of the testis (figure 1.1). This compartment represents about 60-80% of the total testicular volume, and it contains the germ cells, the peritubular cells and the Sertoli cells (Weinbauer et al., 2000). The testis is divided by septa of connective tissue into about

250-300 lobules, each one containing 1-3 highly convoluted seminiferous tubules. Overall, the human testis contains about 600 seminiferous tubules (Weinbauer et al., 2000), each one covered by a layer of collagen and the peritubular cells (myofibroblasts), which are poorly differentiated myocytes with the capacity of spontaneous contraction. It is believed that mature sperm are transported towards the exit of the seminiferous tubules by contraction of these cells. On the other hand, the Sertoli cells are somatic cells located within the basal membrane of the germinal epithelium, representing about 35-40% of it (Weinbauer et al., 2000). These cells coordinate the spermatogenic process topographically and functionally, and are responsible for the final testicular volume and sperm production in the adult (Cheng et al., 2010). Sertoli cells create and maintain a special environment within the tubulus lumen, where they synthesize and secrete a large variety of factors such as: proteins, cytokines, growth factors, opioids, steroids, prostaglandins, modulators of cell division, and tubular fluid, which contains high concentrations of K^+ ions, low concentration of Na^{2+} ions, plus Cl^- ions, $HCO3^-$, Mg^+, inositol, glucose, carnitine, amino acids, and glycerol-phoshorylcholine (Cooper et al., 1992). Another function of the Sertoli cells is the formation of the blood testis barrier, which is pivotal for the spermatogenesis (Cheng et al., 2010). Two important roles for this barrier are: physical isolation of the germinal cells to prevent recognition for the immune system (the so-called autoimmune orchitis that destroys the germinal epithelium) and preparing the special milieu for the meiotic events involved in sperm development (Weinbauer et al., 2000). Proliferation and maturation of Sertoli cells, and thereby testicular volume and spermatogenesis, is mainly stimulated by the follicle stimulating hormone (FSH) and testosterone (Petersen and Soder, 2006). In the interstitial compartment, which represents 12-15% of total testicular volume, are the Leydig cells. These cells secrete the most important male sexual hormone, testosterone (Svechnikov et al., 2010). They are rich in smooth endoplasmic reticulum and mitochondria with tubular cristae, characteristics that are typical

for steroids-producing cells (Weinbauer et al., 2000). Leydig cells develop from mesenchymal cells and from fibroblast-like cells in the interstitium, a process induced by the luteinizig hormone (LH) (Svechnikov et al., 2010). Recent investigations evidenced that these cells possess neuroendocrine properties in addition to their endocrine functions, as they can express serotonin, catecholamine synthesizing enzymes, different antigens characteristic for nerve cells as well as neurohormones and their receptors, neuropeptides, cell adhesion molecules, and numerous growth factors and their receptors (Holstein et al., 2003).

Spermatogenesis (figure 1.2) starts with the division of stem cells and ends up with the formation of mature sperm. The overall duration of the spermatogenesis is calculated as 70 days (Heller and Clermont, 1966). The entire process can be divided into three phases (Weinbauer et al., 2000):

- Mitotic proliferation and differentiation of diploid germ cells (spermatogonia).
- Meiotic division of tetraploid germ cells (spermatocytes).
- Transformation of haploid germ cells (spermatids) into mature spermatozoa (spermiogenesis).

Gonadal cells originate spermatogonia which lie at the base of the seminiferous epithelium and are classified as type A and type B. The formation of spermatogonia seems to be particularly sensitive to high temperature (Ivell, 2007). Type A spermatogonia can be subdivided, from a cytological and physiological point of view, into dark spermatogonia (Ad) and pale spermatogonia (Ap) (Ivell, 2007). The Ad spermatogonia do not show any proliferating activity and are considered the stem cells of the spermatogenesis (Schlatt and Weinbauer, 1994). Conversely, the Ap spermatogonia divide and differentiate into two B

spermatogonia (Sharpe, 1994). The B spermatogonia divide to form diploid germ cells called primary spermatocytes, which commence the DNA synthesis and go through the different phases of two meiotic divisions (Weinbauer et al., 2000), where extensive RNA synthesis, recombination of genetic material and reduction of chromosome number take place.

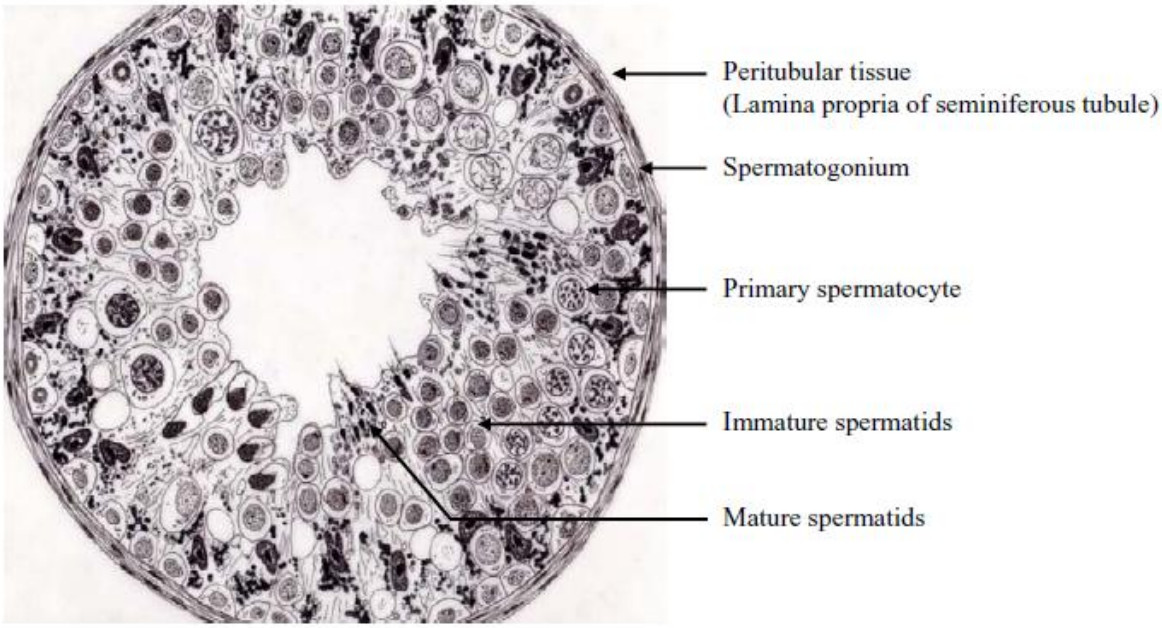

Figure 1.1: Drawing of a cross section of a seminiferous tubule from a fertile man.

(Holstein et al., 2003)

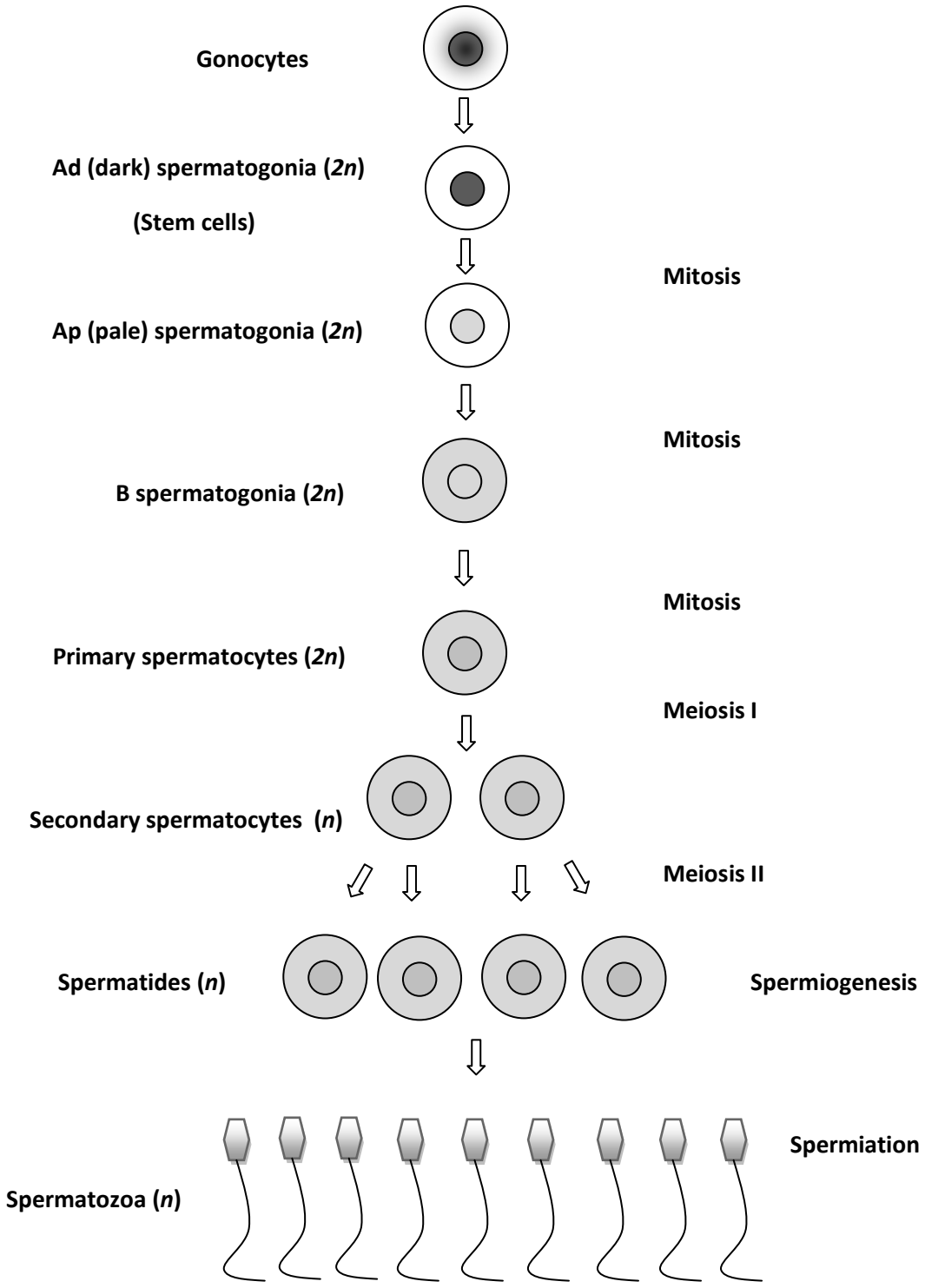

Figure 1.2: Schematic illustration of the human spermatogenesis.

The result of the first meiotic division is the formation of haploid germ cells called secondary spermatocytes, a process that is also heat sensitive (Ivell, 2007), then these cells experience a second meiotic division that lead to the formation of haploid germ cells called spermatids, a process called spermiogenesis. Spermatids are round cells mitotically active that are the precursors of the mature spermatozoa. They undergo a dramatic transformation where the cells acquire unique and definitive accessory structures that are necessary for the detachment of sperm from the seminiferous tubules and acquisition of fertilizing potential.

The last phase of spermatogenesis can be divided into spermiogenesis and spermiation (Sutovsky and Manandhar, 2006). The principal events at the organelle level comprise: a) the cells become elongated (Sutovsky and Manandhar, 2006); b) the acrosome develops from the Golgi, covering the cranial half of the spermatid (Moreno et al., 2000); c) the nucleus becomes extremely condensed and the majority of histones are substituted by protamines (Meistrich et al., 2003); d) the cytoplasm is extruded as the so-called residual body (which is phagocytosed by Sertoli cells) (Weinbauer et al., 2000); and e) the sperm flagellum, with the completed axonema, is formed (Oko, 1998). In parallel with degradation of the residual bodies, a new spermatogenic cycle begins (Weinbauer et al., 2000). After all these changes, the cells are transformed in highly specialized structures capable of acquiring progressive motility and fertilizing potential, and just at this stage the cells are called spermatozoa.

The release of sperm into the tubular lumen is designated as spermiation, where fully differentiated spermatozoa detach from each other and from the apical surface of seminiferous tubules, traveling through the lumen to the rete testis (Sutovsky and Manandhar, 2006). Finally, the sperm leave the testis to reach the epididymis, a tubular organ located over each testis, where they will experience further maturation processes and will be stored in a

quiescent state until the ejaculation.

Spermatogenesis is a process of high levels of redundancy in terms of production: germ cell loss during spermatogenesis is very elevated. Calculating the potential spermatogenetic capacity of a testis with 100%, it must be realized that 75% of the developed germ cells are lost by apoptosis or degeneration (Holstein et al., 2003), that leaves about 25% of the germ cells with the capacity to reach the ejaculate.

1.3 Sperm Structure

The spermatozoon is composed of two major parts: sperm head and sperm tail or flagellum. At the same time, the flagellum could be divided in connecting piece (neck), midpiece, principal piece and endpiece (figure 1.3). Both sperm head and sperm tail are covered by sperm plasma membrane or plasmalemma (Sutovsky and Manandhar, 2006). The sperm head is composed of two main regions: the acrosomal region and postacrosomal region. The acrosomal region is further subdivided in the anterior acrosomal region and posterior acrosomal region (equatorial segment) (Toshimori and Ito, 2003). The sperm head contains the nucleus, which possesses highly condensed DNA that allows the hydrodynamic shape permissive of sperm motility and penetration through the egg vestments (Brewer et al., 2002, Dadoune, 2003). The nucleus is covered by a reduced nuclear envelope, although protection is provided by the perinuclear theca, a rigid shell composed of disulfide bond-stabilized structural proteins amalgamated with various other protein molecules (Oko, 1995).

Unlike the relatively loose structure of chromatin in somatic cells, sperm chromatin is very tightly compacted by virtue of the unique associations between the DNA and sperm nuclear

proteins (Brewer et al., 1999, Zini and Sigman, 2009). During the later stages of spermatogenesis, the spermatid nucleus is remodeled and condensed, and this is associated with the displacement of histones by transition proteins and then by protamines (Steger et al., 2000). The DNA strands are tightly wrapped around the protamine molecules, forming tight and highly organized loops (Brewer et al., 1999). Intermolecular and intramolecular disulfide bonds between the cysteine-rich protamines are responsible for the compaction and stabilization of the sperm nucleus, and it is believed that this nuclear compaction is important to protect the sperm genome from external disturbances such as oxidation or temperature elevation (Kosower et al., 1992, Zini and Sigman, 2009). In humans, sperm chromatin is tightly packaged by protamines, but up to 4% of the DNA remains packaged by histones (Hammoud et al., 2009). The histone-bound DNA sequences are less tightly compacted and are correlated with early embryo development (Hammoud et al., 2009). Infertile men have a higher sperm histone to protamine ratio when compared with fertile controls (Oliva, 2006).

The acrosome is a Golgi-derived structure that covers the anterior half to two thirds of the head, and is surrounded by the outer acrosomal membrane and the inner acrosome membrane. These structures form a cap in the anterior head of the sperm that harbors proteases and receptors required for sperm interaction with the layers of the oocyte (Toshimori and Ito, 2003, Sutovsky and Manandhar, 2006). During the fertilization the inner acrosomal membrane remains while the outer acrosome membrane is lost to vesiculation during the acrosomal exocytosis, which is induced by the binding of the sperm plasma membrane/outer acrosomal membrane complex to the zona pellucida of the oocyte, a key event that allows the sperm penetration of the oocyte's vestments and its fusion with the egg (Sutovsky and Manandhar, 2006).

The sperm tail or flagellum provides a motile force for the spermatozoon, which is based upon a 9 + 2 arrangement of microtubules within the flagellar axoneme (Afzelius, 1959). The 9 + 2 arrangement refers to nine peripheral, symmetrically arranged microtubule doublets connected doublet-to-doublet by dynein arms and to a central pair of microtubules by radial spokes (Sutovsky and Manandhar, 2006). The peripheral doublets are surrounded by the outer dense fibres, which provide flexible, yet firm support during flagellar movement (figure 1.4) (Sutovsky and Manandhar, 2006). Topologically, the flagellum could be subdivided progressing from proximal to distal end in: a) connecting piece (containing the outer dense fibres and the centriole); b) midpiece (covered for the mitochondrial sheet, which generates the energy for motility and site of localization of enzymes, ion channels and ion exchangers); c) principal piece (covered for the fibrous sheet, which provides structural support for the sperm axoneme and site of localization of protein kinases); and finally d) end piece (containing the end of the axoneme and the fibrous sheet) (Sutovsky and Manandhar, 2006). The fibrous sheet is composed of three longitudinal columns attached to microtubule doublets 3 and 8 that run along the principal piece of the spermatozoa (Oko et al., 1990). This structural arrangement and the stabilization provided by disulfide bonds, suggest that fibrous sheet participates in flexibility, the plane of flagellar motion and the shape of flagellar beat (Eddy et al., 2003). Protein kinase A anchoring proteins (AKAPs) and different glycolitic enzymes are located in the fibrous sheet (Eddy et al., 2003, Miki et al., 2004). Interestingly, AKAPs represent more than 50% of the fibrous sheet mass in some species (Eddy et al., 2003).

Flagella are powered by dyneins, a group of motor proteins anchored along the length of the doublets. Dyneins belong to the AAA family of ATPases (Mocz and Gibbons, 2001). Dynein arms are complexes consisting of three classes of subunits. The heavy chains (α and β, ≈ 500

kDa) have a central motor part with four ATP- and microtubule -binding sites; the intermediate chains (60-120 kDa) are located at the base of the dynein molecules and play a role in the ATP-insensitive binding of the arms to microtubules; the light chains (8–20 kDa) are involved in processes such as Ca^{2+} binding (Gagnon and De Lamirande, 2006). The dynein arms are activated when phosphorylated by the hydrolysis of ATP (Tash and Means, 1982) the energy source that induces the arms to produce the sliding force for the displacement of the doublets. Each dynein arm slides along its adjacent microtubule doublet, being the result of this action the bending of the axoneme. As soon as ATP binds to the dynein molecule, this protein is released from the doublets and experiences a conformational change (Oiwa and Sakakibara, 2005). ATP is then hydrolyzed and there is a rebinding of dynein to the adjacent microtubules. The products of ATP hydrolysis, i.e., phosphate and ADP, are released from dynein slowly, and the release of ADP is the rate-limiting step of the whole process (Oiwa and Sakakibara, 2005, Vivenes et al., 2009). Dyneins generate force just in one direction; therefore the arms in one side must be active while those on the other are inactive (figure 1.4). These states must switch to propagate bend down the axoneme (Mitchison and Mitchison, 2010). Dynein dephosphorylation by the calmodulin (CaM)-dependent protein phosphatase reverses this process (Tash and Bracho, 1994). Syndromes characterized by genetic defects of dyneins are associated to male infertility due to immotile spermatozoa (Afzelius and Eliasson, 1979, Afzelius and Eliasson, 1983, Zuccarello et al., 2008).

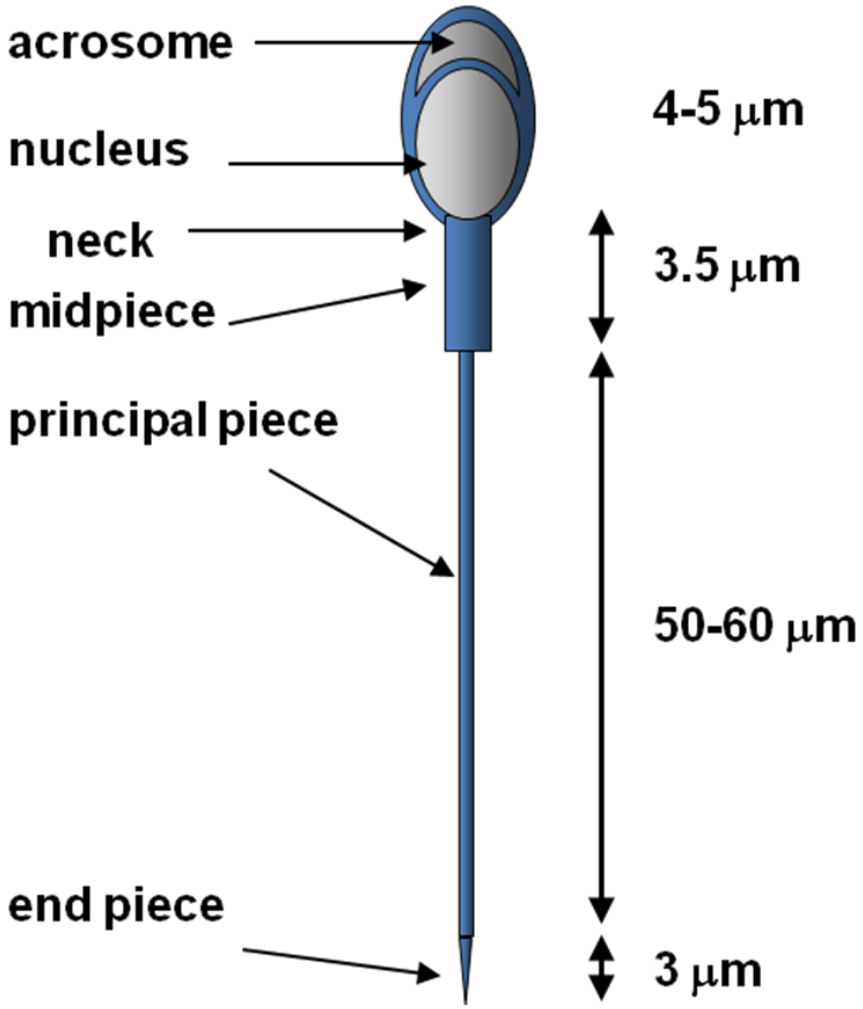

Figure 1.3: Schematic representation of the structure of the mature sperm cell.

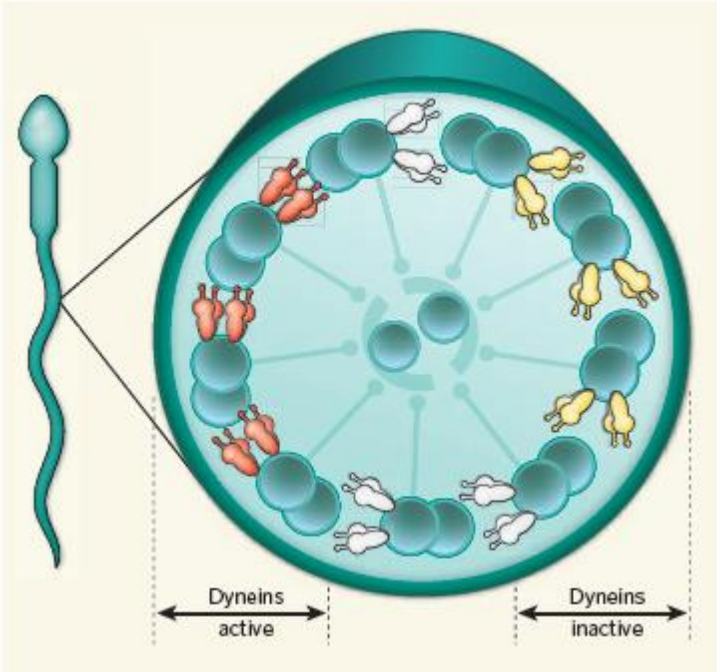

Figure 1.4: Schematic representation of the structure of the sperm axoneme (Mitchison and Mitchison, 2010). The nine microtubule doublets surround a central pair of microtubules. The sliding of microtubules is powered by the action of the dyneins of one side, while those on the other side remain inactive. The mechanism generates bending of the axoneme and the typical flagellar movement.

1.4 Epididymal Maturation

The epididymis is a narrow, tightly-coiled tube connecting the efferent ducts from the rear of each testicle to its vas deferens. It is divided in three regions (proximal to distal): caput (head), corpus (body), and cauda (tail) (Jones, 2004). Spermatozoa shed from the tubular compartment together with the fluid secreted by the Sertoli cells are wafted through the tubuli recti into cavities of the rete testis as the fluid is drawn along by its absorption in the testicular efferent ducts (Cooper and Yeung, 2000). The sperm pass into 12-18 efferent ducts (each 0.2-0.5 m long), which are comprised of ciliated and non ciliated cells whose arrangement, appearance, and height form at least five different tubule types (Cooper and Yeung, 2000). The time for human sperm to pass through the epididymis lies between 2-12 days (Johnson and Varner, 1988) and in this organ the sperm mature and are stored prior ejaculation.

The epididymis has a pseudoestratified epithelium containing a population of principal cells, basal cells and lymphocytes. The principal cells are both resorptive and secretory in nature and they keep an exclusive milieu that allows sperm to be viable for over two weeks (Cooper and Yeung, 2000). The resorptive epithelium is located mainly in the cauda region and concentrates the spermatozoa entering the organ from the testis by mediating the transfer of ions and water (Cooper and Yeung, 2000). Sperm are maintained in a quiescence state in the cauda region. This immotile condition is probably due to low extracellular levels of Na^+ and high levels of K^+ and other compounds, as well as the acidic pH in the surrounding fluids (Wong et al., 1978, Verma, 2001, Yeung et al., 2004). Spermatozoa obtained from epididymal spermatoceles are weakly immotile (Cooper et al., 1992), as are those obtained from the caput region (Yeung et al., 1994). The percentage of motile sperm increases as they pass through the different compartments of the epididymis (Cooper and Yeung, 2006).

Furthermore, the particular ionic environment found in the epididymis is responsible for both the depolarized E_m as well as the slightly acidic intracellular pH seen in the sperm at this level (Cooper and Yeung, 2000).

The epididymis contributes in many processes of sperm maturation such as: volume regulation, motility and fertilization capacity (Cooper and Yeung, 2006) . Subjecting human epididymal sperm to the same procedures as ejaculated sperm for morphological analysis (air-drying smears), results in swelling of the heads of many cells from the caput region but not those from the cauda region (Soler et al., 2000, Yeung et al., 1997). Thus, the presence of spermatozoa with "acorn-shaped" heads may be indication of the presence of immature spermatozoa as a consequence of epididymal disfunction (Cooper and Yeung, 2006). Moreover, the increased intracellular bonding of the sperm during transit trough the epididymis may permit maturing sperm to withstand the osmotic stress associated with air drying (Cooper and Yeung, 2006).

1.5 Capacitation

Once the sperm are released into the female tract they experience a process called capacitation, an event where sperm gain the ability to fertilize. In order to undergo capacitation the cells must reside in the female tract for a certain time (at least 6 hours in humans) (Baldi et al., 2002). Capacitation is associated with changes such as: increase in the fluidity of the membrane by removal of cholesterol and modifications in plasma membrane phospholipids (Cross, 1998, Visconti et al., 1999b, Visconti et al., 1999c); elevation of intracellular pH due to inward fluxes of HCO_3^- (Demarco et al., 2003); increased serine/threonine and tyrosine phosphorylation of flagellar proteins (Visconti et al., 1995b,

Turner, 2006, Bedu-Addo et al., 2005); hyperpolarization of E_m (Zeng et al., 1995, Brewis et al., 2000, Hernández-González et al., 2006); increase of $[Ca^{2+}]_i$ (Baldi et al., 1991, González-Martínez et al., 2002), elevation of cAMP content (Fraser, 2010) among others. All these changes provoke the acquisition of motility and the ability of undertaking acrosome reaction (Yanagimachi, 1988), an essential process to penetrate the layers of the oocyte. The presence of Ca^{2+} is essential for capacitation, hyperactivation and acrosome reaction. Extracellular Ca^{2+} is generally needed for motility in epididymal sperm samples and Ca^{2+} appears to regulate activated and hyperactivated motility (Ho et al., 2002, Lindemann and Goltz, 1988). How the E_m modulates the Ca^{2+} entry during capacitation remains subject of controversy. Resting E_m in human sperm is around -40 and -70 mV in uncapacitated and capacitated cells respectively (Linares-Hernández et al., 1998). Several studies suggest that the sperm E_m hyperpolarization may release T-type voltage-dependent calcium channels (VOCCT) from inactivation (Garcia and Meizel, 1999, González-Martínez et al., 2002) allowing the inward flow of Ca^{2+} into the cell when it is depolarized. Although other studies based on pharmacological inhibition do not show a major role of VOCCT on these events (Bonaccorsi et al., 2001), data from knockout mice has shown that $Ca_v3.2$ is the main T-type Ca^{2+} channel in spermatogenic cells (Stamboulian et al., 2004). Furthermore, $Ca_v3.1$ and $Ca_v3.2$ have been reported to be expressed in human testis and spermatogenic cells (Jagannathan et al., 2002). On the other hand, in recent years the CatSper family of Ca^{2+} channels have been proposed as the main pathway for Ca^{2+} entry. CatSper is located in the principal piece and participates in both depolarization and hyperpolarisation of E_m (Ren et al., 2001, Xia et al., 2007), allowing the entry of Ca^{2+} and the increase of its levels within the cell. This CatSper-dependent rise in $[Ca^{2+}]_i$ is pivotal for hyperactivation .

One of the most studied effects seen on capacitation is protein tyrosine phosphorylation, with

the majority of tyrosine phosphorylation occurring in the flagellum (Visconti et al., 1995a, Visconti et al., 1999d, Bedu-Addo et al., 2005). Increased tyrosine phosphorylation of AKAP proteins in the fibrous sheet of the flagellum has been associated with increased sperm motility and hyperactivation (Luconi et al., 2005). In human spermatozoa AKAP82 and its precursor pro-AKAP82, and fibrous sheath protein 95 (FSP95) are the most prominent tyrosine phosphorylated proteins during capacitation (Carrera et al., 1996). Tyrosine phosphorylation is believed to be initiated by activity of cAMP-regulated PKA, a serine/threonine kinase activated by HCO_3^- and removal of cholesterol (Visconti et al., 1990, Visconti et al., 1999a). When spermatozoa are resuspended in medium that do not support capacitation, tyrosine phosphorylation clearly reverses, and after reversal, rephosphorylation occurs in capacitating medium (Bedu-Addo et al., 2005). Phosphorylation of serine/threonine proteins occurred in presence of either bovine serum albumin alone or HCO_3^- alone (key components of the capacitating medium) (Bedu-Addo et al., 2005). The induction of serine/threonine phosphorylation (immediate upon suspension in capacitating medium) was much more rapid than tyrosine phosphorylation (3 hours to reach maximum), suggesting that the generation of cAMP and activation of PKA occurs immediately upon suspension of spermatozoa in a medium supporting capacitation, but the tyrosine phosphorylation is a more gradual process (Moseley et al., 2005, Bedu-Addo et al., 2005).

1.6 Motility and Hyperactivation

Mammalian sperm exhibits two general forms of motility: activated and hyperactivated. Activated motility, as observed in freshly ejaculated sperm, displays a relative low-amplitude flagellar beat. This mode of swimming, which is effective in low-viscosity medium allowing the sperm to follow a “linear” path, is used in propelling the sperm through the initial stages

of the female reproductive tract (up to the utero-tubal junction). These initial portions have low viscosity and although some immotile sperm could reach the oviduct (probably as result of contractions of the female reproductive tract), most sperm lacking activated motility fail to reach the uterotubal junction and so are incapable of *in vivo* fertilisation (Turner, 2006). This pattern of motility is stimulated by serine/threonine and tyrosine phosphorylation of flagellar proteins, which is regulated in part by the action of cAMP on protein kinase A (PKA), which in turn may be activated by soluble adenylate cyclase (Darszon et al., 2006). This enzyme is regulated by $HCO3^-$ and Ca^{2+}, suggesting that ion channels controlling the inward fluxes of these ions at the plasma membrane are involved. There are two types of adenylate cyclase responsible for cAMP synthesis in eukaryotes, a transmembrane adenylate cyclase (tmAC) and a soluble adenylate cyclase (sAC). Both enzymes are regulated by different pathways; the soluble adenylate cyclase is activated by $HCO3^-$ and Ca^{2+}, is insensitive to G-protein or forskolin regulation and is more active in presence of Mn^{2+} than Mg^{2+} (Wuttke et al., 2001), whereas the transmembrane adenylate cyclase is principally regulated by both G proteins and Ca^{2+} (Wuttke et al., 2001).

Sperm motility requires high levels of ATP to support coordinated movement of the central axonema with the surrounding flagellar structures. ATP is then hydrolyzed by the dynein ATPases that will generate the force to produce flagellar movement. Potential sources of ATP in sperm are compartmentalized in distinct regions along the length of the flagellum (Miki et al., 2004). Oxidative phosphorylation is confined to the midpiece where the mitochondria are located. In contrast, glycolytic enzymes such as phosphoglycerate kinase 2 (PGK2) and glyceraldehyde 3-phosphate dehydrogenase-S (GAPDS) appear to be restricted to the principal piece (Miki et al., 2004, Danshina et al., 2010). GAPDS is bound to the fibrous sheet, the cytoskeletal structure that extends along the entire length of the flagellum (Miki et

al., 2004). Experiments with gene targeting for disruption of GAPDS expression in mice reported profound defects on sperm motility that lead to infertility (Miki et al., 2004). Moreover, although mitochondrial oxygen consumption was conserved, sperm from *Gapds* $^{-/-}$ mice had ATP levels that were only 10.4% of those of sperm from wild type mice (Miki et al., 2004). In addition, the targeted disruption of PGK2 by homologous recombination eliminated PGK activity in sperm, with marked reduction of sperm motility and ATP levels, along with severely impaired male fertility with no affectation of spermatogenesis (Danshina et al., 2010). These results suggest that mutations or environmental factors that disrupt the activity of glycolytic enzymes or their genes, might contribute to male infertility for failure in sperm motility.

Hyperactivated motility is observed at the final stages of the female reproductive tract, and frequently coincides with the onset of the capacitation (Ho and Suarez, 2001). It consists of exaggerated, large amplitude flagellar beats that cause the sperm to swim in a characteristic "figure of eight" formation when in low-viscosity medium, but in a medium with high viscosity (like the oviduct) it can swim in a relatively straight line (Suarez, 2008). Remarkably, sperm that show parameters of activated motility instead of hyperactivated can not advance progressively trough the oviduct, which suggests that hyperactivation helps out sperm to detach from the oviductal epithelium, to attain the fertilisation site, and to penetrate the egg vestments (Suarez and Ho, 2003). It is clear that Ca^{2+} ions within the neck region interact with the axonema of the flagellum for the initiation and maintenance of hyperactivation (Suarez and Ho, 2003, Bedu-Addo et al., 2008). Hyperactivation can be induced by caffeine, thapsigargin and thimerosal (Ho and Suarez, 2001). Interestingly, when $[Ca^{2+}]_o$ was buffered below 50 nM, the response to caffeine was significantly reduced; however the responses to thapsigargin and thimerosal were not affected (Ho and Suarez,

2001). The authors concluded that intracellular stores were important regulators of hyperactivated motility.

More evidence supporting the involvement of ion channels in Ca^{2+} regulation and motility comes from studies in CatSper channels (Ren et al., 2001), a selective Ca^{2+} channel whose expression is restricted to the sperm flagellum. CatSper knockout mice are infertile due to loss of hyperactivated motility (Ren et al., 2001, Qi et al., 2007). It is postulated that CaSper contributes to the Ca^{2+} influx in the flagella that is required for the sperm hyperactivation. 4-aminopyridine (an inhibitor of voltage-activated K^+ channels) caused an instant and dramatic transition of motility in the human sperm population, increasing hyperactivated motility by more than 10-fold (Gu et al., 2004). Application of 2 mM 4-aminopyridine caused a dose dependent, tonic increase in $[Ca^{2+}]_i$ in human sperm (Bedu-Addo et al., 2008). This was clearly visible in fluorimetric records from populations and in imaging experiments where a similar sustained, reversible rise in $[Ca^{2+}]_i$ occurred in the neck-midpiece region associated with asymmetric bending of the proximal flagellum (Bedu-Addo et al., 2008). When cells in "nominally Ca^{2+} free" medium were treated with bis-phenol, an inhibitor of both sarcoplasmic endoplasmic reticulum Ca^{2+} ATPase and secretory pathway Ca^{2+} ATPAse (SPCA) (Harper et al., 2005), the response to 4-aminopyridine was greatly reduced (Harper et al., 2005). These data suggest that 4-aminopyridine is mobilising Ca^{2+} from intracellular stores in human spermatozoa that generates the Ca^{2+} signal required for the initiation of the hyperactivation.

1.7 Acrosome Reaction

The acrosome reaction (figure 1.5) is a modified exocytotic event that is induced by binding to the zona pellucida, a highly glycosylated matrix that surrounds the oocyte (Kopf, 1999).

The binding to the zona pellucida is mediated by the protein ZP3, a glycoprotein that binds to receptors in the anterior head of acrosome-intact sperm (Evans and Florman, 2002). Adhesion to the zona pellucida occurs through association of receptors in sperm with O-linked oligosaccharides (carbonate chains attached to polypeptide by serinyl/threoninyl: N-acetylgalatosaminyl linkages) present in ZP3 (Evans and Florman, 2002). During this process, fusion of the outer acrosomal membrane with the overlying plasma membrane of the sperm occurs at multiple points, causing the release of acrosomal enzymes (including hyaluronidase and acrosin) that digest the substance of the zona pellucida. This phenomenon, in combination with the vigorous motility exhibited by hyperactivated sperm, facilitates the penetration of the sperm through the zona and allows its fusion with the plasma membrane of the oocyte (Talbot, 1985, Kirkman-Brown et al., 2002). It is estimated that the acrosome reaction might last between 15 to 20 minutes (Morales et al., 1994).

One of the more striking features of the acrosome reaction is the lost of the outer crosomal membrane with the sperm plasma membrane as hybrid vesicles. This hybrid vesicle formation is preceded by acrosomal swelling and membrane docking (Zanetti and Mayorga, 2009), a process where SNARE proteins (soluble N-ethylmaleimide-sensitive-factor attachment protein receptor) are heavily involved.

The evidence indicates that before reaching the oocyte and undergoing acrosome reaction, human sperm seems to be subject of "priming" by factors, mainly progesterone and nitric oxide, present in the follicular or oviductal fluid during the ovulation (Serrano and Garcia-Suarez, 2001, Machado-Oliveira et al., 2008). Progesterone is produced at levels of 5 to 10 µM in the vestments of the oocyte during ovulation (Osman et al., 1989), and the presence of progesterone receptors in human sperm has been documented (Losel et al., 2005). The main

role of progesterone on the acrosome reaction resides in the induction of rapid activation of Ca^{2+} influx which does appear to be regulated nongenomically (Blackmore et al., 1990). A universally reported finding is transient elevation of $[Ca^{2+}]_i$ followed by a sustained elevation in the acrosomal region of the sperm head. The transient rise in $[Ca^{2+}]_i$ is abolished in a low-Ca^{2+} medium, supporting the idea that extracellular influxes of Ca^{2+} through specific channels are responsible for this response (Blackmore et al., 1990, Foresta et al., 1995, Kirkman-Brown et al., 2002). On the other hand, the sustained Ca^{2+} elevation is mostly observed in cells that have had transient elevation first (Kirkman-Brown et al., 2000), and it is seems that is due to mobilization of intracellular stores (Bedu-Addo et al., 2007), although there is certain degree of controversy in this matter yet (Correia et al., 2007).

As a consequence of $[Ca^{2+}]_i$ elevation, rapid hydrolysis of phosphatidylinositol 4,5-biphosphate to the second messenger, inositol 1,4,5-triphosphate (IP_3) and dyacilglycerol (DAG) occurs (Correia et al., 2007). These second messengers act releasing Ca^{2+} from intracellular stores like the IP_3 receptor, and activating or regulating plasma membrane channels. On the other hand, cAMP also plays a pivotal role in the acrosome reaction by means of the phosphorylation of Ca^{2+} channels via PKA (Branham et al., 2006).

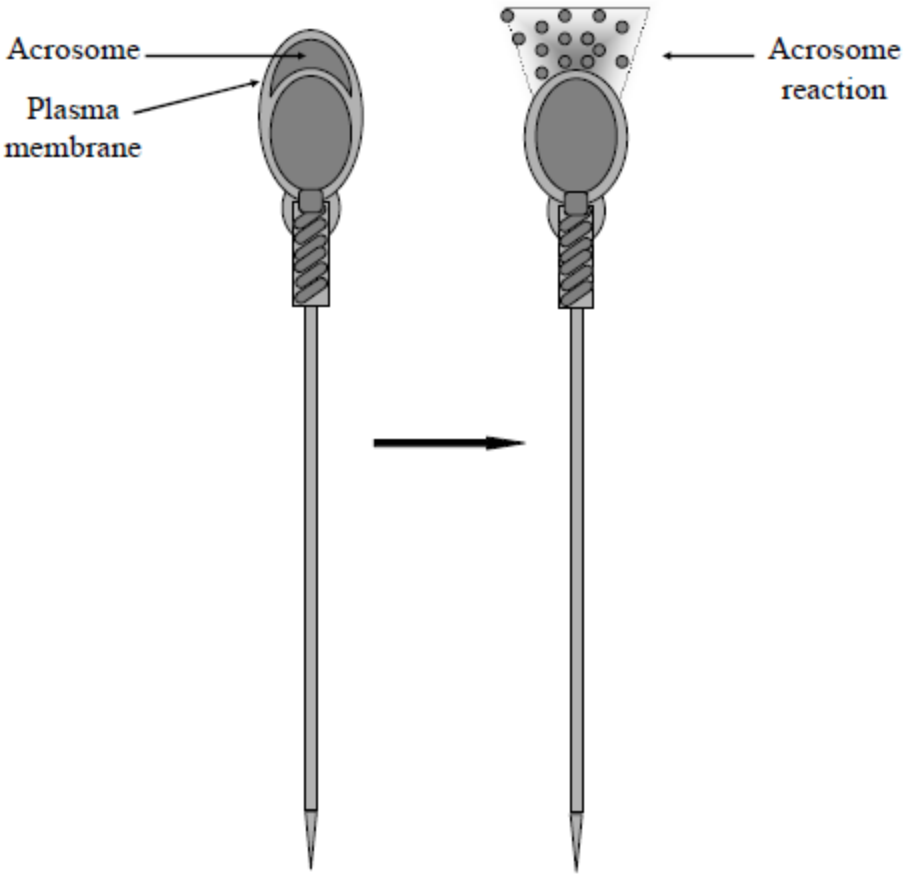

Figure 1.5: Schematic representation of the acrosome reaction.

1.8 Calcium Signalling in Human Spermatozoa

1.8.1 Regulation of Ca^{2+} at the plasma membrane

$[Ca^{2+}]_i$ is strongly buffered in resting cells ($<10^{-7}$ M) whereas $[Ca^{2+})_o$ and $[Ca^{2+}]$ within intracellular organelles is in the range 10^{-4} – 10^{-3} M (Berridge, 2004). Two mechanisms involved in $[Ca^{2+}]_i$ regulation at the plasma membrane have been described in sperm, the plasma membrane Ca^{2+} pump type 4 (PMCA4) (Okunade et al., 2004, Schuh et al., 2004), and the Na^+/Ca^{2+} exchanger (NCX) (Wennemuth et al., 2003, Krasznai et al., 2006). There are four isoforms of PMCA (designated PMCA1-4) and approximately a dozen splice variants (Carafoli and Brini, 2000), but western and northern analysis showed that more than 90% of PMCA protein in mouse sperm is PMCA4 and the remaining 10% is PMCA1 (Okunade et al., 2004). Immunolocalization has showed that PMCA4 is located at the principal piece of the flagellum (Okunade et al., 2004, Schuh et al., 2004). Null knockout rodents for PMCA4 exhibited male infertility accompanied with loss of hyperactivated motility (Okunade et al., 2004). Measurement of $[Ca^{2+}]_i$ showed that, after 60 min of incubation in capacitating conditions, resting $[Ca^{2+}]_i$ was increased from 157 to 370 nM in PMCA4-deficient mice (Schuh et al., 2004). The NCX exports an intracellular Ca^{2+} for three Na^+ ions, using the energy derived from the Na^+ gradient at the plasma membrane (Jimenez-Gonzalez et al., 2006, DiPolo and Beaugé, 2006). The exchanger can also operate in a reverse mode to import Ca^{2+} ions depending on the condition that the cell experiences (DiPolo and Beaugé, 2006). NCX has been reported to participate in Ca^{2+} homeostasis and has been located in rat sperm flagella and tails of sperm sea urchin (Bradley and Forrester, 1980, Su and Vacquier, 2002).

1.8.2 Ca^{2+} channels

As sperm prepare for fertilization, different Ca^{2+} channels at the plasma membrane must open up to guarantee an adequate Ca^{2+} influx for the Ca^{2+}-mediated events. Voltage-dependent calcium channels (VOCCs) are a family of transmembrane channel-forming proteins (Ertel et al., 2000). An important function of VOCCs in sperm is likely to be mediation of the HCO_3^- / cAMP signal (Jimenez-Gonzalez et al., 2006), as in mouse sperm the depolarization-evoked Ca^{2+} entry is enhanced by HCO_3^- through a PKA-dependent mechanism (Wennemuth et al., 2000). A number of VOCCs appear to be present in sperm cells. The existence of mRNAs for all three T-type Ca^{2+} channels ($Ca_v3.1$, $Ca_v3.2$ and $Ca_v3.3$) have been documented in human sperm (Jimenez-Gonzalez et al., 2006). In addition, high voltage activated Ca^{2+} channels ($Ca_v1.2$, $Ca_v2.2$ and $Ca_v2.3$) have also been reported in human sperm (Wennemuth et al., 2000, Jimenez-Gonzalez et al., 2006). It is probable that these channels are participating in processes like acrosome reaction, capacitation and others. Another family of voltage-sensitive Ca^{2+} channels that seems to have special importance in sperm physiology is CatSper. CatSper has four subunits which show restricted expression in sperm cells and testis (Qi et al., 2007). In sperm they are located in the principal piece of the flagellum. Experiments with knockout mice have shown that deletion of any of the four genes encoding CatSper proteins (CatSper1, CatSper2, CatSper3 and CatSper4) leads to loss of progressive motility, inhibition of hyperactivation and finally male infertility (Ren et al., 2001, Qi et al., 2007). Moreover in mice CatSper -/- mutants, the rapid increase in flagellar $[Ca^{2+}]_i$ that occurs upon application of cell-permeant cAMP/cGMP did not occur (Jimenez-Gonzalez et al., 2007). This observation suggested that CatSper might be cAMP gated (Ren et al., 2001). Alkalinisation dramatically increases CatSper open probability thereby potentiating CatSper-Ca^{2+} entry which enhances flagellar bending (Qi et al., 2007). Cyclic nucleotide gated Ca^{2+} channels (CNG) have also been identified in the principal piece of spermatozoa of bovine

(Weyand et al., 1994). In the flagellum, CNG channels are more sensitive to cGMP than cAMP (Wiesner et al., 1998). Manipulation of cGMP and cAMP levels in mouse sperm showed a transient elevation of $[Ca^{2+}]_i$ (Kobori et al., 2000), This effect was greatly reduced in low Ca^{2+} medium or in presence of Ca^{2+} channel blockers, suggesting a role of CNG channels in $[Ca^{2+}]_i$ mobilization. Moreover cGMP was more effective inducing this $[Ca^{2+}]_i$ mobilization (Kobori et al., 2000). CNG channels are crucial for sea urchin sperm chemotaxis (Bonigk et al., 2009), but their role in humans is still not clear. Finally, mobilization of internal Ca^{2+} is thought to activate store operated Ca^{2+} channels (SOCs) at the sperm plasma membrane (capacitive Ca^{2+} entry) (Blackmore, 1993). This Ca^{2+} influx produces a sustained increase in $[Ca^{2+}]_i$ that might be triggering the acrosome reaction (Gonzalez-Martinez et al., 2001, O'Toole et al., 2000). Some members of the canonical transient receptor potential (TRPC) channel superfamily have been suggested as candidates for SOC in mouse sperm (Jungnickel et al., 2001, Stamboulian et al., 2005). These channels show expression in the anterior sperm head and play a role in the Ca^{2+} elevation seen in zona pellucida-induced acrosome reaction (Jungnickel et al., 2001).

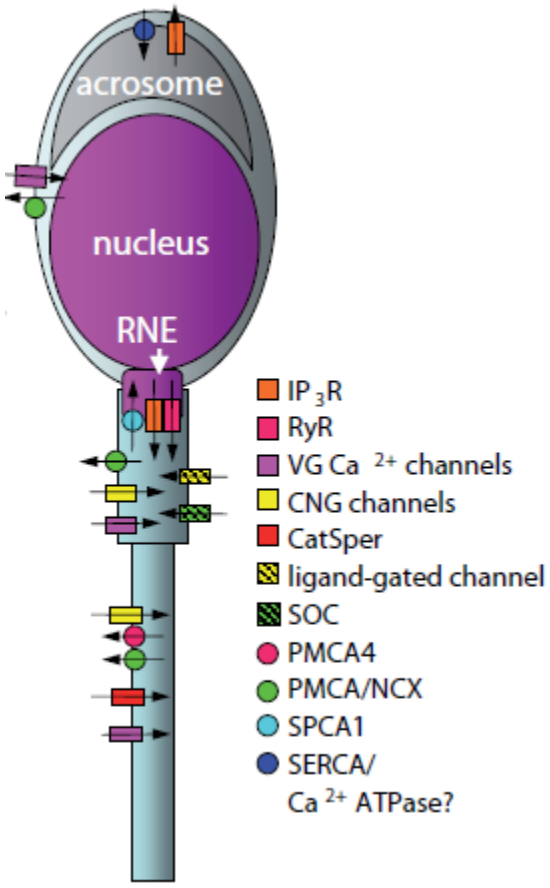

Figure 1.6: Schematic representation of the Ca^{2+} signalling "toolkit" of human sperm (Bedu-Addo et al., 2008). CNG channel, cyclic nucleotide regulated channel; PLC, phospholipase C; PMCA, plasma membrane Ca^{2+}-ATPase; NCX, Na^{+}/Ca^{2+} exchanger; RyR, ryanodine receptor; RNE, redundant nuclear envelope; SERCA, sarcoplasmic-endoplasmic reticulum Ca^{2+}-ATPase; SOC, store-operated channel; SPCA, secretory pathway Ca^{2+}-ATPase.

1.8.3 Intracellular stores

In order to be considered as a *bona fide* intracellular store, organelles must possess at least two types of Ca^{2+} transporters, enabling both loading of the store and release of Ca^{2+} in a controlled fashion (Costello et al., 2009). Intracellular storage of Ca^{2+} is present in sperm as demonstrated by various research groups, the most convincing evidence being that stimulus-induced Ca^{2+} signals can be observed in sperm incubated in Ca^{2+}- free or very low-Ca^{2+} medium (Rossato et al., 2001, Harper et al., 2005, Bedu-Addo et al., 2008). Data suggesting that sperm possess sarcoplasmatic reticulum Ca^{2+} ATPases (SERCAs) has come up from different laboratories (Blackmore, 1993, Dragileva et al., 1999, Rossato et al., 2001, Williams and Ford, 2003); however, the existence of SERCA in sperm is still controversial as it lacks endoplasmic reticulum and because of the high doses of thapsigargin (SERCA blocker) used in those reports (Harper et al., 2005). On the other hand, redundant nuclear envelope and calreticulin-containing vesicles are present in human sperm, and it is more likely that they are (along with mitochondria in the midpiece) the principal Ca^{2+} reservoirs in these cells as indicated by confirmation of secretory pathway Ca^{2+} ATPase (SPCA) activity (Naaby-Hansen et al., 2001, Harper et al., 2005, Bedu-Addo et al., 2008).

Ca^{2+} accumulation in reservoirs is achieved by ATPases such as SERCA and SPCA, along with some co-transporters (Costello et al., 2009), suggesting that SPCA may be the principal "pump" in charge of filling intracellular stores in human sperm. Ryanodine receptors (RyRs) have been identified in human sperm (Harper et al., 2004) and there is evidence showing that they are sensitive to Ca^{2+}, IP_3 , and nitric oxide (NO) (Machado-Oliveira et al., 2008, Bedu-Addo et al., 2008). IP_3 receptors are stimulated by the second messenger inositol 1,4,5-triphosphate (IP_3), which is a by-product of the hydrolysis of phosphatidylinositol 4,5-biphosphate by phospholipase C (PLC) (Walensky and Snyder, 1995). Interestengly, SPCA

(Harper et al., 2005), IP_3 receptors (Naaby-Hansen et al., 2001) and RyRs (Harper et al., 2004) have been reported to be located in the neck region. In addition, mitochondria (located in the midpiece) can accumulate $[Ca^{2+}]_i$ through the mitochondrial Ca^{2+} antiporter located in the inner mitochondrial membrane (Wennemuth et al., 2003), but at the same time is able to release Ca^{2+} in a controlled fashion through a Na^+/Ca^{2+} exchanger (Bernardi, 1999). Finally, the acrosome is also able to store Ca^{2+} and has IP_3 receptors on its outer membrane which are lost once the acrosome reaction occurs (Naaby-Hansen et al., 2001, Rossato et al., 2001, Bedu-Addo et al., 2008).

1.8.4 Progesterone

Progesterone is a hormone present at micromolar concentrations in the follicular fluid (Osman et al., 1989), and is synthesized, both before and after ovulation, by the cells of the cumulus oophorus that surround the egg (Bedu-Addo et al., 2008). Exposure to progesterone, at nanomolar or micromolar range, causes an almost immediately increase in $[Ca^{2+}]_i$ in non capacitated and capacitated cells (Blackmore et al., 1990, Baldi et al., 1991, Bedu-Addo et al., 2005). In capacitated cells exposure to the hormone causes a dose-dependent induction of acrosome reaction (Yanagimachi, 1994, Baldi et al., 1991, Bedu-Addo et al., 2008). Progesterone can induce Ca^{2+} oscillations in human sperm, which is attributed to a form of Ca^{2+}-induced Ca^{2+} release (Bedu-Addo et al., 2008). Oscillations were not affected by inhibition of IP_3 generation or IP_3 receptors. In contrast, pharmacological inhibition of ryanodine receptor altered the frequency of oscillations, and ryanodine and caffeine transformed irregular Ca^{2+} "ripples" in a series of organized transients (Bedu-Addo et al., 2008).

1.8.5 Nitric oxide

NO is produced from L-arginine by the NOS synthase (Palmer et al., 1988). Generation of NO is implicated in gamete interaction and fertilization. NO activates soluble guanylate cyclase (sGC) leading to downstream cGMP actions such as kinase activation, gating of ion channels and s-nitrosylation of exposed protein thiols (that mimics the effects of protein phosphorylation) (Machado-Oliveira et al., 2008). Previous work has shown that human sperm is able to produce NO, which contributes to capacitation and acrosome reaction (Machado-Oliveira et al., 2008, de Lamirande et al., 2009). Immunofluorescent studies showed that cells from the cumulus oophorus (cellular layer investing the egg) synthesize NO (Machado-Oliveira et al., 2008). NO induced an increase in $[Ca^{2+}]_i$ in the neck/midpiece of human sperm, leading to modulation of flagellar activity (Machado-Oliveira et al., 2008). This effect was seen in absence of external Ca^{2+} from the medium, suggesting mobilization from intracellular stores. Human sperm ryanodine receptors are targeted by s-nitrosylation (Lefievre et al., 2007b), suggesting that these stores are responsible for the response seen to NO. Thus, when progesterone was incubated with NO there was a prolonged $[Ca^{2+}]_i$ transient within the sperm cells that was correlated with a prolonged enhancement of flagellar beating (Machado-Oliveira et al., 2008). According to these findings it has been postulated that spermatozoa encounter NO and progesterone in the fallopian tubes, and upon approaching and entering the cumulus oophorus they provide a potent stimulus that act synergistically to mobilize Ca^{2+} in the neck/midpiece (by s-nitrosylation of ryanodine receptors that leads to Ca^{2+} release) that will modulate flagellar bending needed for the hyperactivation (Machado-Oliveira et al., 2008).

1.9 Fertilisation

Fertilization is the process of union of the male and female gametes, sperm and egg. Once the

sperm cells are detached from the seminiferous epithelium in the testis, they are transported through the epididymis where maturation takes place, and finally will be stored in the cauda epididymis (Cooper, 1996). Upon ejaculation the cells become capacitated and hyperactivated in the female tract, which will enable them to reach the oocyte through the mucus-filled oviduct and helping them to penetrate the cumulus oophorus and zona pellucida of the oocyte (Suarez, 1996). It has been postulated that spermatozoa may be guided to the fertilization site by substances generated by the cumulus cells that surround the egg, or the oocyte itself, e.g. progesterone and nitric oxide, a process called sperm chemotaxis (figure 1.7) (Machado-Oliveira et al., 2008, Teves et al., 2010).

After penetration of the zona pellucida, sperm adhere to and fuse with the plasma membrane of the egg. The involvement of sperm fertilin-α (also known as a disintegrin and a metalloprotease domain 1 (ADAM1)), fertilin-β (ADAM2) and cyritestin (ADAM3), as well as CRISP1 and CRISP2 (cysteine-rich secretory protein1 and 2) in sperm–egg adhesion are indicated by studies using antibodies, peptides, and native or recombinant proteins (Evans, 1999, Ellerman et al., 2010). In addition, sperm from fertilin-β and cyritestin knockout mice show greatly reduced abilities to adhere to the egg membrane, although some of the few sperm that adhere can go on to fuse with the egg (Cho et al., 1998, Nishimura et al., 2001). Integrins found on the surface of eggs are thought to be receptors for sperm ADAMs (Evans and Florman, 2002). Recent evidence implicates α9β1 integrin as a binding partner for fertilin-β (Eto et al., 2002). These adhesion-mediating proteins on both gametes are likely to function within the context of multimeric complexes at the plasma membranes (Evans and Florman, 2002). In addition, the integrin-associated protein tetraspanin CD9, has been reported to be located in the egg plasma membrane and seems to be important for sperm–egg interactions (Evans and Florman, 2002). Sperm do not fuse with eggs from CD9 knockout

mice (Miyado et al., 2000), and anti-CD9 antibodies inhibit sperm–egg fusion and the binding of sperm ADAMs to eggs (Evans and Florman, 2002).

CRISP1 is synthesized in an androgen-dependent manner by the proximal segments of the epididymis, and associates with the sperm surface during epididymal maturation (Kohane et al., 1980b, Kohane et al., 1980a). It is initially located in the dorsal region of the sperm head but after the acrosome reaction it migrates towards the equatorial segment, which is the region where sperm fuses with the egg (Rochwerger and Cuasnicu, 1992). Results using the hamster oocyte penetration test showed that incubation of human sperm with an anti-hCRIPS1 antibody produced a significant decrease in the sperm ability to penetrate the eggs without affecting any other sperm functional parameter (Cohen et al., 2001, Cohen et al., 2008). CRISP2 was found to be present in the acrosome and the outer dense fibers of the flagellum, and remains there after the acrosome reaction occurs (O'Bryan et al., 2001, Cohen et al., 2008). The role of CRISP2 in human sperm was evaluated by the same hamster oocyte test, where a polyclonal antibody against CRISP2 decreased the percentage of penetrated oocytes without affecting sperm motility, acrosome reaction or sperm binding to the plasma membrane of the egg (Busso et al., 2005); suggesting that this protein is also involved in fusion.

After fusion of the gametes the embryonic development is initiated. In all animals and plants where this phenomenon has been studied, an early event in egg activation is the increase in $[Ca^{2+}]_i$ to approximately 1 µM (Evans and Florman, 2002). The rise in $[Ca^{2+}]_i$ seems to occur between several seconds and a few minutes after the establishment of membrane continuity between gametes, and often occurs as a "wave" that travels across the egg (Stricker, 1999, Runft et al., 2002). This $[Ca^{2+}]_i$ initiates the mitosis and the exocytosis of cortical granules,

the contents of which modify the zona pellucida to prevent fertilization for additional sperm cells (polyspermy) (Schultz and Kopf, 1995). Other responses seen in egg activation include the recruitment of maternal mRNAs for translation, changes in protein synthesis, and zygotic genome activation (Schultz and Kopf, 1995, Evans and Florman, 2002).

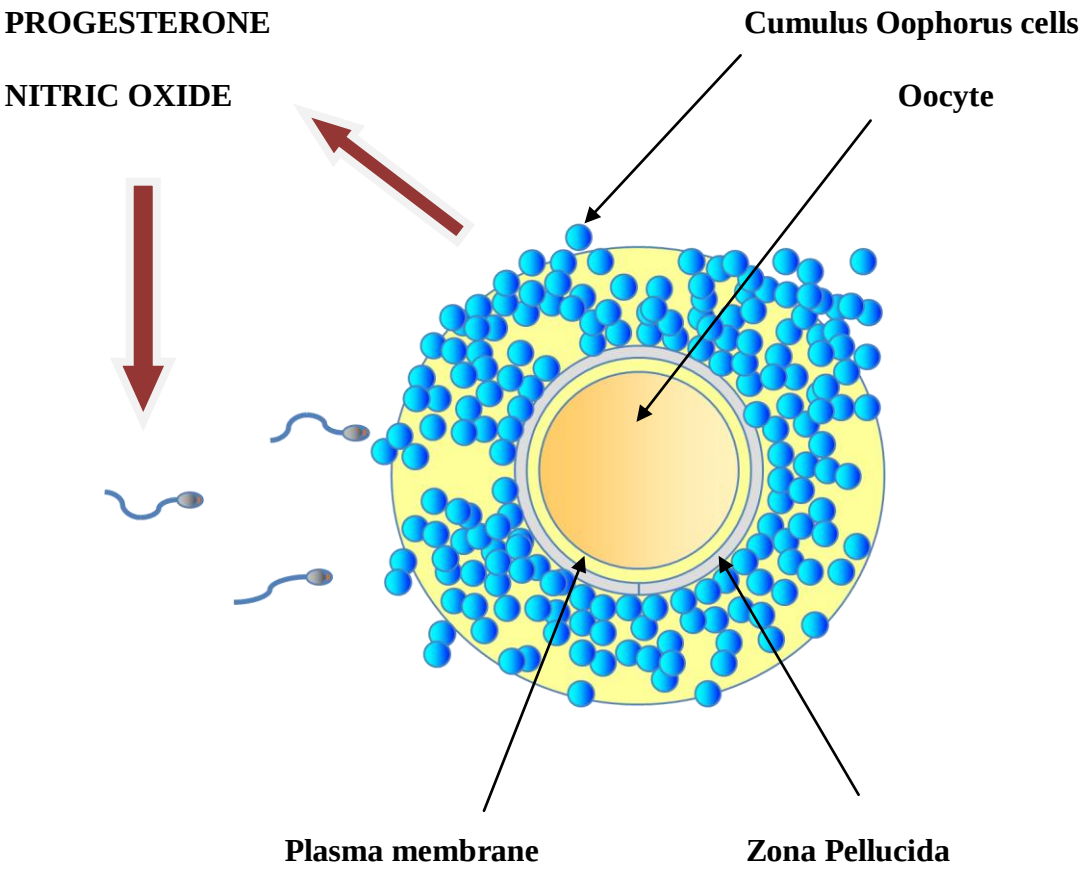

Figure 1.7: Schematic representation of the sperm chemotaxis to the oocyte.

1.10 Ion Channels in Human Spermatozoon

At the plasma membrane a single ion channel exists as a "pore" that allows the passage of millions of charged particles (ions) per second from one side to the other. The ionic gradients generated by these flows are pivotal to the maintaining and functioning of key cellular mechanisms such as: membrane potential (E_m), enzymatic systems, exchangers, pH and Ca^{2+} regulation, further channel activity and modulation of other second messengers. Indeed, a vast quantity of drugs used in the cardiovascular and neurological therapeutic acts directly on ion channels modifying their activity. Ion channels are known to play a crucial role in sperm physiology and function (Darszon et al., 2006), including motility (Ren et al., 2001), volume regulation (Yeung et al., 2003, Barfield et al., 2005, Yeung et al., 2005), capacitation (Zeng et al., 1995, Darszon et al., 1999, Muñoz-Garay et al., 2001, Navarro et al., 2007), hyperactivation (Qi et al., 2007), and induction of acrosome reaction (Darszon et al., 1999, Florman et al., 1992, Kirkman-Brown et al., 2002).

Electrophysiological recording of ion channel activity in mature human spermatozoon has proved difficult, due to the small size of the cell. As a strategy, ion channels have been isolated from human sperm plasma membranes and then reconstituted into lipid planar bilayers via fusion, in order to perform patch clamp studies. Through this technique it has been possible to identify the presence of K^+, Na^+, Ca^{2+} and Cl^- channels (Shi and Ma, 1998). The conductances for these channels were 40 pS, 26 pS, 40 pS and 30 pS respectively, and no apparent voltage dependence was found for these channels, although the percentage of open channel events was different (Shi and Ma, 1998). However, this experimental technique cannot mimic completely the physiological conditions seen in intact cells. In a previous study three different types of channels (Type 1, 2 and 3) were detected in the equatorial region of spermatozoa using the cell attach approach, but the most common records were from high-

conductance, multi-state channels sensitive to 4-aminopyridine (Gu et al., 2004). Application of 2 mM 4-aminopyridine (a dose sufficient to cause channel blockade) caused an instant and dramatic transition of motility in the sperm population increasing hyperactivated motility by more than 10-fold (Gu et al., 2004).

In a second study, records obtained from the equatorial and anterior acrosomal regions in the sperm head showed that two of these channels (referred to as type 1 and type 2) were superficially similar (conductance 28 and 23 pS respectively), exhibiting flickering between the open and close state with periodic longer openings (Jimenez-Gonzalez et al., 2007). Current through these channels reversed at a value of membrane potential approximately 55 mV positive to resting potential. Type 3 showed a kinetic very different (with a conductance of 31 pS), with more stable and prolonged openings, particularly at depolarized potentials. The reversal potential was estimated to be 70-75 mV positive to resting potential. Interestingly, the use of the inside-out approach revealed that this same channel was a Cl^- -permeable anion channel, with reversal potential of 24 mV positive (Jimenez-Gonzalez et al., 2007), but the channels type 1 and 2 could not be detected under this configuration. A particular characteristic found in these currents was their distribution, which followed a regionalized pattern. Whereas type 1 was distributed randomly between the anterior acrosomal and equatorial regions, type 2 was seen only in the equatorial region as well as type 3. These observations demonstrated that human sperm channel activity is both structurally and physiologically regionalized and tightly grouped (Jimenez-Gonzalez et al., 2007).

Very recently, elegant experiments using whole cell patch clamp in human sperm showed the existence of a proton channel (Hv1) confined to the principal piece of the flagellum, where it

is expressed in unusually high quantities (Lishko et al., 2010). Hv1 is responsible for most of the proton conductance and is activated by depolarization, extracellular alkalinization, the endocannabinoid anandamide, and removal of extracellular zinc (a potent Hv1 blocker) (Lishko et al., 2010). Hv1 only allowed outward transport of protons and it is suggested that its main role is to induce intracellular alkalinization for activation of human spermatozoa.

1.11 Chloride Channels and Cell Function

Anion channels allow the passive diffusion of negatively charged ions along their electrochemical gradient. Although these channels may conduct other anions (e.g., I^- or NO_3^-) better than Cl^- , they are often called Cl^- channels because Cl^- is the most abundant anion in organisms and hence is the predominant permeating species under most circumstances (Jentsch et al., 2002). Cl^- channel gating may depend on the transmembrane voltage (in voltage-gated channels) (Dutzler, 2004), cell swelling (Nilius et al., 1996, Do and Civan, 2006), binding of signaling molecules (as in ligand-gated anion channels of postsynaptic membranes) (Lynch, 2004), H^+ (pH) (Nobles et al., 2004), Ca^{2+} (Yang et al., 2008, Zhu et al., 2009), phosphorylation of intracellular residues by various protein kinases (Geiger et al., 2009), and the binding or hydrolysis of ATP (El Hiani and Linsdell, 2010). Like other ion channels, Cl^- channels may perform their functions at the plasma membrane and in the membranes of the intracellular organelles. The activity of the channels has a dual function, transport of charge, i.e., the electric current passing through the channels (Hogg et al., 1994), and the transport of matter, i.e., the bulk flow of chloride in response to osmotic challenges (Cooper and Yeung, 2007). Currents flowing through Cl^- channels are thought to be important in regulation of excitability in nerve and muscle as well as the activity of the electrogenic H^+ -ATPase that acidifies several intracellular compartments (Jentsch et al.,

2002). On the other hand, bulk flow of chloride is important in the events of cell volume regulation and epithelial transport (Hoffmann et al., 2009).

An important function of Cl^- channels is related to membrane electrical excitability. Loss of a specific type of Cl^- channel that stabilizes the resting potential in skeletal muscle leads to myotonia, an intrinsic disorder characterized by muscle hyperexcitability (Macias et al., 2007). In contrast to skeletal muscle, in smooth muscle the electrochemical potential of Cl^- is significantly higher than the resting potential (Chipperfield and Harper, 2000). Thus, an opening of Cl^- channels will lead to depolarization that may be strong enough to induce flux of Ca^{2+} through VOCCs, a mechanism that might be important for the response of vascular resistance to mechanical stress (Manoury et al., 2010).

Cl^- channels participate in the regulation of pH within the cells, which is tightly controlled by the Na^+/H^+ exchanger and the Na^+ HCO_3^-/H^+ Cl^- exchanger (Vaughan-Jones and Spitzer, 2002). Both exchangers need a parallel pathway for recycling chloride that is provided by the Cl^- channels (Jentsch et al., 2002). Conversely, the cells may decrease their pH by action of the $Cl^-/$ HCO_3^- exchanger (Casey et al., 2009) that also require a parallel shunt of chloride ions. Cl^- channels are also needed for the transport of salt and fluid across many epithelia. The polarized expression of Cl^- channels and secondary active Cl^- uptake mechanisms ensures the directionality of transport. For example, airway epithelia, acinar cells of many glands, and the intestine can actively secrete Cl^- across their apical membrane. Because Cl^- channels only permit passive transport by diffusion, the intracellular Cl^- concentration is raised above equilibrium by Na^{2+} - K^+ - $2Cl^-$ cotransporters that often need K^- channels for recycling potassium (Jentsch et al., 2002). In intestinal crypt cells that secrete Cl^-, the Na^{2+} - K^+ - $2Cl^-$ cotransporters, together with the K^+ channels needed for recycling, are located

basolaterally, whereas the Cl^- leaves the cell apically via CFTR channels (Sandle et al., 2007). In acinar cells regulation of Cl^- secretion depends on Ca^{2+}-activated Cl^- channels, which remarks the importance of Ca^{2+} in some subtypes of Cl^- channels (Petersen, 1992). In addition Ca^{2+}-activated Cl^- channels might be important in signal transduction of the olfactory cell's response (Pezier et al., 2010) and regulation of cell volume (Chien and Hartzell, 2007).

1.12 Chloride Channels in Human Spermatozoon

The ClC family constitutes a large family of transmembrane transporters that either function as Cl^- channels or as H^+/Cl^- exchangers. The nine homologues in human are located either at the plasma membrane or in the membranes of intracellular components, being involved in various processes ranging from electrical depolarization in muscle to epithelial ion transport and acidification of intracellular compartments (Dutzler, 2007) Data obtained from bacteria shows that ClC is a homodimeric protein whose two structurally identical subunits each harbor an independent ion translocation pore. The subunit exhibits a complex topology with two structurally related halves spanning the membrane with opposite orientations to form an "antiparallel architecture" (Dutzler et al., 2002). The Cl^- translocation path is located at the interface between the two halves and contains a Cl^- selectivity filter in the neck of an hourglass-like shaped pore (Dutzler, 2007). This narrow filter harbors three selective anion-binding sites that can bind Cl^- anions at the same time with mM affinity (Lobet and Dutzler, 2006). In this family of Cl^- channels, ClC2 and ClC3 have been suggested to participate in volume regulation, but only the ClC3 has been identified in human sperm (Yeung et al., 2005).

Three more Cl^- channels have been identified in human sperm, the glycine receptor/Cl^-

channel (GlyR), the $GABA_A$ receptor/Cl^- channel and the cystic fibrosis transmembrane conductance regulator (CFTR). The GlyR is a member of the nicotinic acetylcholine receptor family of ligand-gated ion channels as well as $GABA_A$ receptors. Ligand-gate ion channels permit cells to respond rapidly to changes in their external environment (Lynch, 2004). The molecule is a membrane-embedded protein, formed of one type of β subunit in combination with one of several different α subunit types to yield a pentamer of three α subunits and two β subunits, that contains an integral Cl^- selective pore (Lynch, 2004). When glycine binds to its site on the external receptor face, the pore opens allowing Cl^- to passively diffuse across the membrane leading the membrane potential rapidly toward the Cl^- equilibrium potential (Lynch, 2004). Presence of GlyR has been confirmed in human sperm (Bray et al., 2002). This study shows that when an antagonist of GlyR is used, inhibition of the typical rise of intracellular Ca^{2+} related with the acrosome reaction occurs. Therefore, it is suggested that this channel may play a role in the early signal transduction cascades associated with the acrosome reaction, presumably via depolarization of E_m (Bray et al., 2002). Moreover, glycine is able to initiate the porcine and human acrosome reaction, and this event could be inhibited by strychnine (an inhibitor of GlyR) at 50 nM (Meizel, 1997).

$GABA_A$ receptors are also members of the nicotinic superfamily of heteropentameric ligand-ion channels. The subunit structure of all these receptors consists of a large N-terminal extracellular domain followed by four transmembrane domains and a large cytoplasmic loop between the segments 3 and 4. On the other hand, the C termini of subunits face the extracellular membrane but barely extrude from the membrane (Lüscher and Keller, 2004). These channels exhibit extensive structural heterogeneity as indicated by the 19 different subunits genes that encode the subunits of pentameric receptors (Sieghart et al., 1999). As well as GlyR, these channels seem to participate in the depolarizing events during the

acrosome reaction (Shi and Roldan, 1995, Turner and Meizel, 1995). In order to support this assumption, human spermatozoa were exposed to chlordane and endosulfan, which are chlorinated cyclodiene blockers of insect neuronal $GABA_A$ receptor/Cl^- channels. The results showed that these chemicals strongly inhibited the acrosome reaction initiated by progesterone or glycine, even at nanomolar concentrations (Turner et al., 1997).

The CFTR protein is made up of two homologous repeats, each containing six transmembrane regions followed by an intracellular nucleotide-binding domain. These two halves are joined by an intracellular regulatory domain (Linsdell, 2005). The crystal structure of CFTR shows membrane-spanning regions lining a central pore; the pathway through which Cl^- ions cross the membrane (Rosenberg et al., 2004). This overall structure is common with ligand-gated Cl^- channels (Unwin, 2003, Linsdell, 2005). CFTR is a cAMP-modulated Cl^- channel and a regulator of several transporters and proteins, including K^+ channels, such as ROMK1 and ROMK2 (Kunzelmann and Schreiber, 1999, Briel et al., 1998), anion exchangers, aquaporins, and epithelial sodium channels (EnaCs) (Liu et al., 1999). Activation of CFTR reciprocally inhibits EnaCs (Schwiebert et al., 1999). Additionally, cystic fibrosis, the most prevalent human genetic disease is caused by CFTR mutations (Guggino and Stanton, 2006), and around 95% of men with the disease present male infertility. Reduced sperm quality in patients with CFTR mutations is common, including defective sperm capacitation and egg-fertilizing ability; being hypothesized that CFTR may be directly or indirectly involved in mediating $HCO3^-$ transport and its alteration may contribute to impairment of the capacitation (Chan et al., 2006). Previous experimental data have documented the presence of CFTR in the midpiece of both mouse and human sperm, and DPC (an inhibitor of CFTR) blocked the capacitation-associated hyperpolarization and prevented the EnaCs closure in mouse (Hernández-González et al.,

2007).

1.13 Physiology of Volume Regulation

Osmolality is defined as the number of osmotically active particles per kilogram of water. The animal cell membrane is, with a few exceptions, highly permeable to water. Cell water content and cell volume are thus determined by the cellular content of osmotic active compounds and by extracellular tonicity (Hoffmann et al., 2009). The osmotic water permeability in animal cells is several orders of magnitude greater than the permeability towards Na^+, K^+, and Cl^- (Hoffmann et al., 2009). Cells contain impermeable, polyvalent anionic macromolecules which are constantly threatened by colloid osmotic cell swelling due to entrance of diffusible ions and water (Hoffmann et al., 2009). According to the "pump and leak" concept, cell swelling and lysis are avoided because a combination of a low Na^+ permeability and active Na^+ extrusion via the Na^+-K^+ -ATPase renders the plasma membrane effectively impermeable to Na^+ (Leaf, 1959, Tosteson and Hoffman, 1960).

Osmotically swollen cells release KCL, nonessential organic osmolytes, and cell water in order to reduce cell volume to its original value, a process called regulatory volume decrease (RVD). On the other hand, osmotically shrunken cells initiate a net gain of KCL and cell water, thereby increasing cell volume towards the original value, a process called regulatory volume increase (RVI) (Hoffmann et al., 2009). RVD is a process dependent on increases in the net efflux of Cl^-, K^+, and organic osmolytes, whereas RVI involves activation of Na^+, K^+-$2Cl^-$ co-transport, Na^+/H^+ exchange, and nonselective cation channels (Hoffmann et al., 2009).

Cells need to control their volume in the face of internal and external challenges. For instance, in the proximal gastrointestinal tract or in the kidney, the cells may be exposed to significant changes in extracellular osmolarity (Snow et al., 1993, De Smet et al., 1995, Jentsch et al., 2002). Epithelial cells involved in transepithelial transport need to balance their apical and basolateral ion transport rates to maintain their volume within certain limits (Crowe et al., 1995, Jentsch et al., 2002, Brochiero et al., 1995). Small volume changes may actually serve to couple transport rates between the two cell surfaces by recruiting swelling-regulated transporters for the vectorial transport of solutes and water (Jentsch et al., 2002). It is noteworthy to mention that cell volume changes during growth, apoptosis, invasion and cell division (Doroshenko et al., 2001, Eggermont et al., 2001, Hoffmann et al., 2009). Thus volume regulation is probably a universal feature of all vertebrate cells that is necessary for diverse biological functions.

In general, one can separate the events elicited by cell volume changes in three major categories: 1) macromolecular crowding, 2) cellular ionic strength or concentrations of specific ions , or 3) mechanical/chemical changes of the lipid bilayer (Hoffmann et al., 2009). Macromolecular crowding refers to the high concentrations of proteins, nucleic acids, and/or polysaccharides in intracellular compartments that could significantly affect the chemical reactivity of individual macromolecules as well as of cell water (Minton et al., 1992). Macromolecular crowding has been suggested to play determinant roles in the modulation of some cellular responses to volume perturbation in red blood cells (Parker, 1993, Dunham, 1995). Changes in intracellular ionic strength associated with volume perturbations may participate in the activation of signalling cascades (e.g., modulation of phosphatidylinositol 4, 5 biphosphate levels) and volume-activated transport proteins like the Na^+ -K^+ -$2Cl^-$ cotransporter (Nielsen et al., 2007, Hoffmann et al., 2009). Mechanical/chemical changes in

lipid bilayer induced by osmotic stress may regulate membrane transport, proteins, receptors, and enzymes (Perozo, 2006, Hoffmann et al., 2009). The existence of specific K^+ channels that are activated by cell stretching only and others activated by cell volume only (Hammami et al., 2009), constitutes evidence of the role of the physical stimulus in the cellular response to changes in volume. Changes in lipid composition resulting from the action of osmosensitive specific phospholipases and phospholipid kinases can alter membrane curvature, which in turn can modify the function of transporters and channels that participate in volume regulation (Hoffmann et al., 2009).

Cell swelling induces a characteristic anion-selective conductance in most of the vertebrate cells where whole cell patch clamp have been implemented (Bond et al., 1998, Jentsch et al., 2002, Auzanneau et al., 2006, Matsuda et al., 2010). This current displays moderate outward rectification, lacks conspicuous time-dependent activation upon depolarization, and shows variable inactivation at voltages more positive than +40 mV (Jentsch et al., 2002, Nobles et al., 2004, Do and Civan, 2006). In some cells, the swelling activated Cl^- current shows less rectification and inactivation (Nilius et al., 1996), possibly suggesting a molecular diversity of underlying channel proteins.

1.14 Physiology of Sperm Volume Regulation

The sperm cell has to deal with constant osmotic changes in the fluids surrounding it, which suggest that sophisticated mechanisms able to regulate cellular volume are required. Failure in controlling the intracellular volume will translate in cell deformation that will affect the ability of sperm to swim, and therefore, to fertilize the oocyte. The osmolality of fluid bathing human sperm in the testis approximates that in the blood (300 mOsm), but as sperm are

transported through the epididymal duct over a course of a week, they encounter a gradually increasing osmotic environment as a result of the androgen-dependent secretion of low molecular weight, water-soluble compounds by the epididymal epithelium (Cooper and Yeung, 2007), along with absorption of Na^{2+} and water, a process estrogen-dependent (Cooper and Yeung, 2000). After all these changes, epididymal sperm end up bathed in an osmolality of about 340 mOsm (Hinton et al., 1981).

The absorption of fluid concentrates the spermatozoa and epididymal secretions in the lumen. The components secreted are believed to be taken up for spermatozoa during maturation in order to keep them quiescent before ejaculation, as well as serving as osmolytes for volume regulation when they pass through the female tract (Cooper and Yeung, 2000, Cooper and Yeung, 2003). Among these compounds are organic osmolytes like L-carnitine, glutamate, *myo*-inositol, taurine, hypotaurine, and glycerophosphocoline (Yeung et al., 2006); and the inorganic osmolyte K^{+} (Cooper and Yeung, 2007). It has been hypothesized that the intake of osmolytes by spermatozoa is mediated by a process of isovolumetric regulation (IVR) (Cooper and Yeung, 2003), in which osmolytes are taken up by the cells that draw in water osmotically in order to counteract dehydration in such hypertonic medium, but the importance of such osmolytes in sperm RVD is still debatable (Yeung et al., 2003).

Sperm experience a decrease in extracellular osmolality before ejaculation once it has contact with hypotonic secretions coming from glands located within the urethra, which have an osmolality of about 294 mOsm (Cooper et al., 2005). Upon ejaculation, sperm are still maintained at lower osmolalities in the female tract, being 280-294 mOsm for the uterine fluid (Casslen and Nilsson, 1984), and about 270 mOsm for fallopian tubes (hydrosalpinx) (Ng et al., 2000, Granot et al., 1998). That means that sperm suffers an osmotic difference of

about 46 mOsm within the urethra and cervical mucus, and 70 mOsm within the fallopian tubes when is compared to that in the epididymis, which would produce cell swelling unless corrective measures were taken. In this context, the regulatory volume decrease (RVD) comes into action, and its failure leads to subsequent cell swelling and impairment of both migration and penetration through cervical mucus (Yeung and Cooper, 2001).

During RVD an efflux of K^+ occurs through potassium channels (Yeung and Cooper, 2001, Klein et al., 2006), driving water out of the cell which prevents swelling. These K^+ fluxes would hyperpolarize the cell in excess. In order to maintain the electro-balance and to increase the efficiency of RVD, separate Cl^- or anion channels are evoked to allow the efflux of anions. This is corroborated by evidence that ClC3 is present along the human sperm tail and the use of Cl^- channels blockers inhibited the RVD (Yeung et al., 2005).

The clinical relevance for RVD is confirmed for data showing that defects in RVD are cause of infertility in laboratory rodents and domestic animals by angulations or coiling of the sperm flagellum, which occurs as a consequence of the tail's swelling into various sizes and shapes to accommodate the increase in cell volume (Yeung et al., 2001, Cooper and Yeung, 2007). It is important to mention that swelling and the resultant deformation of the human sperm tail has been widely utilized in fertility clinics to establish sperm vitality in the HOS test (hyposmotic shock) where ejaculated sperm is incubated with a drastically hyposmotic solution at 150 mmol/kg (WHO, 1999). Swelling of the tail indicates intact membranes or living sperm, whereas dead cells retain their normal tail shape because of leaky membranes (Cooper and Yeung, 2000).

1.15 Cell signalling in sperm volume regulation

In somatic cells, RVD mediated by Cl^- and K^+ channels involves signalling cascades mediated by phosphorylation and dephosphorylation of diverse proteins (Klein et al., 1993, Robson and Hunter, 1994, Petrunkina et al., 2007, Hoffmann et al., 2009). Previous evidence suggests that sperm cell volume under hypertonic conditions is mediated by protein tyrosine kinase pathways (PTK) (Petrunkina et al., 2005). Sperm from c-*ros* tyrosine kinase receptor knockout mice were infertile and showed impaired motility and other characteristics commensurate with a volume regulatory disturbance (Yeung et al., 2004).

Petrunkina et al (Petrunkina et al., 2005) reported differential effects of the PTK inhibitor lavendustin and the general protein kinase inhibitor staurosporine (especially potent against protein kinase C, PKC), which suggests that phosphorylation mediated by PTK and/or by serine- threonine kinases such as PKC may participate in volume regulation (Petrunkina et al., 2005). Activation of PKC led to sperm swelling in hypotonic media in boar (Petrunkina et al., 2007). The inhibitor-induced swelling did not take place in a medium in which Cl^- had been replaced with sulphate, suggesting that PKC was acting largely on Cl^- channels (Petrunkina et al., 2007). cAMP plays a major role in ion channel activation. At low concentrations, forskolin, a potent stimulator of adenylate ciclase, increased isotonic volumes and enhanced RVD in response to hypotonic conditions (Petrunkina et al., 2007). Moreover papaverine, a phosphodiesterase inhibitor, led to a significant increase in both isotonic volume and RVD, and at the same time it was able to reverse the inhibition of RVD by okadaic acid, a potent inhibitor of protein phosphatases (Petrunkina et al., 2007). Therefore is very likely that cAMP is involved in the opening of ion channels during RVD. This group has proposed two models of osmo-signaling pathways in spermatozoa (Petrunkina et al., 2007). The first model establishes that PKC is involved in the sequence that leads to deactivation of

the osmo-dependent regulatory mechanism, probably by closing and keeping closed volume-sensitive anion channels. Inhibition of PKC would result in premature activation of the channels, increased isotonic cell volume and prolonged volume regulation. Phosphatase 1 (PP1) would be involved in the sequence that leads to activation of RVD, probably by opening of these channels (Petrunkina et al., 2007). Thus, inhibition of PP1 would result in blocked RVD. The second model postulates that activation of RVD during hypotonicity is cAMP-sensitive. An increase in intracellular cAMP would be only associated to activation of mechanisms normally "dormant" during isotonic conditions, therefore these channels would be specially recruited to overcome the osmotic challenges imposed by hyposmotic environments (Petrunkina et al., 2007).

RESEARCH AIMS

To:

Evaluate the influence of Cl^- channels, through the use of different Cl^- channel blockers, on motility of human spermatozoa exposed to hyposmotic shock.

Assess the effect of different Cl^- channel blockers on morphology of human spermatozoa exposed to hyposmotic shock.

Investigate the effect of hyposmotic shock and different Cl^- channel blockers on intracellular Ca^{2+} signalling of human spermatozoa.

CHAPTER 2

EFFECT OF DIFFERENT CLHORIDE BLOCKERS IN THE MOTILITY OF THE HUMAN SPERMATOZOON

2.1 Abstract

The role of Cl^- channels in human sperm motility remains poorly understood. The Cl^- channels blockers DIDS, NPPB and niflumic acid were used to evaluate their possible effects on motility of human spermatozoa incubated at different degrees of osmolality (295, 270 and 200 mOsm, equivalent to the osmotic conditions of cervical mucus, fallopian tubes, and non physiological respectively). The results show that at 295 and 270 mOsm, 50 and 100 µM DIDS inhibited motility whereas 400 µM abolished it. Conversely, 100 µM NPPB and 200 µM niflumic acid did not affect motility. In non physiological conditions (200 mOsm), 50 µM DIDS reduced motility at 30 min, whereas 100 and 400 µM DIDS were effective reducing motility at both 30 and 60 min. 100 µM NPPB failed to produce any significant modification in the percentage of motile cells and niflumic acid decreased motility at 60 min. Western blots show that DIDS produce a reduction of serine/threonine phosphorylation of proteins in sperm cells. HCO_3^- is important for soluble adenylate cyclase activity, cAMP production, and phosphorylation of proteins. The evidence suggests that DIDS inhibits the transport of HCO_3^- , probably by targeting the HCO_3^- / Cl^- exchanger, which might be affecting cAMP production and therefore phosphorylation of proteins essential for sperm motility.

2.2 Introduction

Motility is one of the most important characteristics for assessing fertility potential of human spermatozoa. Mature spermatozoa are quiescent in the epididymis, but upon ejaculation they become motile. Capacitation is a complex set of events that spermatozoa experience during transit through the female tract which results in their achieving full fertilizing potential (for more information see chapter 1, page 19). Among the changes induced by the capacitation is the ability to acquire the correct motility patterns for reaching the fertilization site (where the oocyte lies), and to penetrate the egg vestments.

Protein phosphorylation reflects the balance between the enzymatic activities of phosphatases and kinases. After the ejaculation into the female tract, mammalian spermatozoa initiate flagellar beating, which is regulated by serine/threonine and tyrosine phosphorylation of flagellar proteins (Goto and Harayama, 2009). One of these proteins is dynein (Tash and Means, 1982, Tash and Bracho, 1994). Serine/threonine phosphorylation is regulated in part by the action on protein kinase A (PKA) of cAMP, which in turn may be activated by soluble adenylate cyclase (Darszon et al., 2006). This enzyme is regulated by $HCO3^-$ and Ca^{2+}, suggesting that mechanisms that control the inward fluxes of these ions at the plasma membrane are involved. Sperm hyperactivation is also regulated by serine/threonine protein phosphatases (Suzuki et al., 2010).

There is a lack of information about the possible role of Cl^- channels in human sperm motility. A previous report has shown that the anion channel blocker DIDS at 100 µM did not affect sperm motility in hamster, whereas at 1 mM there was a decrease in velocity and increase in the curvature radius of the flagellum but not in percentage of motile cells (Visconti et al., 1990). The same study reported that 200 µM DIDS inhibited cAMP

accumulation induced by an activator of PKC in capacitated cells, but 1 mM DIDS failed to do so (Visconti et al., 1990). The authors concluded that the effect of DIDS on cAMP is due to alteration of HCO_3^- transport (HCO_3^- / Cl^- exchanger) required for capacitation rather than inhibition of adenylate cyclase *per se* (Visconti et al., 1990). A second study reported that 100 µM DIDS (EC_{50}) inhibited spontaneous acrosome reaction in hamster sperm (50% at 8h of incubation); reaching maximum inhibition at 600 µM (Visconti et al., 1999d). However, no effect on motility was observed (Visconti et al., 1999d). At 600 µM the levels of cAMP were significantly lower, suggesting that HCO_3^- modulates sperm cAMP metabolism through a DIDS sensitive mechanism (Visconti et al., 1999d). Another group described that 25 µM DIDS had no direct effect on adenylate cyclase activity of pig sperm (Tajima and Okamura, 1990); reaching the same conclusion that HCO_3^- was the main factor involved. However, in this study they reported that DIDS + HCO_3^- enhanced motility, respiration rate and the cAMP content to a greater extent than HCO_3^- alone (Tajima and Okamura, 1990).

The Cl^- channel blocker NPPB (50 µM) did not impair motility in mouse sperm, but increased the number of kinked tails (Yeung et al., 1999); such effect was attributed to failure in RVD. There is another study reporting that niflumic acid (10-20 µM) increased flagellar bending in response to speract (an egg-derived sperm-activating peptide) in sea urchin (Wood et al., 2007). Moreover, the drug augmented the amplitude and duration of Ca^{2+} increases in the flagella that are associated to such bending (Wood et al., 2007). In spite of these reports, it is far from clear how such chemicals modify the motility parameters of human spermatozoa.

The goals of the work reported in this chapter were to evaluate the effect of different Cl^- channel blockers –DIDS, NPPB, and niflumic acid– on human sperm motility at different

ranges of osmolality.

2.3. Materials and Methods

2.3.1 Materials

The chloride blockers 4,4′-Diisothiocyanatostilbene-2,2′-disulfonic acid disodium salt hydrate **(**DIDS), 5-Nitro-2-(3-phenylpropylamino)benzoic acid **(**NPPB**)** and niflumic acid; dimethyl sulfoxide (DMSO), Percoll, chemicals to prepare M medium, sodium dodecyl sulphate (SDS), TBS and sodium dodecyl sulphate polyacrylamide gel electrophoresis (SDS-PAGE), and salts used to prepare supplemented Earle's Balanced Salt Solution (EBSS) were all purchased from Sigma Aldrich (Dorset, UK). Fatty-acid free bovine serum albumin (BSA) was purchased from SAFC Biosciences (Lenexa, KS, USA). Nitrocellulose membrane was supplied by GE Healthcare UK Ltd. (St. Giles, Bucks, UK). Serine–threonine phosphatase inhibitors calyculin A and okadaic acid were purchased from New England Biolabs (Hitchin, Hertfordshire, UK) and Calbiochem (Merck Biosciences, Beeston, Nottingham, UK), respectively. Phospho-serine/threonine PKA substrate antibody was obtained from New England Biolabs (Hitchin, Hertfordshire, UK). Secondary antibody conjugated with horseradish peroxidase was purchased from Jackson ImmunoResearch Laboratories (Stratech Scientific, Soham, Cambridgeshire, UK). Lumi-GLO, an enhanced chemiluminescence kit, was purchased from Insight Biotechnology Ltd. (Wembley, Middlesex, UK). The Silver Stain Plus was supplied by Bio-Rad Laboratories Ltd. (Hempstead, Hertfordshire, UK). All chemicals were cell culture-tested grade where available. Osmolalities were determined with an Osmometer 3MO Plus (Advanced Instruments, Norwood, MA, USA).

2.3.2 Preparation of spermatozoa

All donors were recruited at the Birmingham Women's Hospital (HFEA Centre #0119), and the School of Biosciences of the University of Birmingham in accordance with the Human Fertilisation and Embryology Authority Code of Practice. Only normal samples in accordance with the World Health Organization guidelines were selected (WHO, 1999). Approval was obtained from the Local Ethical Committee (#0472, #5570) and all donors gave informed consent. Semen was collected by masturbation and after semen liquefaction for approximately 30 min; motile sperm was harvested by swim-up (Mortimer, 1994). Under this method 1 ml of sEBSS [NaCl (116.4 mM), KCl (5.4 mM), $CaCl_2$ (1.8 mM), $MgCl_2$ (1 mM), glucose (5.5 mM), $NaHCO_3$ (25 mM), Na pyruvate (2.5 mM), Na lactate (19 mM), $MgSO_4$ (0.81 mM) and 0.3% BSA, pH 7.4], adjusted at pH 7.3-7.4, was underlayered with 0.3 ml of liquefied sample in polystyrene Falcon round-bottom tubes (Becton Dickinson, USA). After 1 hour of incubation at 37°C, 5% CO2 and at an angle of 45° (to maximize yield), the top layer of each tube, containing the motile cells, was collected into a 15 ml polystyrene Falcon tube (Becton Dickinson, USA). Sperm concentration was determined using a Neubauer counting chamber in accordance with the World Health Organization methods (WHO, 1999). Cells were then concentrated to 2-3 million/ml and prepared for the assays with sEBSS as described previously (Kirkman-Brown et al., 2000). For the western blotting, semen was layered over 1 ml fractions of 45% and 90% Percoll (made isotonic with M medium; see Appendix I for details). Samples were then centrifuged at 2000 g for 20 minutes, and the concentration of spermatozoa was calculated using the Neubauer chamber. Percoll-washed sperm were further washed with PBS to eliminate Percoll. Cells were then transferred to the tubes for the experiments.

2.3.3 Sperm motility

Motile spermatozoa were selected through a swim up gradient as described before. The sperm concentration and motility were determined using a CASA machine (Computer Assisted Semen Analysis, Hamilton Thorne, Beverly, USA). Only the percentage of forward progressives sperm (a + b) was taken into account. Experiments were carried out by incubating 100 µl of motile spermatozoa at 37ºC (5 % CO_2), in the presence and absence of 10, 50, 100 and 400 µM DIDS, 100 µM NPPB, 200 µM niflumic acid, (inhibitors of chloride channels). Motility parameters were determined loading 6 µL of sample into a disposable 2 cell (3 µL in each cell) MicroCell counting chamber of 20 microns depth (Conception Technologies, San Diego, USA), then the chamber was placed inside the CASA machine for determination of the different motility values. Readings were obtained at 30 and 60 minutes after incubation with the different Cl^- channel blockers. The media were adjusted at osmolalities of 295, 270 and 200 mOsm. Despite 200 mOsm is a non physiological condition, it was chosen in order to mimick the HOS (hyposmotic shock) test for sperm vitality used in fertility clinics. During HOS test sperm is incubated with a solution at 150 mmol/kg (WHO, 1999). Swelling of the tail indicates intact membranes or living sperm, whereas dead cells retain their normal tail shape because of leaky membranes (Cooper and Yeung, 2000). Kinematic parameters included progressive velocity: distance between the first and the last track points; track velocity: the time-averaged velocity obtained from distances between two consecutive track points (a measure of cell vigour); mean path velocity (VAP): the time-averaged velocity obtained from smoothing the original path which joined up consecutive track points, using a 5-point running average; beat cross frequency (BCF): average rate at which the curvilinear path crosses the average path; linearity (LIN): the linearity of a curvilinear path (progressive velocity/track velocity); straightness: linearity of the average path (progressive velocity/VAP); amplitude of lateral head displacement (ALH) of the head:

the width of head oscillation measured as twice the maximum value of the distance of any point on the original track from the corresponding 5-point average (Mortimer and Mortimer, 1990, Yeung et al., 1992).

2.3.4 Immunodetection of proteins by Western blot

Detection of serine/threonine phosphorylation of proteins was performed according to the protocol of Lefièvre et al (Bedu-Addo et al., 2005, Lefievre et al., 2007a). Briefly, percoll-washed sperm samples were aliquoted in the following conditions: A) non capacitating EBSS (with no HCO_3); B) capacitating EBSS (with HCO_3); C) capacitating EBSS + 10 µM DIDS; D) capacitating EBSS + 50 µM DIDS; E) capacitating EBSS + 100 µM DIDS; F) capacitating EBSS + 400 µM DIDS. The total sperm concentration was 2 million sperm/ eppendorf tube. The samples were incubated for 30 min at 37ºC (5 % CO_2) before the addition of solubilization buffer. Solubilization buffer contained (final concentration): 2% (w/v) sodium dodecyl sulphate (SDS), 10% glycerol (v/v), 1.4% dithiothreitol (DTT) (w/v), 62.5 mM Tris–HCl pH 6.8, 0.1 mM vanadate, 10 nM okadaic acid, and 50 nM calyculin A. Samples were then boiled at 100°C for 5 min, sonicated and centrifuged at 14 000 *g* for 5 min. Proteins were separated by electrophoresis on SDS–polyacrylamide gel electrophoresis (SDS–PAGE) (12%) gels (Laemmli, 1970) and electrotransferred (Towbin et al., 1979) onto nitrocellulose membrane. Non-specific binding sites on the nitrocellulose membrane were blocked with 5% (w/v) dry skim milk in Tris-buffered saline (0.9% NaCl (w/v), 20 mM Tris–HCl, pH 7.8) supplemented with 0.1 % (v/v) Tween-20 (TTBS) for the detection of phosphoserine/threonine proteins. The nitrocellulose membranes were incubated overnight at 4°C or for 1 h at room temperature with the antiphosphoserine/threonine PKA substrate antibody (1:1000). The membranes were then extensively washed with TTBS, incubated with

the secondary antibody conjugated with horseradish peroxidase (1:10000) for 1 h and again extensively washed with TTBS. Positive immunoreactive bands were detected by chemiluminescence using LumiGLO, an enhanced chemiluminescence kit, according to the manufacturer's instructions. Silver staining of the proteins transferred on the nitrocellulose membrane was performed after the detection to confirm that the transferred protein patterns were similar for all samples (Jacobson and Karsnas, 1990). These experiments were made in collaboration with Dr. Linda Lefièvre.

2.3.5 Statistical Analysis

Statistics was performed with the software OriginPro 8 Student Version (Origin Lab Corporation, Northampton, MA, USA). The results are expressed as mean ± standard error for the number of indicated assays in each case. The standard errors of the differences were calculated for paired data. Data analysis was performed with Student's Test for paired data, "*n*" being the number of repeated assays with different preparations. Only probabilities < 0.05 were accepted as significant.

2.4 Results

2.4.1 Effect of Cl^- channel blockers on human sperm motility at 295 mOsm

With few exceptions, Cl^- channel blockers are rather inespecific and have a low potency, with effective concentrations in the range of micromolar to even milimorar. The low specificity for individual ion channels is compounded by side effects of these substances, mainly on ion transporters and components of intracellular signaling pathways (Jentsch et al., 2002). The effect of DIDS (10, 50, 100 and 400 µM), NPPB (100 µM) and niflumic acid (200 µM) in

motility after 30 and 60 min of incubation, were tested on cells exposed to media with osmolality of 295 mOsm. These drugs had never been tested in human sperm motility, but a previous work reported that 400 µM DIDS and 100 µM NPPB were able to induce cell swelling in human sperm (Yeung et al., 2005). In the same study 200 µM niflumic acid rather than increasing cell size produced cell shrinkage (Yeung et al., 2005). According to the authors the drugs only produced changes in cell size at these concentrations. Based upon these findings I decided to use the same range of drug concentrations plus lower doses of DIDS (10 and 50 µM) to evaluate the effect on motility. DIDS is an irreversible blocker in contrast with NPPB and niflumic acid wich are reversible (Jentsch et al., 2002). The reversibility of the effects caused by the different drugs couldn't be tested since it implied further centrifugations of the samples, which are detrimental to sperm's integrity and motility, with loss of cells during the washing. Readings were obtained at 30 and 60 minutes after incubation with the different Cl^- channel blockers (time needed to analyse the kinematic characteristics of the cells between each experiment). DMSO was used as a vehicle to prepare all the chemicals employed in the experiments and was present in every control condition (0.2% for NPPB and niflumic acid and 0.5% for DIDS).

The data reported here show that 10 µM DIDS did not modify the sperm motility neither at 30 min (79.5 ± 4.2 vs 72.5 ± 9.6 SEM) nor at 60 min (82.3 ± 4.2 vs 75.5 ± 10.2 SEM) (figure 2.1.A). On the other hand 50 and 100 µM DIDS reduced motility significantly ($P < 0.05$) after 30 (90.5 ± 2.5 vs 46.1 ± 7.6 SEM for 50 µM DIDS, and 79.8 ± 7.5 vs 37 ± 11.3 SEM for 100 µM DIDS) and 60 min of incubation (93.6 ± 0.8 vs 57.8 ± 10 SEM for 50 µM DIDS, and 87.5 ± 4.2 vs 44.8 ± 11.3 SEM for 100 µM DIDS) (figures 2.1.D and 2.2.A), whereas 400 µM DIDS abolished the human sperm motility (91.6 ± 3.4 vs 0.5 ± 0.5 SEM at 30 min, and 86.5 ± 3.9 vs 0 ± 0 SEM at 60 min) ($P < 0.001$) (figure 2.2.D). Both NPPB (82.6 ± 4 vs 79.3

± 4.6 SEM at 30 min, and 82.6 ± 3.4 vs 75 ± 5.3 SEM at 60 min) and niflumic acid (82.3 ± 5.9 vs 76.3 ± 8.6 SEM at 30 min, and 80.3 ± 3.8 vs 82.5 ± 5.4 SEM at 60 min) failed to exert any significant effect (figures 2.3.A and 2.4.A).

With regards to the motility parameters at 30 min (table 1.1), 10 µM DIDS reduced the progressive velocity, track velocity, linearity and mean path velocity; 50 µM DIDS affected progressive velocity, straightness, track velocity, linearity, mean path velocity and lateral head displacement; 100 µM DIDS reduced the progressive velocity, track velocity, linearity and mean path velocity, and 400 µM DIDS reduced all the parameters significantly. NPPB (100 µM) just affected beat cross frequency, and niflumic acid (200 µM) altered progressive velocity, track velocity and mean path velocity. At 60 min (table 1.2), 10 µM DIDS reduced the progressive velocity, track velocity, and mean path velocity significantly; 50 µM DIDS affected progressive velocity, track velocity, linearity, and mean path velocity; 100 µM DIDS reduced the progressive velocity, track velocity, and mean path velocity, and 400 µM DIDS completely reduced all the parameters. NPPB (100 µM) inhibited progressive velocity, linearity and mean path velocity, and niflumic acid (200 µM) altered progressive velocity, track velocity, straightness, linearity, and mean path velocity.

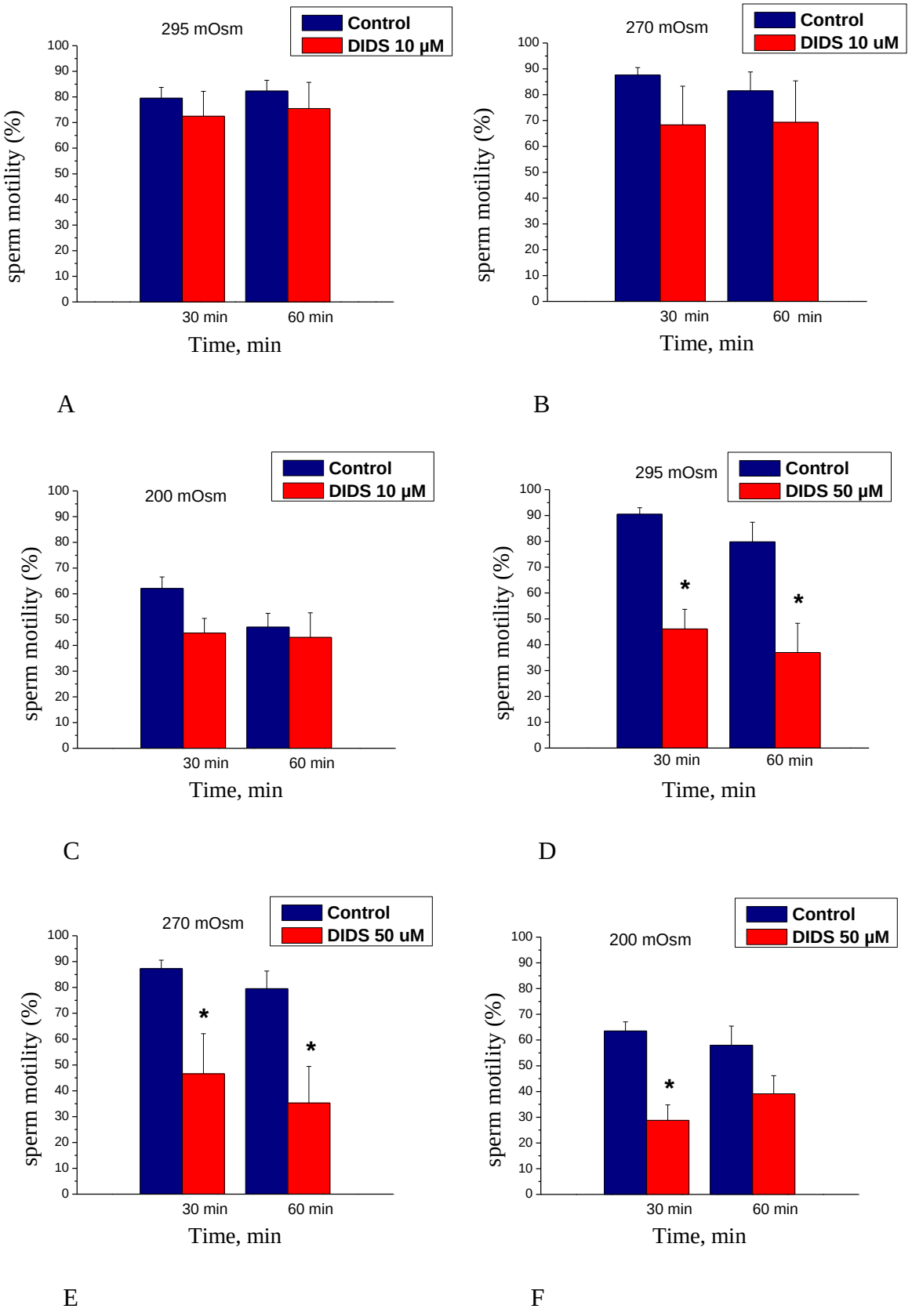

Figure 2.1: Effect of 10 and 50 µM DIDS in human sperm motility under different

osmotic conditions. The graphs represent 10 µM DIDS at 295 mOsm (A), 270 mOsm (B), 200 mOsm (C); and 50 µM DIDS at 295 mOsm (D), 270 mOsm (E), and 200 mOsm (F). Cell samples were prepared with sEBSS (295, 270 and 200 mOsm) and incubated for 30 and 60 min with the drug. Values expressed as mean ± SEM (n=6 experiments).

2.4.2 Effect of Cl^- channels blockers on human sperm motility at 270 mOsm

The data show that 10 µM DIDS did not modify the sperm motility (87.6 ± 2.9 vs 68.3 ± 15 SEM at 30 min, and 81.5 ± 7.3 vs 69.3 ± 16 SEM at 60 min) (figure 2.1.B). On the other hand, 50 µM DIDS (87.3 ± 3.2 vs 46.6 ± 15.4 SEM at 30 min, and 79.5.3 ± 6.8 vs 35.3 ± 14.1 SEM at 60 min) and 100 µM DIDS (94.1 ± 1.4 vs 75 ± 5.6 SEM at 30 min, and 92.5 ± 2.1 vs 78.1 ± 6.5 SEM at 60 min) reduced motility significantly ($P < 0.05$) after 30 and 60 min of incubation (figures 2.1.E and 2.2.B), whereas 400 µM DIDS (76.1 ± 6 vs 0 ± 0 SEM at 30 min, and 69.6 ± 5 vs 0 ± 0 SEM at 60 min) abolished the human sperm motility ($P < 0.001$) (figure 2.2.E). Both NPPB (70.5 ± 4.7 vs 68.5 ± 6.7 SEM at 30 min, and 68 ± 8.3 vs 67 ± 7.1 SEM at 60 min) and niflumic acid (76 ± 5 vs 69.6 ± 6.6 SEM at 30 min, and 77 ± 6.5 vs 62.1 ± 8.3 SEM at 60 min) did not exert any significant effect (figures 2.3.B and 2.4.B).

With regards to the motility parameters at 30 min (table 1.3) only 400 µM DIDS reduced all the parameters significantly, the rest of the concentrations of DIDS used and NPPB and Niflumic Acid did not alter any parameter. At 60 min (table 1.4) the same inhibition by 400 µM DIDS was observed. In addition, niflumic acid reduced significantly the beat cross frequency and increased the lateral head displacement when compared with the controls.

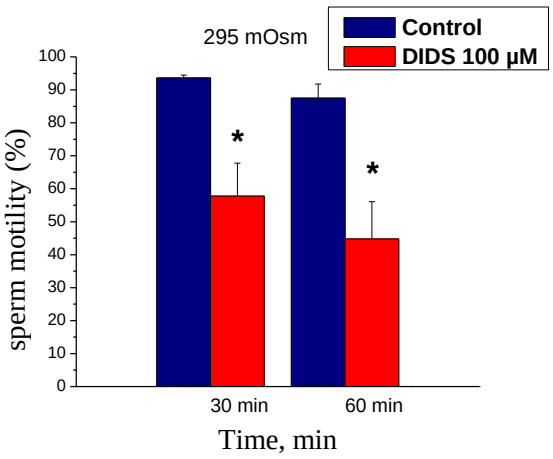
295 mOsm
Control
DIDS 100 µM
sperm motility (%)
Time, min
30 min
60 min
*
*

A

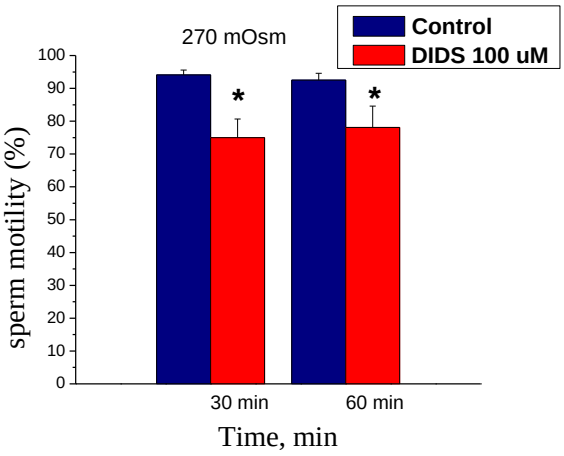
270 mOsm
Control
DIDS 100 uM
sperm motility (%)
Time, min
30 min
60 min
*
*

B

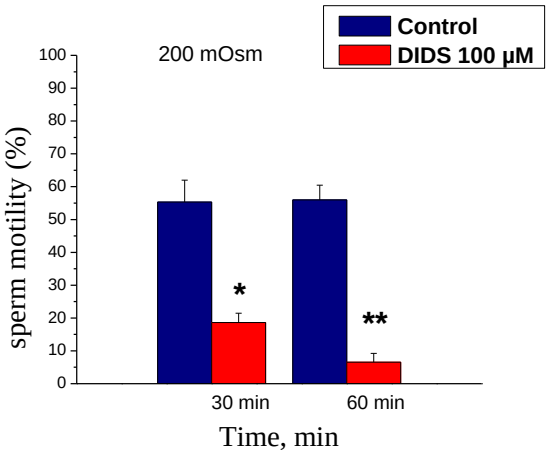
200 mOsm
Control
DIDS 100 µM
sperm motility (%)
Time, min
30 min
60 min
*
**

C

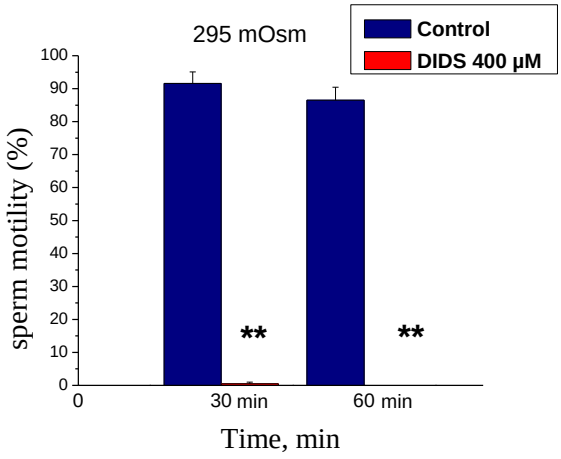
295 mOsm
Control
DIDS 400 µM
sperm motility (%)
Time, min
30 min
60 min
**
**

D

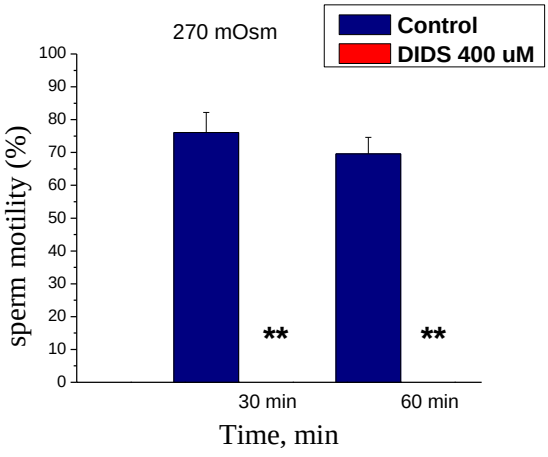
270 mOsm
Control
DIDS 400 uM
sperm motility (%)
Time, min
30 min
60 min
**
**

E

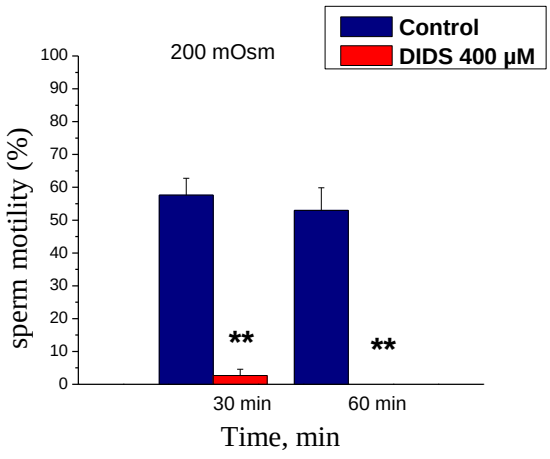
200 mOsm
Control
DIDS 400 µM
sperm motility (%)
Time, min
30 min
60 min
**
**

F

Figure 2.2: Effect of 100 and 400 µM DIDS in human sperm motility under different osmotic conditions. The graphs represent 100 µM DIDS at 295 mOsm (A), 270 mOsm (B), 200 mOsm (C); and 400 µM DIDS at 295 mOsm (D), 270 mOsm (E), and 200 mOsm (F). Cell samples were prepared with sEBSS (295, 270 and 200 mOsm) and incubated for 30 and 60 min with the drug. Values expressed as mean ± SEM (n=6 experiments).

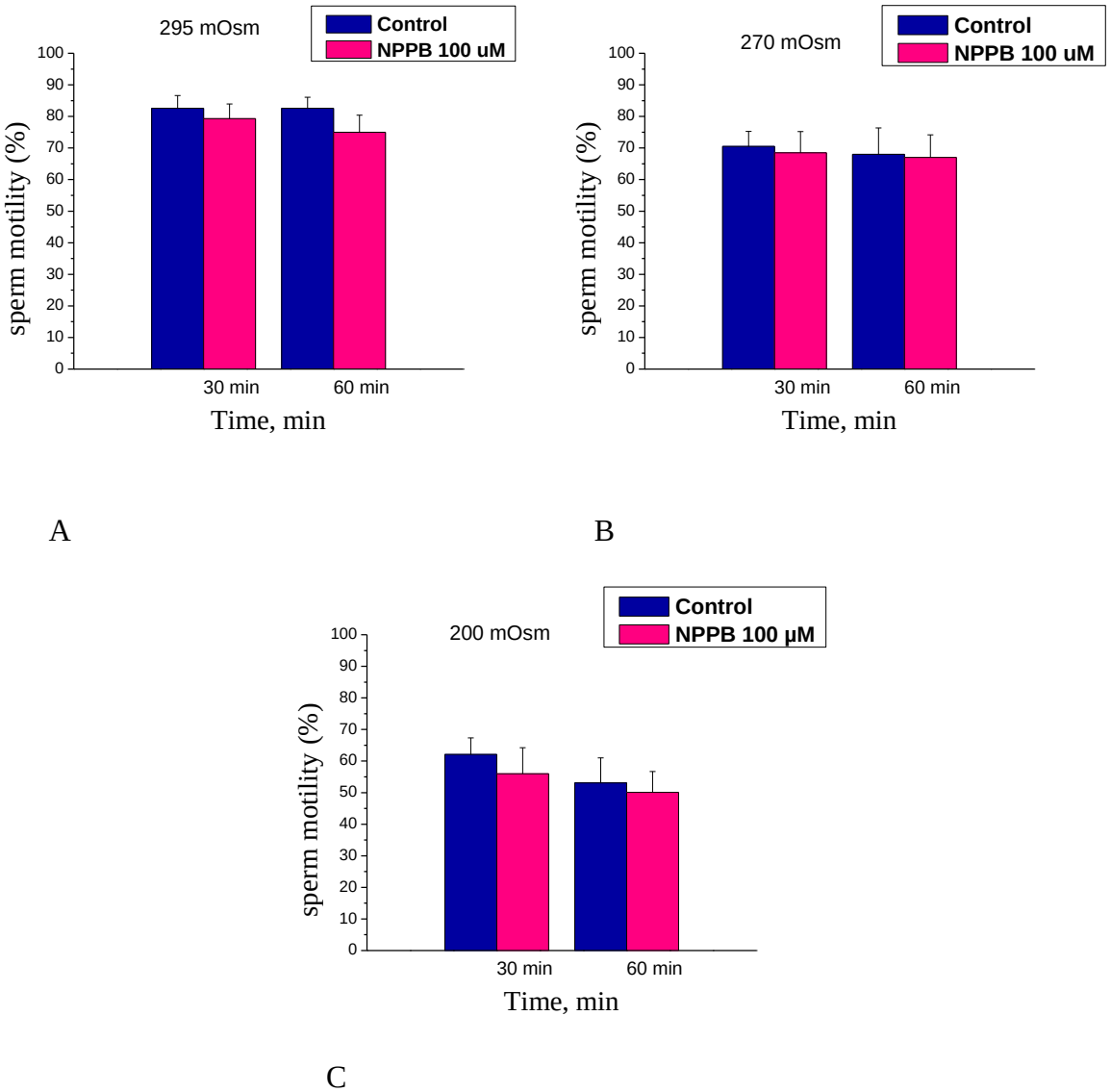

Figure 2.3: Effect of 100 µM NPPB in human sperm motility under different osmotic conditions. The graphs represent 100 µM NPPB at 295 mOsm (A), 270 mOsm (B), 200 mOsm (C). Cell samples were prepared with sEBSS (295, 270 and 200 mOsm) and incubated

for 30 and 60 min with the drug. Values expressed as mean ± SEM (n=6 experiments).

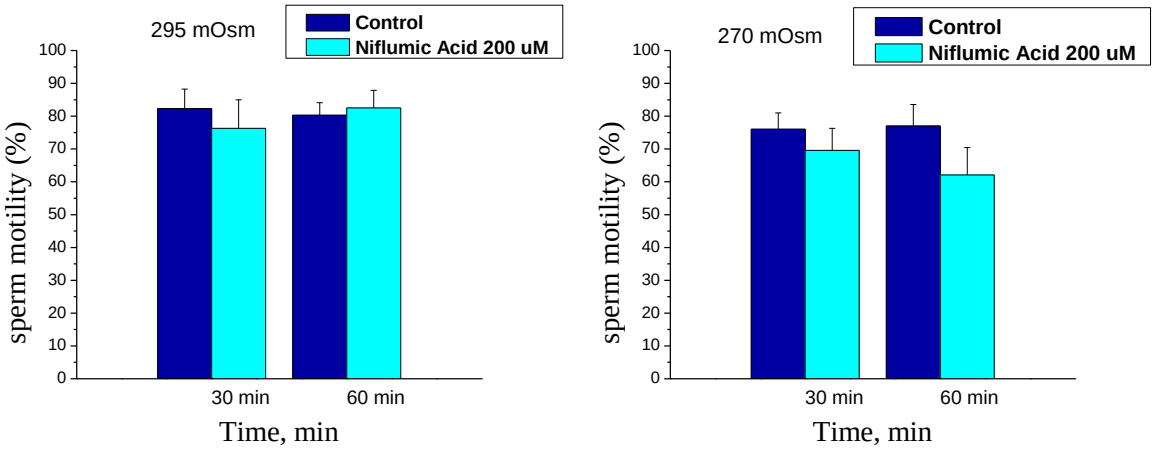

A B

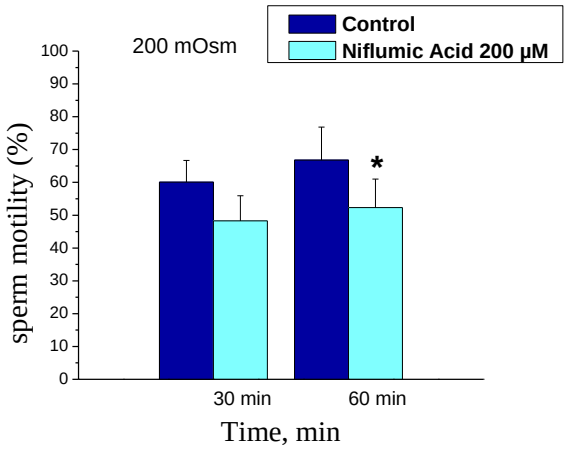

C

Figure 2.4: Effect of 200 µM Niflumic Acid in human sperm motility under different osmotic conditions. The graphs represent 200 µM niflumic acid at 295 mOsm (A), 270 mOsm (B), 200 mOsm (C). Cell samples were prepared with sEBSS (295,270 and 200 mOsm) and incubated for 30 and 60 min with the drug. Values expressed as mean ± SEM (n=6 experiments).

Condition	Progress Velocity	Track Velocity	BCF	Straight	LIN	VAP	ALH
Control	**70.4 ± 6.9**	**114.6 ± 8.2**	**29.9 ± 2.4**	**90.3 ± 1.2**	**61.6 ± 2.4**	**76.6 ± 6.7**	**4.2 ± 0.2**
10 µM DIDS	**48.9 ± 5.4***	**87.8 ± 6.8***	**28.5 ± 1.6**	**87 ± 1.6**	**53.5± 2.7***	**54.2 ± 5.4***	**4.1 ± 0.1**
Control	**67.6 ± 7**	**113.2 ± 8.2**	**30.3 ± 2.2**	**88.5 ± 1.6**	**59.8 ± 3**	**74.2 ± 6.7**	**4.2±0.3**
50 µM DIDS	**29 ± 4.7***	**61.2 ± 5****	**29.6 ± 1.4**	**81.5± 2.3***	**45.3 ±3.7***	**34.1±4.3****	**3.3± 0.2***
Control	**66.7 ± 4.7**	**108.1 ± 5**	**29 ± 2.5**	**90.3 ± 1.4**	**62 ± 2.8**	**72.6 ± 4.3**	**4 ± 0.2**
100 µM DIDS	**35.6 ± 6.1***	**68.7 ± 7.2***	**28.3 ± 2.5**	**83.1 ± 2.8**	**49.1± 3.8***	**34 ± 9***	**2.3 ± 0.7**
Control	**69.1 ± 5**	**110.4 ± 7.3**	**30.2 ± 2.5**	**90.6 ± 1**	**62.3 ± 2.4**	**74.8 ± 5.1**	**4 ± 0.3**
400 µM DIDS	**3.2 ± 3.2****	**4.6 ± 4.6****	**5 ± 5***	**14.8±14.8 ***	**11.6±11.6 ***	**3.6± 3.6****	**0****
Control	**59.7 ± 5.8**	**101.5 ± 8.2**	**28.3 ± 1.9**	**89.1 ± 1**	**57.6 ± 1.7**	**65.5 ± 5.9**	**4.2 ± 0.2**
100 µM NPPB	**56.1 ± 4.7**	**97.8 ± 4.8**	**30.4± 1.6***	**88 ± 1.3**	**56.3 ± 2.3**	**61.9 ± 4.3**	**4.2 ± 0.1**
Control	**64.8 ± 5.6**	**106.9 ± 8.3**	**28.5 ± 2**	**90.1 ± 0.7**	**60.6 ± 1.7**	**70.7 ± 5.7**	**4.2 ± 0.3**
200 µM Niflumic Acid	**55.2 ± 5.9***	**98.1 ± 7.3***	**26.6 ± 2.1**	**87.5 ± 1.7**	**55.8 ± 2.5**	**61.5 ± 5.7***	**4.4 ± 0.1**

Table 1.1: Motility parameters at 30 min at 295 mOsm (BCF: beat cross frequency; Straight: Straightness; LIN: Linearity; VAP: mean path velocity; ALH: lateral head displacement). Significant values are coloured in dark red. Values expressed as mean ± SEM (n=6 experiments).

* $P < 0.05$ vs control

** $P < 0.001$ vs control

Condition	Progress Velocity	Track Velocity	BCF	Straight	LIN	VAP	ALH
Control	**68.5 ± 9**	**113 ± 12.8**	**29.4 ±2.2**	**90.3 ± 1.1**	**60.3 ± 2.6**	**70.4 ± 9.3**	**4.4 ± 0.4**
10 µM DIDS	**47.5 ± 9.9***	**87.3±11.7***	**28.4 ±2.3**	**83.8 ± 2.8**	**50.8 ± 4.6**	**54 ± 9.8***	**4 ± 0.1**
Control	**65.1 ± 8.2**	**109.4±10.6**	**27.4 ± 2.5**	**88.5 ± 1.6**	**58.5 ± 2.5**	**71.5 ± 8.1**	**4.3 ± 0.2**
50 µM DIDS	**25.2 ± 5.3***	**55.7 ± 7.6***	**26.4 ± 2.4**	**82.8 ± 2.3**	**44.8± 2.1***	**29.8± 5.4***	**3.3 ± 0.8**
Control	**61.5 ± 8.8**	**103.7 ± 10**	**26.3 ± 2.4**	**89.1 ± 2.1**	**58.5 ± 3.8**	**75.3 ± 6.2**	**4.3 ± 0.3**
100 µM DIDS	**25.9 ± 9.6***	**48.8±17.8***	**17.7 ± 6**	**59.3± 18.7**	**35.8± 11.5**	**28.7±10.5***	**2.5 ± 0.8**
Control	**59.3 ± 7,4**	**93.5 ± 10.6**	**30.3 ± 1.9**	**91.3 ± 1.8**	**64.1 ± 6.9**	**63.7 ± 7.6**	**3.4 ± 0.5**
400 µM DIDS	**0****	**0****	**0****	**0****	**0****	**0****	**0****
Control	**67.8 ± 6.1**	**112 ± 8.6**	**31.1 ± 1.9**	**90.1 ± 0.9**	**60.3 ± 1.6**	**73.7 ± 6.2**	**4.2 ± 0.2**
100 µM NPPB	**59.4 ± 5.1***	**104± 5.2**	**29.8 ± 1.2**	**89.5 ± 1.2**	**56.5 ± 2***	**65 ± 4.8***	**4.5 ± 0.1**
Control	**70.1 ± 4.9**	**115.2 ± 7.1**	**31.5 ± 1.6**	**90.5 ± 1**	**61 ± 1.5**	**76 ± 4.9**	**4.3 ± 0.2**
200 µM Niflumic Acid	**53.3 ± 5.5***	**97.5 ± 5.6***	**26.3 ± 2.1**	**86.8± 1.6***	**54.3± 2.6***	**60.1± 5.1***	**4.4 ± 0.1**

Table 1.2: Motility parameters at 60 min at 295 mOsm (BCF: beat cross frequency; Straight: Straightness; LIN: Linearity; VAP: mean path velocity; ALH: lateral head displacement). Significant values are coloured in dark red. Values expressed as mean ± SEM (n=6 experiments).

* $P < 0.05$ vs control

** $P < 0.001$ vs control

Condition	Progress Velocity	Track Velocity	BCF	Straight	LIN	VAP	ALH
Control	**59.9 ± 6.9**	**99.4 ± 7.1**	**27.7 ± 2.3**	**89.3 ± 1.9**	**59.1 ± 3.9**	**66 ± 6**	**4. ± 0.2**
10 µM DIDS	**59.9 ± 12.8**	**103.6±21.8**	**24.6 ± 5**	**74.1±14.9**	**49.1± 10.3**	**63.3 ± 13.9**	**3.9 ± 0.8**
Control	**59.8 ± 7.3**	**103.6±11.4**	**27.1 ± 3.1**	**88.1± 2.2**	**57.5 ± 2.8**	**68.7 ± 7.2**	**4.3 ± 0.4**
50 µM DIDS	**41.2 ± 14.1**	**77.9 ±21.8**	**28.3 ± 7**	**70.1 ±14.2**	**41.3 ± 9.6**	**50.7 ± 15.6**	**3.2 ± 1**
Control	**52.1 ± 7.1**	**100.2±10.2**	**26.2 ± 2.3**	**84 ± 4.4**	**50.6 ± 4.8**	**62.2 ± 6.4**	**4.3 ± 0.5**
100 µM DIDS	**48.2 ± 9.6**	**90.6 ±13.8**	**25 ± 2.3**	**83.3 ± 4.2**	**51.6 ± 3.6**	**50.1± 12.8**	**3.4 ± 0.7**
Control	**57.5 ± 1.8**	**94.7 ± 3.8**	**31.3 ± 2.1**	**89.3 ± 0.6**	**59.8 ± 1.4**	**62.7 ± 2**	**3.7 ± 0.2**
400 µM DIDS	**0****	**0****	**0****	**0****	**0****	**0****	**0****
Control	**52.9 ± 2.4**	**88.2 ± 2.8**	**32.3 ± 1.9**	**87.8 ± 1.8**	**58 ± 1.8**	**56.5 ± 2.2**	**3.7 ± 0.1**
100 µM NPPB	**50.3 ± 2.2**	**87.8 ± 3.5**	**30.5 ± 1.4**	**88.8 ± 0.7**	**55.3 ± 1.3**	**54.1 ± 2.4**	**3.9 ± 0.1**
Control	**56.3 ± 4.4**	**91.1 ± 4.5**	**30 ± 1.9**	**89.8 ± 1.1**	**59.6 ± 2.4**	**60.8 ± 4.2**	**3.7 ± 0**
200 µM Niflumic Acid	**41.8 ± 2.4**	**74.6 ± 4.4**	**26.5 ± 1.9**	**86 ± 0.7**	**53.1 ± 0.9**	**41.2 ± 5.4**	**3.9 ± 0.2**

Table 1.3: Motility parameters at 30 min at 270 mOsm (BCF: beat cross frequency; Straight: Straightness; LIN: Linearity; VAP: mean path velocity; ALH: lateral head displacement). Significant values are coloured in dark red. Values expressed as mean ± SEM (n=6 experiments).

* $P < 0.05$ vs control

** $P < 0.001$ vs control

Condition	Progress Velocity	Track Velocity	BCF	Straight	LIN	VAP	ALH
Control	**59.5 ± 6.2**	**100.3 ± 8.1**	**28.2 ±1.8**	**89 ± 1.5**	**57.8 ± 2.4**	**65.1 ± 6.2**	**4.1 ± 0.2**
10 µM DIDS	**56.6 ± 13.4**	**100 ± 22 .1**	**23.3 ±4.7**	**73 ± 14.6**	**46.6± 9.7**	**62.9 ± 14.6**	**4.1 ± 0.8**
Control	**59.2 ± 7**	**100.3±10.2**	**28.8 ± 1.5**	**88.5 ± 1.3**	**58.1 ± 2.6**	**65.2 ± 7.2**	**4 ± 0.3**
50 µM DIDS	**40.7 ± 13.4**	**76.7 ± 20.8**	**23.3 ± 5.1**	**68.5± 13.9**	**42.5 ± 9.2**	**47.1 ± 14.1**	**3.4 ± 0.7**
Control	**57.2 ± 8.4**	**101.2 ± 8**	**27.5 ± 2.2**	**85.6 ± 4.4**	**55.1 ± 5.2**	**64.3 ± 7.3**	**4.3 ± 0.3**
100 µM DIDS	**44 ± 10.4**	**78.7 ± 17**	**23.2 ± 4.9**	**71.5± 14.4**	**45.1 ± 9.6**	**49.4 ± 11.1**	**3.5 ± 0.7**
Control	**59.7 ± 4.2**	**95.6 ± 3.8**	**31.6 ± 1.8**	**90.3 ± 0.8**	**60 ± 2.4**	**64.2 ± 4.2**	**3.8 ± 0.1**
400 µM DIDS	**0****	**0****	**0****	**0****	**0****	**0****	**0****
Control	**51.7 ± 6**	**86.8 ± 5.7**	**32.3 ± 2**	**89.3 ± 1.3**	**58.6 ± 3.4**	**57.7 ± 5.9**	**3.6 ± 0.1**
NPPB	**51.8 ± 4.1**	**88.1 ± 5.2**	**31. 5 ± 1.1**	**88.8 ± 0.9**	**57 ± 2**	**56.7 ±**	**3.7 ± 0.2**
Control	**53.1 ± 5.6**	**86.6 ± 4.7**	**31.3 ± 1.5**	**88 ± 1.9**	**59.5 ± 3.8**	**57.4 ± 5.3**	**3.5 ± 0.1**
Niflumic	**39.5 ± 2.3**	**78.7 ± 4.6**	**26.8±1.7***	**85.5 ± 0.8**	**51 ± 1.1**	**47 ± 3.2**	**3.9± 0.1***

Table 1.4: Motility parameters at 60 min at 270 mOsm (BCF: beat cross frequency; Straight: Straightness; LIN: Linearity; VAP: mean path velocity; ALH: lateral head displacement). Significant values are coloured in dark red. Values expressed as mean ± SEM (n=6 experiments).

* P < 0.05 vs control

** P < 0.001 vs control

2.4.3 Effect of Cl^- channel blockers on human sperm motility at 200 mOsm

The data show that 10 µM DIDS (62.1 ± 4.4 vs 44.8 ± 5.6 SEM at 30 min, and 47.1 ± 5.3 vs 43.1 ± 9.5 SEM at 60 min) did not modify the sperm motility (figure 2.1.C). On the other hand 50 DIDS (63.5 ± 3.5 vs 28.8 ± 5.9 SEM at 30 min, and 58 ± 7.4 vs 39.1 ± 7 SEM at 60

min) reduced motility significantly (P< 0.05) at 30 min only (figure 2.1.F). 100 µM DIDS inhibited sperm motility at 30 min (55.3 ± 6.6 vs 18.6 ± 2.8 SEM) (P < 0.05) and 60 min (56 ± 4.4 vs 12 ± 2.6 SEM) (P < 0.001) (figure 2.2.C), whereas 400 µM DIDS (57.6 ± 5.1 vs 2.6 ± 1.9 SEM at 30 min, and 53 ± 6.8 vs 0 ± 0 SEM at 60 min) almost abolished the motility (P < 0.001) (figure 2.2.F). Incubation with NPPB (62.1 ± 5.2 vs 56 ± 8.2 SEM at 30 min, and 53.1 ± 7.8 vs 50.1 ± 6.6 SEM at 60 min) did not produce any significant change (figure 2.3.C), but niflumic acid (60.1 ± 6.5 vs 48.3 ± 7.6 SEM at 30 min, and 66.8 ± 10.7 vs 52.3 ± 8.7 SEM at 60 min) decreased the sperm motility at 60 min (P < 0.05) (Figure 2.4.C).

With regards to the motility parameters at 30 min (table 1.5), 50 µM DIDS affected track velocity; 100 µM DIDS reduced the progressive velocity, track velocity, linearity and mean path velocity, and 400 µM DIDS reduced all the parameters significantly. NPPB increased progressive velocity and mean path velocity, and reduced beat cross frequency. Niflumic Acid reduced track velocity, straightness, linearity, and mean path velocity. At 60 min (table 1.6), 50 µM DIDS reduced beat cross frequency and straightness, and 400 µM DIDS suppressed all the parameters. On the other hand, NPPB increased lateral head displacement.

Condition	Progress Velocity	Track Velocity	BCF	Straight	Lin	VAP	ALH
Control	**31.4 ± 2.2**	**69.6 ± 2.8**	**35.5 ± 1.6**	**86.1 ± 1**	**46 ± 1.2**	**35.7 ± 2.2**	**3 ± 0.2**
10 µM DIDS	**33.1 ± 4.5**	**68.1 ± 7**	**38.8 ± 2.2**	**87.6 ± 2.3**	**48.8 ± 2.8**	**36.9 ± 4.3**	**2.8 ± 0.2**
Control	**31.8 ± 2.7**	**70.4 ± 4.2**	**37.1 ± 1.8**	**85 ± 1.4**	**45.3 ± 1.7**	**36 ± 2.6**	**2.9 ± 0.1**
50 µM DIDS	**25.5 ± 2.9**	**53.3 ± 4.5***	**35.9 ± 2.8**	**85.3 ± 2.1**	**46 ± 1.2**	**28.7 ± 2.9**	**2.4 ± 0.1**
Control	**29.1 ± 1.5**	**62.1 ± 3.3**	**37.2 ± 1.4**	**87.5 ± 1**	**46.6 ± 1.5**	**32.5 ± 1.6**	**2.6 ± 0.1**
100 µM DIDS	**18.9 ± 1.3***	**42.5 ± 3.5***	**28.1 ± 6.6**	**88.3 ± 2.5**	**50.1 ± 5.6**	**21.3 ± 1.5***	**1.7± 0.3***
Control	**30.1 ± 2.4**	**68.4 ± 3.6**	**39.8 ± 0.5**	**86.5 ± 0.9**	**44.8 ± 2.7**	**34.2 ± 2.4**	**2.8 ± 0.2**
400 µM DIDS	**13.5 ± 6.5**	**26.2±12.8***	**19.4 ± 9**	**43.1± 19.3**	**25.6± 11.6**	**15 ± 7.2**	**1.2 ± 0.6**
Control	**31.5 ± 2.8**	**68.9 ± 3.1**	**38.1 ± 0.8**	**86.6 ± 1.7**	**46.1 ± 2.2**	**35.6 ± 2.6**	**3 ± 0.1**
100 µM NPPB	**36.9 ± 3.4***	**74 ± 4.5**	**35.8± 0.8***	**87.1 ± 1.1**	**49.3 ± 1.6**	**41.1± 3.3***	**3.1 ± 0.2**
Control	**36.3 ± 1.8**	**74.2 ± 1.9**	**38.9 ± 0.6**	**88.1 ± 1**	**48.3 ± 2.2**	**40.3 ± 1.8**	**3 ± 0.1**
200 µM Niflumic Acid	**21.9 ± 1.3**	**59 ± 2.1***	**36.3 ± 2.4**	**81.1 ± 1***	**39.5± 1.9***	**26.7± 1.5***	**2.8 ± 0.1**

Table 1.5: Motility parameters at 30 min at 200 mOsm (BCF: beat cross frequency; Straight: Straightness; LIN: Linearity; VAP: mean path velocity; ALH: lateral head displacement). Significant values are coloured in dark red. Values expressed as mean ± SEM (n=6 experiments).

* $P < 0.05$ vs control

** $P < 0.001$ vs control

Condition	Progress Velocity	Track Velocity	BCF	Straight	Lin	VAP	ALH
Control	**26.4 ± 2.6**	**60.1 ± 4.9**	**37 ± 2.2**	**86 ± 1.4**	**44 ± 2.6**	**30.4 ± 2.6**	**2.5 ± 0.1**
10 µM DIDS	**24.4 ± 4.9**	**50.5 ± 10.2**	**30.8 ± 6.2**	**72.6± 14.5**	**40.6 ± 8.3**	**27.2 ± 5.5**	**2.2 ± 0.4**
Control	**31.4 ± 2.8**	**69.2 ± 3.1**	**38.9 ± 0.7**	**87 ± 1**	**45.5 ± 2.1**	**35.3 ± 2.8**	**2.8 ± 0.1**
50 µM DIDS	**30.8 ± 3.6**	**71.6 ± 10**	**32.2± 3.8***	**83.5± 1.3***	**46.6 ± 2.4**	**36.1 ± 4.3**	**2.9 ± 0.3**
Control	**27.9 ± 1.8**	**63.6 ± 3.3**	**35.4 ± 1.3**	**85.2 ± 2.8**	**45.2 ± 3.1**	**32.4 ± 1.7**	**2.8 ± 0.3**
100 µM DIDS	**27.5 ± 15**	**51.1 ± 20.4**	**21.7 ± 7.3**	**63.5± 21.2**	**33.5± 11.8**	**30.1± 15.2**	**1.7 ± 1.1**
Control	**34.1 ±3.8**	**73.3 ± 5.1**	**37.5 ± 2.5**	**87.1 ± 1.3**	**46.8 ± 2.9**	**38.1 ± 3.9**	**3.1 ± 0.1**
400 µM DIDS	**0****	**0****	**0****	**0****	**0****	**0****	**0****
Control	**37.7 ± 3.2**	**69 ± 2.5**	**36.7 ± 1.9**	**88 ± 1.1**	**54.1 ± 3.1**	**41.8 ± 3**	**3 ± 0.1**
100 µM NPPB	**35.6 ± 2.2**	**70.6 ± 2.1**	**33.4 ± 1.3**	**85.8 ± 0.7**	**49.6 ± 1.8**	**40.4 ± 2.4**	**3.4± 0.1***
Control	**39.1 ± 3.5**	**76.3 ± 3.5**	**35.9 ± 1.8**	**85.8 ± 1.3**	**50.6 ± 3.7**	**44.3 ± 3.3**	**3.5 ± 0**
200 µM Niflumic Acid	**31.4 ± 2.2**	**70.7 ± 4.2**	**34.9 ± 1.6**	**82.8 ± 1.4**	**44.3 ± 2.1**	**36.3 ± 1.9**	**3.7 ± 0.1**

Table 1.6: Motility parameters at 60 min at 200 mOsm (BCF: beat cross frequency; Straight: Straightness; LIN: Linearity; VAP: mean path velocity; ALH: lateral head displacement). Significant values are coloured in dark red. Values expressed as mean ± SEM (n=6 experiments).

* $P < 0.05$ vs control

** $P < 0.001$ vs control

2.4.4 Effect of DIDS on the serine/threonine phosphorylation of human sperm proteins

The effect of DIDS on human sperm serine/threonine phosphorylation was investigated. After

separation with percoll, cells were resuspended for 30 min with EBSS lacking HCO_3^- (non capacitating medium), EBSS alone, and EBSS with 10, 50, 100 and 400 µM DIDS. As expected, the phosphorylation levels were very low in HCO_3^- -free EBSS when compared to normal EBSS (figure 2.5) (Bedu-Addo et al., 2005). On the other hand, DIDS induced a dose-dependent decrease in serine/threonine phosphorylation of two proteins of 105 and 81 kDa (figure 2.5), reaching the maximum level of inhibition at 100 and 400 µM. This pattern was consistent in three experiments with different donors. These results suggest that DIDS is interfering with the activity of the cAMP-regulated PKA in charge of phosphorylation of proteins that might be of importance in sperm motility regulation.

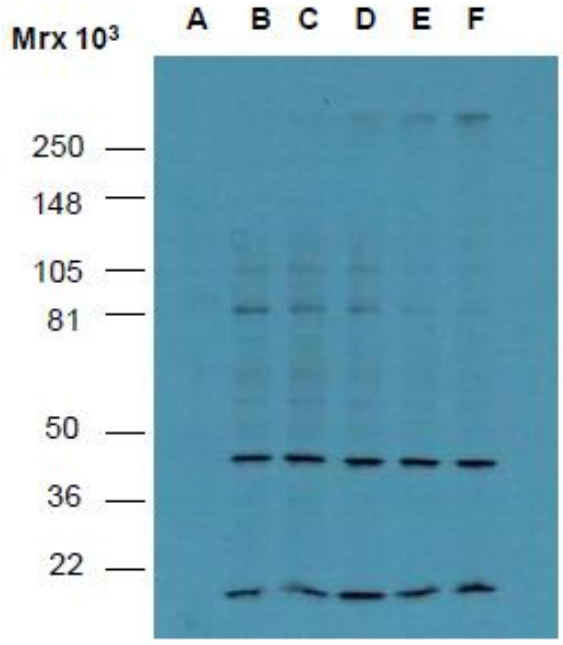

Figure 2.5: Effect of DIDS on serine/threonine phosphorylation of human sperm proteins. **A)** No capacitating EBSS (HCO_3^- -free), **B)** capacitating EBSS, **C)** capacitating EBSS + 10 µM DIDS, **D)** capacitating EBSS + 50 µM DIDS, **E)** capacitating EBSS + 100 µM, **F)**

capacitating EBSS + 400 µM. Lanes exhibit the protein phosphorylation levels after 30 min of treatment for each condition.

2.5 Discussion

The results showed that concentrations of DIDS from 50 µM were effective in reducing sperm motility, and 400 µM DIDS completely suppressed it. Previous report has shown that 400 µM induced cell swelling by impairing RVD mechanisms in human sperm (Yeung et al., 2005). On the other hand, NPPB and niflumic acid did not produce significant changes in the percentage of motile cells despite the fact that NPPB has been reported to produce cell swelling of human sperm, and niflumic induced cell shrinking (Yeung et al., 2005).

Some CASA parameters, including ALH, linearity, track velocity and progressive velocity, have been reported to exhibit significant correlations with fertilization rates during *in vitro* fertilization (IVF) in humans (Liu et al., 1991, Hirano et al., 2001). The fertilizing capacity of rat spermatozoa was correlated with the decline of the progressive velocity (Moore and Akhondi, 1996). 400 µM DIDS suppressed the kinematic parameters (progressive velocity, track velocity, BCF, straightness, LIN, VAP and ALH), in all the conditions of osmolality (excepting at 30 min with 200 mOsm, where only track velocity showed inhibition); this is in agreement with the effects seen in overall motility. During the first 30 min of incubation (295 mOsm), 10, 50 and 100 µM DIDS reduced progressive velocity, track velocity, LIN and VAP, even though 10 µM DIDS did not affected overall motility. Niflumic acid affected the same parameters but failed to significantly reduce overall motility, which was surprising. At 60 min, 10, 50 and 100 µM DIDS reduced progressive velocity, track velocity, and VAP (plus LIN in the case of 50 µM DIDS), but 10 µM DIDS still had no effect on overall

motility. On the other hand, NPPB reduced progressive velocity, LIN and VAP and niflumic acid affected progressive velocity, track velocity, LIN, straightness and VAP, but both chemicals did not affect overall motility. At 270 mOsm there were little modifications on the general parameters. At 200 mOsm, most of the effects were seen at 30 min; 50 µM DIDS affected track velocity and 100 µM DIDS reduced progressive velocity, track velocity, VAP and ALH. Both concentrations inhibited overall motility. NPPB reduced progressive velocity, BCF and VAP, whereas niflumic acid did the same with track velocity, straightness, LIN and VAP. However, both chemicals did not alter overall motility. The high variability of the samples might be a factor determining the variety of results in the kinematic parameters studied, although there was a clear pattern of inhibition produced by DIDS to high concentrations (400 µM).

Western blots analysis indicated that incubation with DIDS inhibited serine/threonine phosphorylation in human sperm cells. The degree of inhibition is proportional to the concentration of DIDS used, being higher with 100 and 400 µM DIDS. Data from sperm cells of diverse species have suggested that HCO_3^- is required for processes such as regulation of soluble adenylate cyclase and consequent generation of cAMP, tyrosine phosphorylation of proteins, capacitation and acrosome reaction (Visconti et al., 1999d). HCO_3^- is also known to stimulate the motility and respiration of spermatozoa (Murdoch and Davis, 1978, Okamura et al., 1986), and influences the appearance of hyperactivated movement (Neill and Olds-Clarke, 1987) (Boatman and Robbins, 1991). DIDS might be affecting the activity of the HCO_3^- / Cl^- exchanger (Tajima and Okamura, 1990), which means that HCO_3^- would not be able to enter into the cell; hence sperm adenylate cyclase would not be stimulated properly with reduction of cAMP production and PKA activity. These series of events would lead to low levels of serine/threonine and tyrosine

phosphorylation of some proteins critical for sperm motility. Moreover, reduction of intracellular HCO_3^- could produce acidification within the cells. An acidic pH can affect the activity of human sperm dynein ATPases, which are responsible of the movement of sperm flagella (Vivenes et al., 2009) and would also lead to closure of the pH-dependent CatSper channels in the flagellar membrane, causing a fall in resting $[Ca^{2+}]_i$. Acidification could also affect other enzymatic and non enzymatic systems that participate in motility (such as ATPases, exchangers, calcium channels, anion channels, etc), including the activity of the adenylate cyclase and therefore the cAMP-regulated PKA.

Failure of RVD and sperm cell swelling induced by quinine has been linked to impairment of both migration and penetration through cervical mucus (Yeung and Cooper, 2001). These findings along with those showing that Cl^- channels blockers like DIDS and NPPB inhibited RVD in human sperm (Yeung et al., 2005), could lead us to assume that cell swelling was the main reason for the alterations in motility exhibited by the cells incubated with DIDS. However, although the influence of cell volume in motility cannot be discarded, it seems that failure of RVD is not the principal cause of DIDS-induced immobility (due to the lack of effect of NPPB). Rather, the effect of DIDS might be a direct consequence of impairment of cell signaling pathways, such as cAMP regulation, phosphorylation of specific proteins and others, that are dependent of the transport of HCO_3^-. This suggests that the mechanisms involved in HCO_3^- transport in human sperm are DIDS-sensitive (specific anion channels/exchangers like the HCO_3^-/ Cl^- exchanger).

In conclusion, DIDS is an effective inhibitor of human sperm motility and is associated to reduced phosphorylation of serine/threonine residues, which might be associated a failure of

HCO_3^- transport due to specific inhibition of the HCO_3^-/ Cl^- exchanger. NPPB and niflumic acid did not affect the overall motility. So more experiments are required to understand the processes involved in cell signalling of volume regulation and motility of human spermatozoa.

CHAPTER 3

EFFECT OF DIFFERENT CLHORIDE BLOCKERS IN THE MORPHOLOGY OF THE HUMAN SPERMATOZOON

3.1 Abstract

I investigated the effect of different chloride channel blockers on the morphology of human sperm tails at different degrees of osmolality. Motile spermatozoa were selected by swim up into sEBSS. Samples were incubated in the presence and absence of 100 and 400 µM DIDS, 100 µM NPPB, and 200 µM niflumic acid for 1 hour. The osmolality of the media were adjusted at 295, 270 and 200 mOsm. The results showed that 400 µM DIDS increased significantly the percentage of sperm cells with coiled or angulated tails in every condition of osmolality examined, but 100 µM DIDS did not produce coiling under the same conditions. NPPB only produced increase in the percentage of coiled sperm at a very extreme degree of osmolality (200 mOsm) when compared with controls. Niflumic acid increased the percentage of coiled sperm at 270 mOsm only. The data suggest that 400 µM is able to inhibit regulatory volume decrease (RVD) mechanisms that cause cell swelling in human sperm, leading to coiling or deformation of the sperm tail. Chloride channel blockers seem to have a role in maintaining the morphological integrity of the human sperm.

3.2 Introduction

The observation in the ejaculate of sperm with coiling and bending back of the tail on itself is not rare. Coiled sperm are classified in the WHO manual (WHO, 1999) as defects in either the midpiece or the tail. There are relatively few data in the literature of the occurrence of coiled sperm in the populations of fertile and infertile men. In four reports on fertile men totalling 2070 subjects, there was an average of 5.8 - 7% of coiled sperm appearing in the ejaculate (Schwartz et al., 1984, Bujan et al., 1988, Auger et al., 2001, Kubo-Irie et al., 2005, Yeung et al., 2009). In another study of infertile men, the 252 men that induced pregnancy had significantly lower levels of coiled sperm (9.3%) than the 142 men that did not (11%) (Jouannet et al., 1988). In a study with electron microscopy of semen from 439 infertile men attending and andrology centre, the researchers found an overall 11% of sperm with different coiled forms (Yeung et al., 2009). Moreover, 12% of the patients had 20% or more of such sperm (Yeung et al., 2009). The percentage of coiled sperm was correlated with age and the epididymal secretory marker neutral α-glucosidase, and associated with smoking and varicocele (Yeung et al., 2009).

The early experiments by Drevius and Ericsson (Drevius and Eriksson, 1966) characterizing the bending or coiling of the sperm tail as a normal phenomenon in response to hyposmotic challenges led to the introduction of the HOS (hyposmotic swelling) test into the andrology clinic as a test for membrane integrity (Jeyendran et al., 1984, WHO, 1999, Yeung et al., 2009). The bending back of the sperm tail upon release from the epididymis of the infertile *c-ros* tyrosine kinase receptor knockout mice into normal culture medium has subsequently been shown to arise from defects in sperm volume regulation associated to abnormalities in the epididymal environment (Yeung et al., 2006, Yeung et al., 1998, Yeung et al., 2009), which reflects the importance of the epididymis in the acquisition of volume regulation

capacity in sperm cells.

Chloride channels play an important part in volume regulation within the spermatozoa. Failure of volume regulation induces swelling and deformation of the sperm tail that has been associated to impaired migration through the female tract (Cooper and Yeung, 2007). In light of the effects that chloride channel blockers might have in volume regulation and hence morphology of sperm tails, I decided to evaluate whether there was any increase in the number of sperm with coiled or angulated tails after exposition to DIDS, NPPB and niflumic acid (chloride channel blockers) at 295 mOsm (similar to the osmolality found in cervical mucus), 270 mOsm (similar to the osmolality found in fallopian fluid), and 200 mOsm (non physiological).

3.3 Materials and Methods

3.3.1 Materials

The chloride blockers 4,4′-Diisothiocyanatostilbene-2,2′-disulfonic acid disodium salt hydrate **(**DIDS), 5-Nitro-2-(3-phenylpropylamino)benzoic acid **(**NPPB) and niflumic acid; dimethyl sulfoxide (DMSO), and salts used to prepare supplemented Earle's Balanced Salt Solution (sEBSS) were all purchased from Sigma Aldrich (Dorset, UK). Fatty-acid free bovine serum albumin (BSA) was purchased from SAFC Biosciences (Lenexa, KS, USA). Osmolalities were determined with an Osmometer 3MO Plus (Advanced Instruments, Norwood, MA, USA).

3.3.2 Preparation of spermatozoa

All donors were recruited at the Birmingham Women's Hospital (HFEA Centre #0119), and

at the School of Biosciences of the University of Birmingham in accordance with the Human Fertilisation and Embryology Authority Code of Practice. Only normal samples in accordance with the World Health Organization guidelines were selected (WHO, 1999). Approval was obtained from the Local Ethical Committee (#0472, #5570) and all donors gave informed consent. Semen was collected by masturbation and after semen liquefaction for approximately 30 min; motile sperm was harvested by swim-up (Mortimer, 1994). Under this method 1 ml of sEBSS [NaCl (116.4 mM), KCl (5.4 mM), $CaCl_2$ (1.8 mM), $MgCl_2$ (1 mM), glucose (5.5 mM), $NaHCO_3$ (25 mM), Na pyruvate (2.5 mM), Na lactate (19 mM), $MgSO_4$ (0.81 mM) and 0.3% BSA, pH 7.4], adjusted at pH 7.3-7.4, was underlayered with 0.3 ml of liquefied sample in polystyrene Falcon round-bottom tubes (Becton Dickinson, USA). After 1 hour of incubation at 37°C, 5% CO2 and at an angle of 45° (to maximize yield), the top layer of each tube, containing the motile cells, was collected into a 15 ml polystyrene Falcon tube (Becton Dickinson, USA). Sperm concentration was determined using a Neubauer counting chamber in accordance with the World Health Organization methods (WHO, 1999). Cells were then concentrated to 2-3 million/ml and prepared for the assays with sEBSS as described previously (Kirkman-Brown et al., 2000).

3.3.3 Sperm morphology

After swim-up the cells were washed and resuspended with sEBSS at 295, 270, and 200 mOSm according to every experiment. The different osmolalities were adjusted by adding NaCl to the stock solution (about 150 mOsm before the addition of NaCl, which is the last ingredient added to the final sEBSS), until achieving the desired level of osmolality. Cells were incubated in these conditions for 1 hour at 37ºC (5 % CO_2), followed for 1 extra hour of incubation in the absence (controls) and presence of 100 and 400 μM DIDS, 100 μM NPPB, and 200 μM niflumic at 37ºC (5 % CO_2) . All the drugs were prepared in DMSO. For each

condition, 10 µl of sample were added onto a 22 x 40 mm coverglass (Menzel-Gläser, Braunschweig, Germany) in duplicate, and then covered with a squared coverslip for visualization in an inverted microscope Nikon TS100 (Nikon, Japan). 100 cells were counted in each coverglass for each condition and then averaged. Only immotile sperm with either coiled or angulated tails, and motile sperm with backward swimming due to similar angulations of the tails were counted as abnormal (figure 3.2).

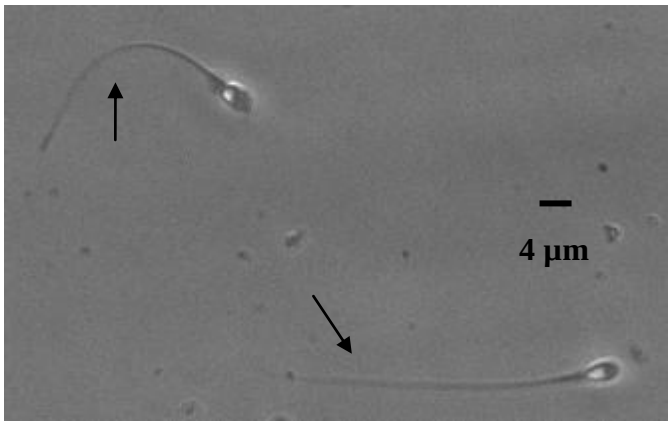

Figure 3.1: Human spermatozoa showing no coiling of the tails.

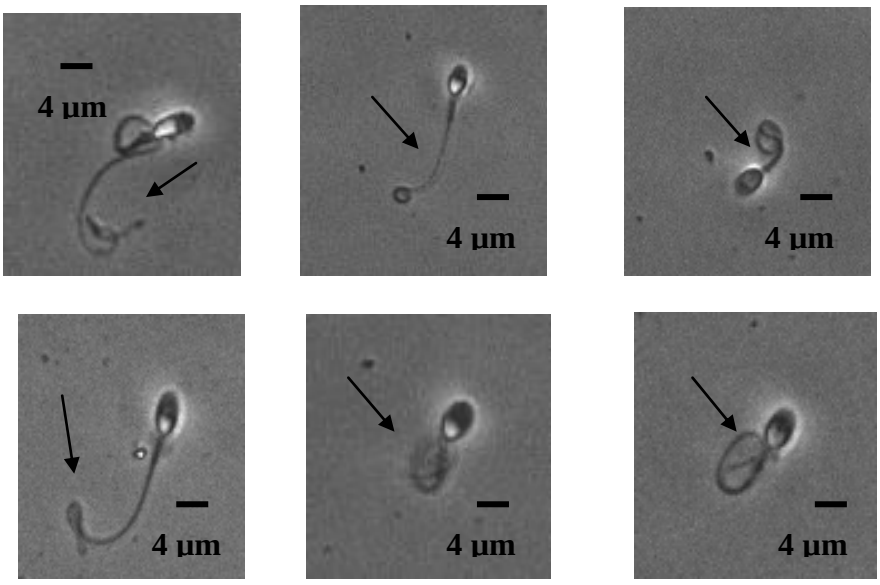

Figure 3.2: Human spermatozoa showing different types of angulations or coiling of the tail due to swelling.

3.3.4 Statistical Analysis

Statistics was performed with the software OriginPro 8 Student Version (Origin Lab Corporation, Northampton, MA, USA). The results are expressed as mean ± standard error for the number of indicated assays in each case. The standard errors of the differences were calculated for paired data. Data analysis was performed with Student's Test for paired data, "*n*" being the number of repeated assays with different preparations. Only probabilities < 0.05 were accepted as significant.

3.4 Results

3.4.1 Effect of hyposmotic shock on sperm morphology

The effect of DIDS (100 and 400 µM), NPPB (100 µM) and niflumic acid (200 µM) on sperm morphology were tested on cells exposed to media with osmolality of 295, 270 and 200 mOsm. A previous work reported that 400 µM DIDS and 100 µM NPPB were able to induce cell swelling in human sperm (Yeung et al., 2005). In the same study 200 µM niflumic acid rather than increasing cell size produced cell shrinkage (Yeung et al., 2005). According to the authors the drugs only produced changes in cell size at these concentrations. Based upon these results and the fact that sperm motility is reduced with 100 and 400 µM DIDS, I decided to evaluate whether the effects seen on motility were related with alterations on morphology. DIDS is an irreversible blocker in contrast with NPPB and niflumic acid wich are reversible (Jentsch et al., 2002). The reversibility of the effects caused by the different drugs couldn't be tested since it implied further centrifugations of the samples, which are detrimental to sperm's integrity and morphology, with loss of cells during the washing. Readings were obtained at 60 minutes after incubation with the different Cl^- channel blockers (time needed to count the cells between each experiment). DMSO was used as a vehicle to prepare all the chemicals employed in the experiments and was present in every control condition (0.2% for NPPB and niflumic acid and 0.5% for DIDS).

In all the conditions there was a percentage of coiling (ranging from 6% ± 0.8 to 9.7% ± 1.4 SEM in cells incubated with 295 mOsm). As expected, the lower the level of osmolality the higher the percentage of flagellar coiling/deformation (ranging from 11.4% ± 1.5 to 19.7% ± 1.6 SEM for 270 mOsm, and 16.6% ± 2.9 to 37.3% ± 4.9 SEM for 200 mOsm). The alterations exhibited the same common patterns of coiling (figure 3.2) in all the conditions.

There was an important variation in the percentages of coiling during the diverse control conditions, which might be attributed to the diversity of the samples obtained from different donors.

3.4.2 Effect of DIDS and hyposmotic shock on sperm morphology

The results show that with a dose of 100 µM DIDS there was no significant increase in the coiling of tails in the conditions tested (6% ± 0.8 vs 5.4% ± 0.5 SEM for 295 mOsm; 12.4% ± 1.7 vs 16.9% ± 2.6 SEM for 270 mOsm; 31.7% ± 5 vs 35.3% ± 4.8 SEM for 200 mOsm) (figure 3.3). On the other hand, 400 µM was able to produce a small but significant increase in the proportion of sperm with angulated or deformed tails in the three conditions of osmolality evaluated (8.1% ± 0.9 vs 14.2% ± 1.4 SEM for 295 mOsm; 16.1% ± 2.1 vs 26.9% ± 1.3 SEM for 270 mOsm; 34.3% ± 4.9 vs 48.6% ± 6.4 SEM for 200 mOsm) (figure 3.4).

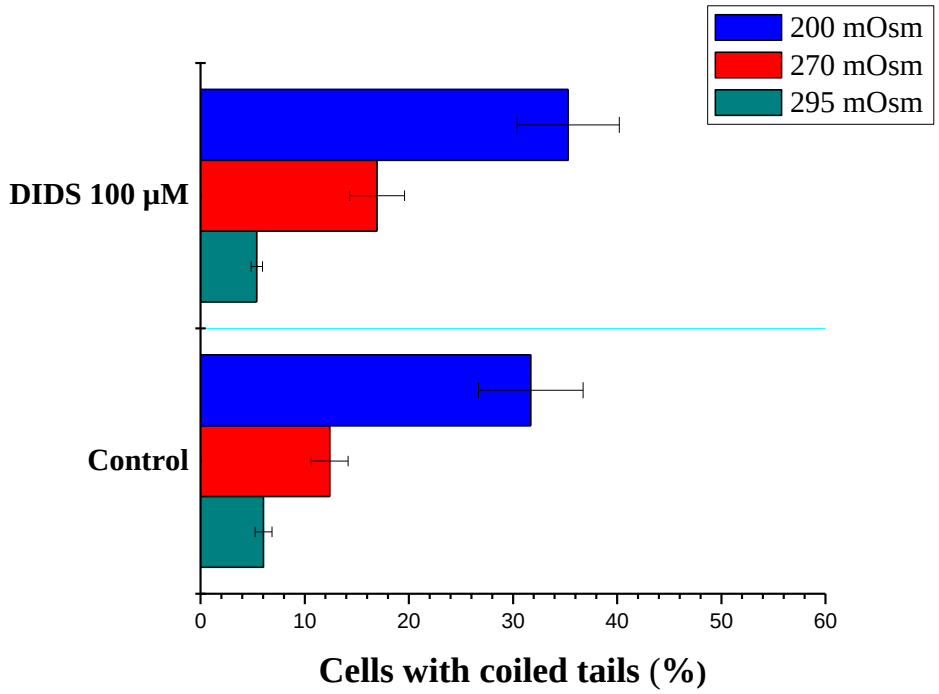

Figure 3.3: Percentage of coiled tails in human spermatozoa incubated with 100 µM DIDS. Values expressed as mean ± SEM (n=10).

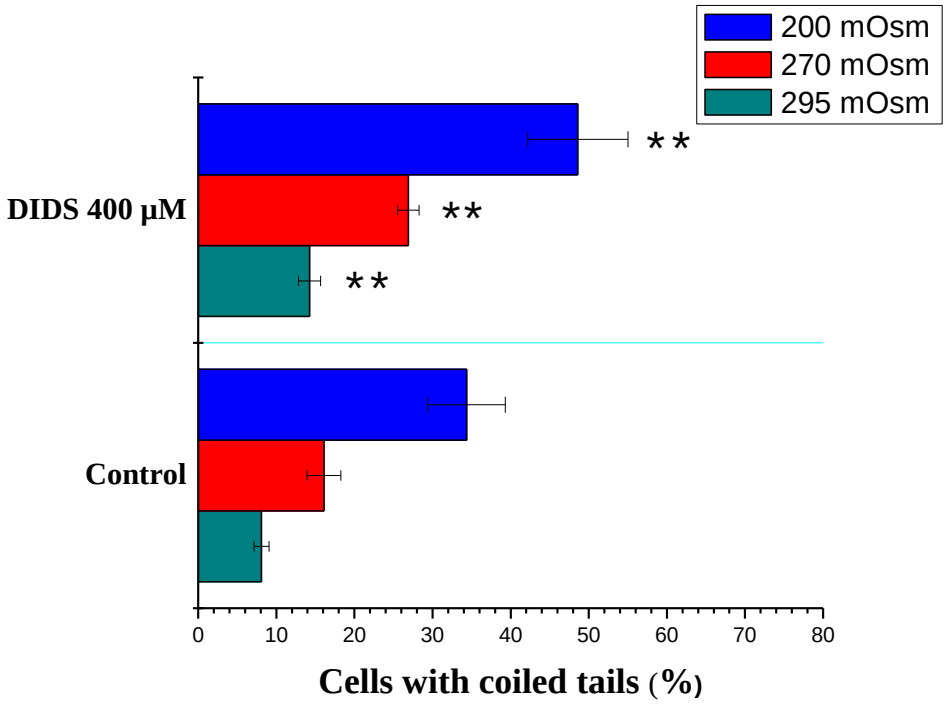

Figure 3.4: Percentage of coiled tails in human spermatozoa incubated with 400 µM DIDS. Values expressed as mean ± SEM (n=10).

** P < 0.001 vs control.

3.4.3 Effect of NPPB and hyposmotic shock on sperm morphology

NPPB is another chloride blocker that was used in the same experimental conditions. As shown in the figure 3.5, 100 µM NPPB was able to produce an increase in the percentage of coiled tails only at 200 mOsm (37.3% ± 4.9 vs 43.5% ± 3.8 SEM), which is a very extreme and non physiological condition. No significant variations were detected at 295 and 270 mOsm (9.7% ± 1.4 vs 7.7% ± 1.2 SEM for 295 mOsm; 20.2% ± 2 vs 19.7% ± 1.6 SEM for 270 mOsm).

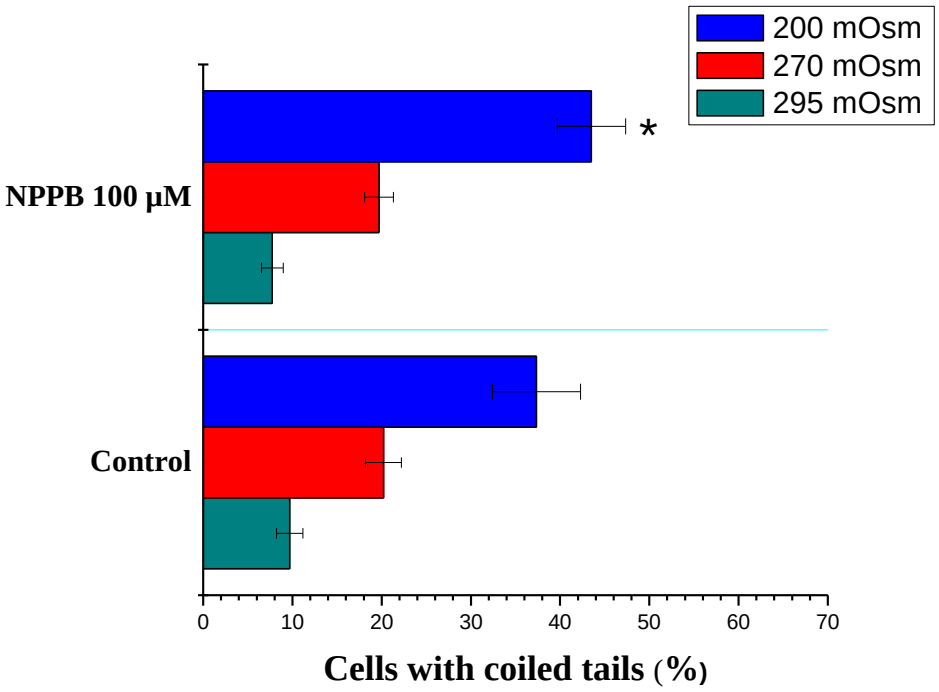

Figure 3.5: Percentage of coiled tails in human spermatozoa incubated with 100 µM NPPB. Values expressed as mean ± SEM (n=10).

* P < 0.05 vs control.

3.4.4 Effect of Niflumic Acid and hyposmotic shock on sperm morphology

Niflumic acid (200 µM) was used in the experimental conditions as described above. The drug was able to produce an increase in the percentage of coiled tails only at 270 mOsm (11.4% ± 1.5 vs 21.2% ± 4.4 SEM), but no significant variations were detected at 295 and 200 mOsm (6.3% ± 1 vs 7.4% ± 1 SEM for 295 mOsm; 16.6% ± 2.9 vs 19% ± 3.6 SEM for 200 mOsm) (figure 3.6).

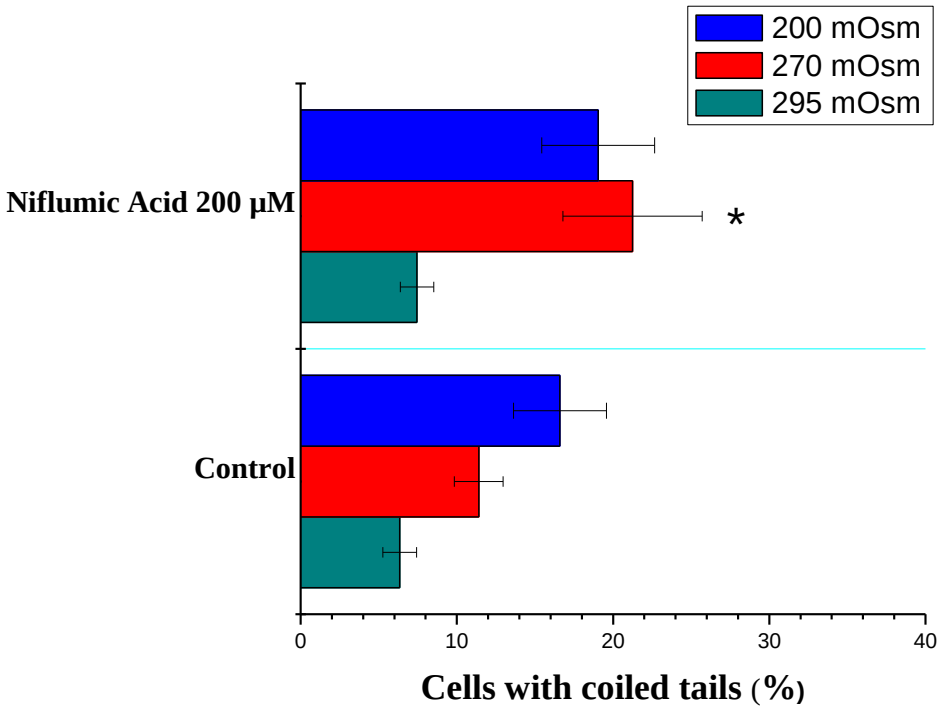

Figure 3.6: Percentage of coiled tails in human spermatozoa incubated with 200 µM niflumic acid. Values expressed as mean ± SEM (n=10).

* $P < 0.05$ vs control.

3.5 Discussion

The behavior of the spermatozoon and its ability to fertilize is especially susceptible to changes in the ionic environment, which causes water movement through the cells that is compensated by activation or inactivation of different types of channels for Na^+, Ca^{2+}, K^+, and Cl^-. Cl^- channels have been linked to volume regulation, because they are activated in response to physiological volume changes and trigger compensatory mechanisms for RVD. When the RVD fails, the sperm cells swell and change their flagellar shape as a compensatory mechanism for avoiding excessive stretching of the plasma membrane. As a

consequence, coiling or angulation of the flagellum occurs in order to accommodate a larger volume within the same surface area (Cooper and Yeung, 2000). Association of coiled or angulated sperm with infertility has been demonstrated in many animal models in the so-called “Dag defect”, which is characterized by high proportions of coiled or bent sperm tails in the ejaculate (Cooper and Yeung, 2003, Cooper and Barfield, 2006).

In this study, the percentage of coiled or bent sperm present in the control conditions was between 6 - 10%, which is similar to the values (5.8 - 7%) reported by other groups in the ejaculate (Schwartz et al., 1984, Bujan et al., 1988, Kubo-Irie et al., 2005). Furthermore, the proportion of sperm coiled or bent ranged from 12 to 20 % when cells were resuspended in 270 mOsm medium, and 32 to 35 % when resuspended in 200 mOsm medium. This is evidence that such alterations in the tails are proportional to the degree of hyspomotic shock induced on the sperm cells. The clear variations in the percentages of coiling during the different control conditions might be attributed to the high level of variability seen between samples obtained from different donors.

In man, swollen sperm fail to penetrate and migrate through surrogate mucus (Yeung and Cooper, 2001). When the efficiency of different chloride blockers is tested, it becomes clear than only 400 µM DIDS produces a significant increase in the percentage of cells with coiling of the tails, but at 100 µM shows no effect. On the other hand, NPPB and niflumic acid only produced alterations at 200 and 270 mOsm respectively, failing to do so in other conditions. The defects seen on morphology after incubation with 400 µM DIDS may reflect failure of RVD mechanisms due to inhibition of channels or exchangers that are not involved in Cl^- transport and are not targeted by the other drugs. A previous report studying the effect of different anion blockers in human sperm volume measured by flow cytometry (in a

medium adjusted at 290 mOsm), showed that the use of 400 µM DIDS induces cell swelling as reflected by the increase in laser-forward scatter compared to the control (Yeung et al., 2005). In the same study 200 µM niflumic acid rather than increasing cell size produced cell shrinkage (Yeung et al., 2005). Although these results are in agreement with the data showed here, they reported that 100 µM NPPB was able to produce a significant increase in cell swelling. NPPB has been effective in inhibiting RVD by spermatozoa from boar, monkey, and mice (for a review see (Cooper and Yeung, 2007). A hypothesis that might explain the difference between my results and those reported by Yeung et al (Yeung et al., 2005), is that changes in cell volume sensitive to NPPB occur primarily in the head and/or the acrosome and not in the tail and therefore, are not reflected in assessment of tail morphology. Small changes in sperm head volume are difficult to discern by microscopy (Yeung et al., 2005). In that case more experiments measuring the size of the head, acrosome and tail would be needed in order to confirm the viability of this hypothesis. DIDS had no detectable effect in bull spermatozoa but induced swelling in boar and interestingly caused shrinkage in murine spermatozoa in hypotonic media (Cooper and Yeung, 2007). On the other hand, niflumic acid had no effect in murine sperm (Cooper and Yeung, 2007). In conclusion, only 400 µM DIDS consistently induced an increment of the percentage of coiled sperm in every osmotic condition, which could have deep implications in sperm motility and ability to fertilize; whereas NPPB and niflumic acid were less effective increasing the coiling and producing visible deformations of the sperm tail.

CHAPTER 4

EFFECT OF HYPOSMOTIC SHOCK AND CHLORIDE CHANNEL BLOCKERS IN CALCIUM SIGNALLING OF THE HUMAN SPERMATOZOON

4.1 Abstract

$[Ca^{2+}]_i$ plays a critical role in volume regulation of many cell lines, however, some cells posses Regulatory Volume Decrease (RVD) mechanisms that are $[Ca^{2+}]_i$ –independent. Human sperm cells experience RVD when exposed to hyposmotic conditions, but there is little known about $[Ca^{2+}]_i$ signalling during RVD. In addition, Cl^- channels blockers like DIDS, NPPB, and Niflumic Acid are reported to impair RVD and mobilise $[Ca^{2+}]_i$ in an important variety of cells through various mechanisms. Human spermatozoa were loaded with Oregon Green 488 BAPTA, and then, in presence or absence of the Cl^- channels blockers, exposed to osmotic conditions that mimicked the hyposmotic shock experienced in the female tract. The results show that when hyposmotic shock is applied there is an substantial increase in $[Ca^{2+}]_i$ that exhibits a biphasic behaviour, with an important and transient peak of fluorescence immediately followed by a plateau with levels that remain more elevated than those observed during the control period. All the drugs produced a significant rise in $[Ca^{2+}]_i$, but only DIDS and Niflumic Acid attenuated the increase in $[Ca^{2+}]_i$ produced by the hyposmotic shock. On the other hand, NPPB failed to prevent the rise in $[Ca^{2+}]_i$ induced by the osmotic shock. These results suggest that $[Ca^{2+}]_i$ might be important for RVD in human spermatozoa.

4.2 Introduction

The importance of Ca^{2+} in the activation of RVD has been clearly established in many cells. However, this Ca^{2+} dependency differs widely between cell lines. As suggested by McCarty and O'Neil (McCarty and O'Neil, 1992), it is possible to classify the Ca^{2+} dependency of RVD in three groups: 1) cells that are highly dependent on extracellular Ca^{2+} and activation of Ca^{2+} influx, supposedly reflecting activation of Ca^{2+} channels, such as observed in rabbit corneal epithelial cells (Wu et al., 1997), and human T lymphocytes (Schlichter and Sakellaropoulos, 1994); 2) cells that are not dependent of extracellular Ca^{2+} and the activation of Ca^{2+} influx but that require a transient Ca^{2+} release from intracellular stores, such as vascular endothelial cells (Jena et al., 1997), and rat cerebellar astrocytes (Rojas et al., 2008); 3) cells that don't show any swelling-induced change in $[Ca^{2+}]_i$ at all, meaning that the RVD is Ca^{2+} independent, such as Ehrlich mouse ascites tumor cells (Jorgensen et al., 1997). There is also a fourth group; cells where there is increase in $[Ca^{2+}]_i$ but it is not necessary for RVD, such as those found in rabbit proximal convoluted tubule (Beck et al., 1991). The reason for these differences could be variations in the type of channels participating in RVD between cell types and species (Galizia et al., 2008), or variations in the Ca^{2+} threshold of RVD mechanisms (McCarty and O'Neil, 1992). This is evidence of the poor understanding of the RVD process and its relationship with Ca^{2+} signalling.

In cells with Ca^{2+} dependent RVD during hyposmotic conditions, it has been postulated that the rise in $[Ca^{2+}]_i$ activates specific K^+ (Galizia et al., 2008) and Cl^- channels (Piper and Large, 2004) (Chien and Hartzell, 2007), which contribute to the efflux of K^+, Cl^- and water to reduce the cell swelling and to guarantee the electrochemical equilibrium at the plasma membrane. Bestrophins and ClC3 are members of the Cl^- channels family that are activated

by cell volume change and Ca^{2+} (Chien and Hartzell, 2007). Interestingly, ClC3 has been identified in human sperm (Yeung et al., 2005).

Previous research with patch clamp techniques has reported the effects of Cl^- channels blockers in the activity of channels activated by volume regulation and Ca^{2+}. DIDS inhibited ClC-3 (Nakazawa et al., 2001), and Ca^{2+}-activated Cl^- channels (Kim et al., 2003) (Xu et al., 2002) (Baron et al., 1991) (Hogg et al., 1994). NPPB blocked swelling activated- Cl^- channels (Isoya et al., 2009) (Tao et al., 2008) and Ca^{2+}-activated Cl^- channels (Kim et al., 2003) . Niflumic acid at 10 µM reduced Ca^{2+}-activated Cl^- channels currents in smooth muscle cells isolated from sheep urethra (Cotton et al., 1997), and with 100 µM further blockade was obtained in sheep (Cotton et al 1997) and mouse (O'Driscoll et al., 2008). Moreover the drug inhibited the Ca^{2+}-activated Cl^- currents in interstitial cells of Cajal linked to pacemaker activity in gastrointestinal muscle (Zhu et al., 2009).

So far, the $[Ca^{2+}]_i$ signaling events, if any, in human spermatozoa under hyposmotic stress remain unknown. Although the effects of the different Cl^- channels blockers aforementioned on $[Ca^{2+}]_i$ has been described in many cell lines, nothing has been made in human sperm cells. It is well known that sperm are equipped with most of the mechanisms involved in Ca^{2+} regulation in cells (PMCA, ryanodine receptors, SERCA, exchangers, Ca^{2+} channels, etc) (Jimenez-Gonzalez et al., 2006), therefore it is important to obtain some understanding about the role of Ca^{2+} in volume regulation.

The goals in this chapter were to evaluate the effects of hyposmotic shock and Cl^- channels blockers (DIDS, NPPB, and niflumic acid) in Ca^{2+} homeostasis of the human spermatozoon.

4.3 Materials and methods

4.3.1 Materials

The chloride blockers 4,4′-Diisothiocyanatostilbene-2,2′-disulfonic acid disodium salt hydrate **(**DIDS), 5-Nitro-2-(3-phenylpropylamino)benzoic acid **(**NPPB) and Niflumic Acid; dimethyl sulfoxide (DMSO), and salts used to prepare supplemented Earle's Balanced Salt Solution (sEBSS) were all purchased from Sigma Aldrich (Dorset, UK). Oregon Green 488 BAPTA 1-acetoxymethyl (OGB-1AM) and Pluronic® F-127 *20% solution in DMSO (to dilute the Oregon Green) were purchased from Invitrogen (Paisley, UK). Poly-D-lysine (PDL) was acquired from BD Biosciences (Oxford, UK). Fatty-acid free bovine serum albumin (BSA) was purchased from SAFC Biosciences (Lenexa, KS, USA). Osmolalities were determined with an Osmometer 3MO Plus (Advanced Instruments, Norwood, MA, USA).

4.3.2 Preparation of spermatozoa

All donors were recruited at the Birmingham Women's Hospital (HFEA Centre #0119), and at the School of Biosciences in accordance with the Human Fertilisation and Embryology Authority Code of Practice. Only normal samples in accordance with the World Health Organization guidelines were selected (WHO, 1999). Approval was obtained from the Local Ethical Committee (#0472, #5570) and all donors gave informed consent. Semen was collected by masturbation and after semen liquefaction for approximately 30 min; motile sperm was harvested by swim-up (Mortimer, 1994). Under this method 1 ml of sEBSS [NaCl (116.4 mM), KCl (5.4 mM), $CaCl_2$ (1.8 mM), $MgCl_2$ (1 mM), glucose (5.5 mM), $NaHCO_3$ (25 mM), Na pyruvate (2.5 mM), Na lactate (19 mM), $MgSO_4$ (0.81 mM) and 0.3% BSA, pH 7.4], adjusted at pH 7.3-7.4, was underlayered with 0.3 ml of liquefied sample in polystyrene

Falcon round-bottom tubes (Becton Dickinson, USA). After 1 hour of incubation at 37°C, 5% CO2 and at an angle of 45° (to maximize yield), the top layer of each tube, containing the motile cells, was collected into a 15 ml polystyrene Falcon tube (Becton Dickinson, USA). Sperm concentration was determined using a Neubauer counting chamber in accordance with the World Health Organization methods (WHO, 1999). Cells were then concentrated to 2-3 million/ml and prepared for the assays with sEBSS as described previously (Kirkman-Brown et al., 2000).

4.3.3 Single cell imaging

Sperm density was reduced to 2-3 million cells/ ml, using the same medium before cell labeling and chamber preparation. 200 µL aliquots of cells were then loaded with 1.2 µL of Oregon Green BAPTA-1 AM ester (OGB) prepared with pluronic F-127 for 10 minutes. Following this, the entire aliquot was transferred to a perfusable imaging chamber (200 µL volume) for 50 min, at 37°C and 5% CO_2. The chamber lower surface was a 0.01% poly-d-lysine (PDL) coated coverslip, allowing cells to adhere, (figure 4.1). The imaging chamber was connected to the imaging system and fresh medium (25°C) was washed through for 5 minutes to eliminate excess dye and unattached spermatozoa. All experiments were performed at 25±0.5°C, in a constant flow of medium, with a perfusion rate of approximately 0.4 ml/minute. Cells were imaged with a Nikon TE200 (figure 4.2) inverted fluorescence microscope, fitted with a Cairn 75W xenon source and an epifluorescence accessory (excitation=485 DF 15, emission=535 DF 35). Images were captured every 10 seconds using a X 40 objective and a Rolera XR, Q Imaging cooled CCD camera (figure 4.3) controlled by iQ software (Andor Technology, Belfast, UK). For a review of our technique for Ca^{2+} imaging see (Nash et al., 2010)

In all the experiments, OGB-1AM loaded sperm were superfused with sEBSS for an initial control period before application of treatments. Control experiments consisted in cell perfusion with sEBSS only and sEBSS + DMSO (used as solvent of the different chemicals tested).

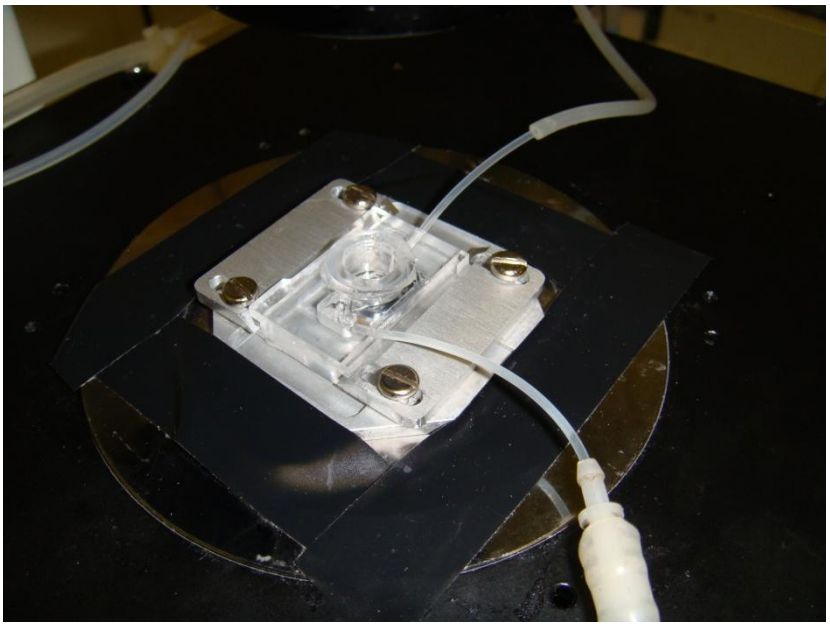

Figure 4.1: Imaging chamber connected to the perfusion system. The floor of the chamber is a slide coated with PDL that allows the cells to adhere and be perfused.

Figure 4.2: Imaging system with microscope Nikon TE200.

Figure 4.3: Camera Rolera-XR Q Imaging connected to the microscope.

4.3.4 Imaging Data Processing

Data were processed offline using iQ software (figure 4.4), a lasso was drawn around the head of each cell in the selected field, considering as many cells as possible. Each cell was directly observed to ensure that only cells where the region of interest remained inside the lasso were used in the analysis. Cells that moved excessively and showed lack of adhesion to the glass surface were excluded, as they are impossible to analyze. Dying cells or dead cells were not included in the analysis. These were easy to identify because either they did not retain dye or gradual loss of fluorescence was visible during the control period (Tesarik et al., 1996). The majority of cells showed vigorous flagellar motility. A small subpopulation of cells showed a clear upward drift of fluorescence during control period or, in some cells, spontaneous oscillation of $[Ca^{2+}]_i$ which may reflect loss of $[Ca^{2+}]_i$ homeostasis. These cells were also excluded from the analysis.

The average fluorescence intensity within the selected area in each spermatozoon was acquired for every image. Raw intensity values were imported into Microsoft Excel© and normalized to pre-stimulus values with the equation:

$$R = [\ (F - F_{rest}) / F_{rest}\ ] \times 100\%$$

R is normalized fluorescence intensity, *F* is fluorescence intensity at a time *t* and F_{rest} is the mean of at least 10 determinations of *F* acquired during the control period. The mean value of R for all cells in the experiment (R_{tot}) was calculated for each time point and the total series of $\mathbf{R}_{tot}$ were plotted to give the mean normalized response of head fluorescent intensity for that experiment. Single cell responses were observed from time-fluorescence intensity plots and the cells were visually sorted into those showing increase, decrease or no change in

fluorescence after treatment.

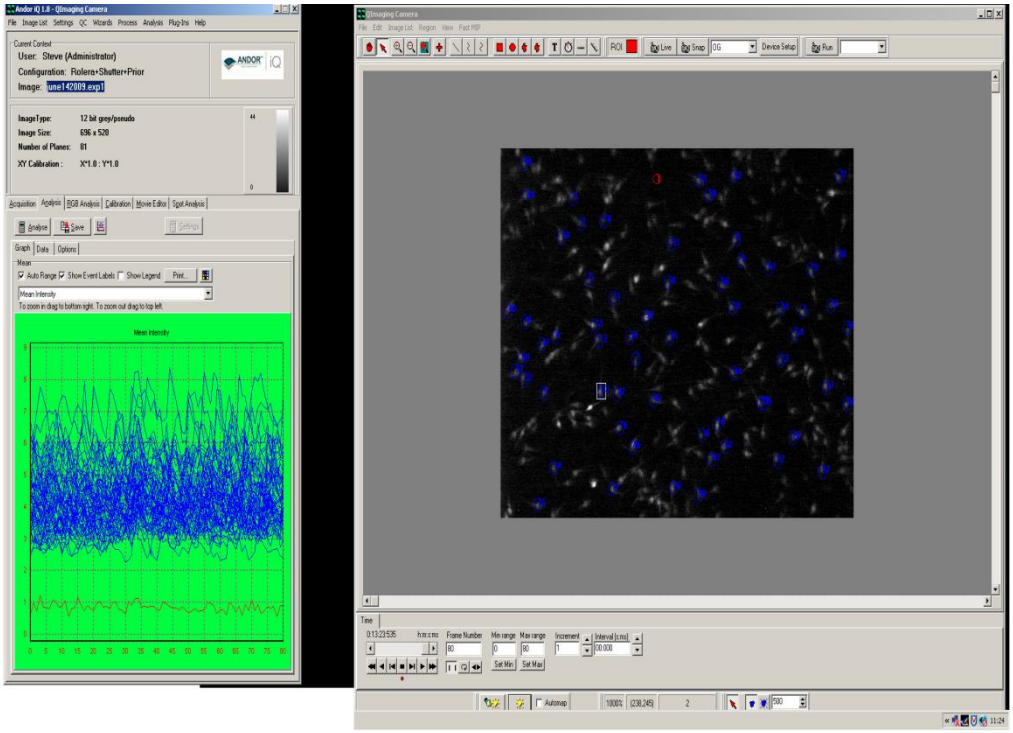

Figure 4.4: Imaging software (Andor iQ, Advanced Imaging, updated version 2007). Cells are selected with a lasso (in blue) and calcium responses are visualized. Raw values are imported into Excel© (Microsoft Office 2007) to be analyzed.

4.3.5 Statistical Analysis

Microsoft Excel© was used to produce the scatter charts and calculate the mean of fluorescence intensity of every cell at the specific point of time where the image was acquired; this translates in 40 images or points per condition, with an interval of 10 second between each one (equivalent to 7 min of recording during per condition examined). The data obtained was used for the statistical analysis. Bar charts and statistics were performed with

the software OriginPro 8 Student Version (Origin Lab Corporation, Northampton, MA, USA). The results are expressed as mean ± standard error for the number of cells indicated in each case. The confidence interval was of 95%. Data analysis was performed with two sample Student's Test (unpaired data), with "*n*" being the number of repeated assays with different preparations. Only probabilities with values < 0.05 were accepted as significant. Though all experiments of a certain type clearly show a pattern of response, only the ones with no important oscillations or drifts of fluorescence during the first minutes before to start the treatments, and with steady responses, were considered for further statistical analysis.

4.4 Results

4.4.1 Effect of the hyposmotic shock on $[Ca^{2+}]_i$ response of human sperm

There are no reports about the effect of DIDS, NPPB and niflumic acid on $[Ca^{2+}]_i$ signalling of human sperm. DIDS (100 and 400 µM), NPPB (100 µM) and niflumic acid (200 µM) were tested on cells exposed to media with osmolality of 295 and 270 mOsm (200 mOsm couldn't be evaluated as the osmotic shoch was so strong that the cells were moved away from the lasso, which impeded any analysis). A previous work reported that 400 µM DIDS and 100 µM NPPB were able to induce cell swelling in human sperm (Yeung et al., 2005). In the same study 200 µM niflumic acid rather than increasing cell size produced cell shrinkage (Yeung et al., 2005). According to the authors the drugs only produced changes in cell size at these concentrations. I decided to use the same range of drug concentrations used in the experiments with morphology (see chapter 3) to evaluate any effect on $[Ca^{2+}]_i$. DIDS is an irreversible blocker in contrast with NPPB and niflumic acid wich are reversible (Jentsch et al., 2002).

In order to investigate the homeostasis of $[Ca^{2+}]_i$ during imposition of osmotic stress, human sperm previously incubated with OGB-1AM and prepared in medium with an osmolality close to that found in the seminal plasma (≈295mOsm) were exposed to a hyposmotic shock, with levels of osmolality similar to those that would be expected to be found in the tubes at the moment of ejaculation (≈270 mOsm). Figure 4.5: A shows that the hyposmotic shock at 270 mOsm induces a rise in $[Ca^{2+}]_i$. This occurred in 86% of the cells in this particular experiment; during the whole series 79% of the cells responded in similar way (99 out of 125 cells, n= 4 experiments). The rise in $[Ca^{2+}]_i$ was immediate, reaching a transient peak of fluorescence that then stabilized at values 12.1 ± 5.3% higher than during control period (figure 4.5: B). This increment in $[Ca^{2+}]_i$ was statistically significant ($P < 0.001$). When cells were challenged again with medium at 295 mOsm $[Ca^{2+}]_i$ gave a transient peak of fluorescence of approximately 1 min of duration, then fell rapidly to control levels before stabilizing at levels (11.4 ± 1.2% above control levels) lower than during exposition to 270 mOsm (figures 4.5: A and 4.5: B). These results suggest that $[Ca^{2+}]_i$ signalling contributes to the mechanisms involved in volume regulation of human spermatozoa under osmotic stress.

DMSO was used as a vehicle to prepare all the chemicals employed in the experiments. Before every experiment 0.5% DMSO (corresponding at the highest concentration of DMSO in the preparations) was used as a control to evaluate the possible effects on the $[Ca^{2+}]_i$ signal evoked by hyposmotic challenge; as the figure 4.6 shows, the behavior of $[Ca^{2+}]_i$ in presence of this concentration of DMSO was very similar to the experiments with complete absence of the solvent.

A

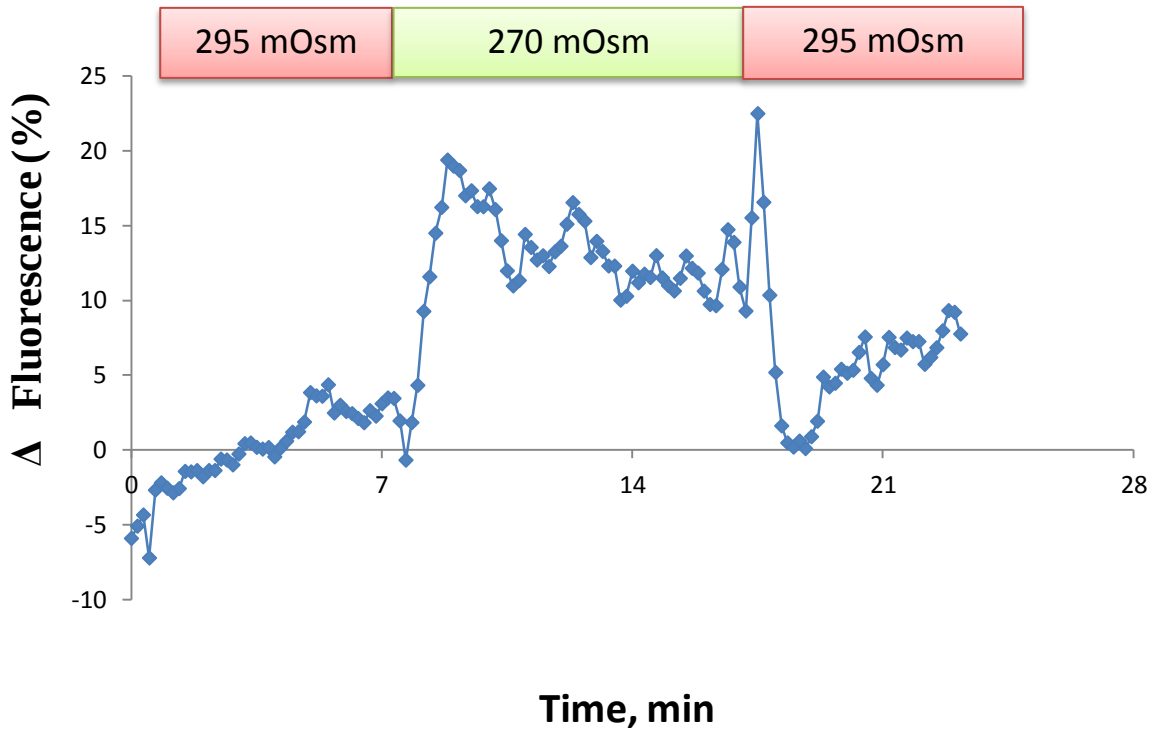
295 mOsm
270 mOsm
295 mOsm
Δ Fluorescence (%)
25
20
15
10
5
0
-5
-10
0
7
14
21
28
Time, min

B

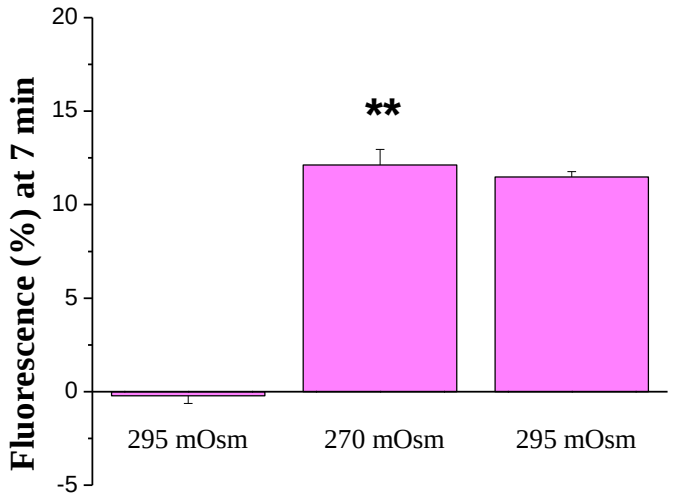
Fluorescence (%) at 7 min
20
15
10
5
0
-5
**
295 mOsm
270 mOsm
295 mOsm

Figure 4.5: A. Effect of hyposmotic shock in $[Ca^{2+}]_i$ in human sperm. Cell samples were perfused with sEBSS (295 mOsm) for 7 min, exposed to 270 mOsm for the same amount of time and then returned to 295 mOsm. The trace represents the average of the typical response obtained from 54 cells (out of 65) in one experiment (a total of four were performed). **B.** Mean $[Ca^{2+}]_i$ during control conditions (295 mOsm), hyposmotic (270 mOsm) and "wash" (295 mOsm). Bar charts show the mean normalized increase in fluorescence of the same cells after 7 min of incubation in each condition. Values expressed as mean ± SEM (n= 54).
** P < 0.001 vs control 295 mOsm

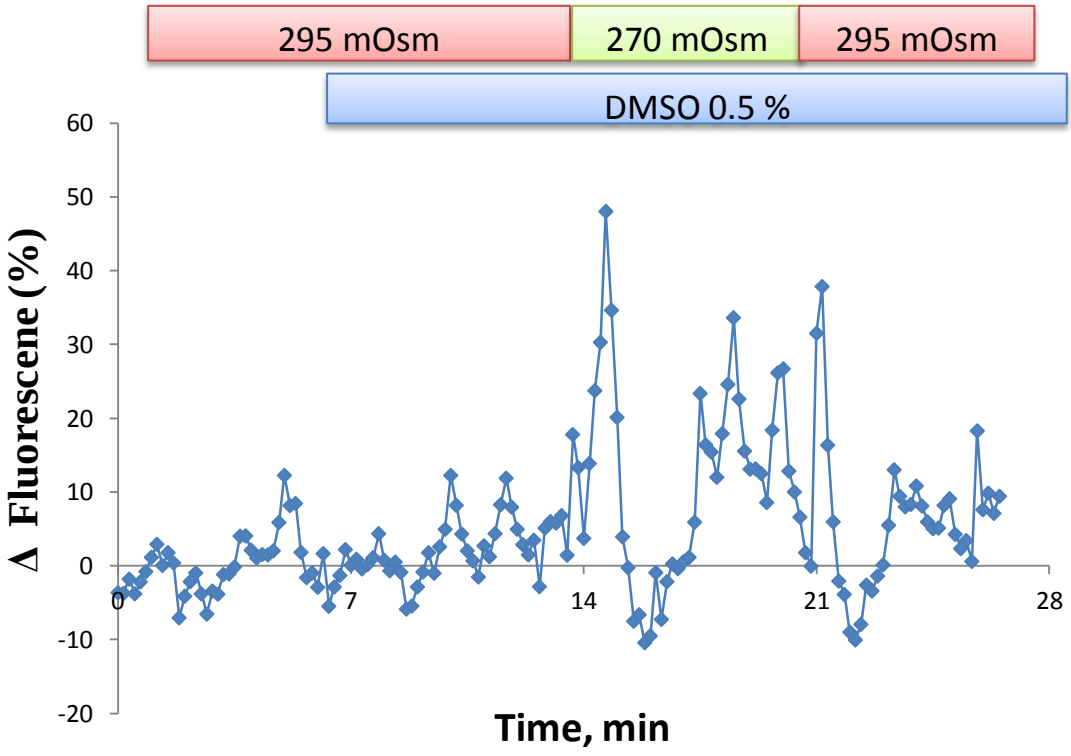

Figure 4.6: Effect of DMSO (0.5%) on the $[Ca^{2+}]_i$ response to hyposmotic schock of human sperm. Cell samples were perfused with sEBSS (295 mOsm) for 7 min, exposed to 270 mOsm for 7 min then returned to 295 mOsm. After the initial control DMSO (0,5%) was present in all the subsequent conditions of osmolality, as shown by the blue bar. DMSO was the vehicle to dilute the chemicals tested and was used as a control in each experiment. The trace represents a single cell response.

4.4.2 Effect of DIDS on the $[Ca^{2+}]_i$ response to hyposmotic shock in human sperm

In order to investigate if DIDS, a potent blocker of chloride channels involved in volume regulation, had any effect in the $[Ca^{2+}]_i$ response during osmotic stress, experiments were carried out to measure the effect of 100 and 400 µM DIDS on human sperm exposed to hyposmotic shock. The cells were prepared as described above and the same sequence of changes in osmolality was used, but this time DIDS was present. The data show that application of 100 µM DIDS produced an increase in $[Ca^{2+}]_i$ almost immediately (figure 4.7: A), with a high transient peak of fluorescence that then stabilized at levels which were 53.3 ± 26.8% higher than during control period ($P < 0.001$) (figure 4.7: B). The rise in $[Ca^{2+}]_i$ occurred in 98% of the cells in this particular experiment and during the whole series 73% of the cells responded in similar way (77 out of 105 cells, n= 3 experiments). When cells were challenged at 270 mOsm in presence of 100 µM DIDS there were no modifications in the fluorescence levels, even though they continued elevated in relation to those observed during control period (65.3 ± 3.6%, $P < 0.05$) (figure 4.7: B). When the osmolality is returned to 295 mOsm, there were no important changes in the fluorescence levels although still remained above than during the control period with drug ($P < 0.001$) (figures 4.7: A and 4.7: B). With 400 µM DIDS there was a significant ($P < 0.001$) and quick rise of $[Ca^{2+}]_i$ followed by a rapid fall in 98% of cells in the experiment (figures 4.8: A and 4.8: B), and 97% of cells during the whole series (193 out of 199 cells, n= 4 experiments). The levels of fluorescence stabilized at 11.2 ± 9.4% (Figure 8.B). At the moment of changing the osmolality to 270 mOsm there was no significant modification in the fluorescence levels (12.6 ± 0.9%) (figure 4.8: B). However, when the osmolality is changed at 295 mOsm there was a significant increase in fluorescence ($P < 0.05$) when compared to the control with drug (figure 4.8: B).

These results suggest that 100 and 400 µM DIDS are able to mobilize $[Ca^{2+}]_i$ in human sperm in an important fashion. Moreover, both concentrations of DIDS are able to attenuate the

usual rise in $[Ca^{2+}]_i$ seen in response to osmotic stress (270 mOsm).

A

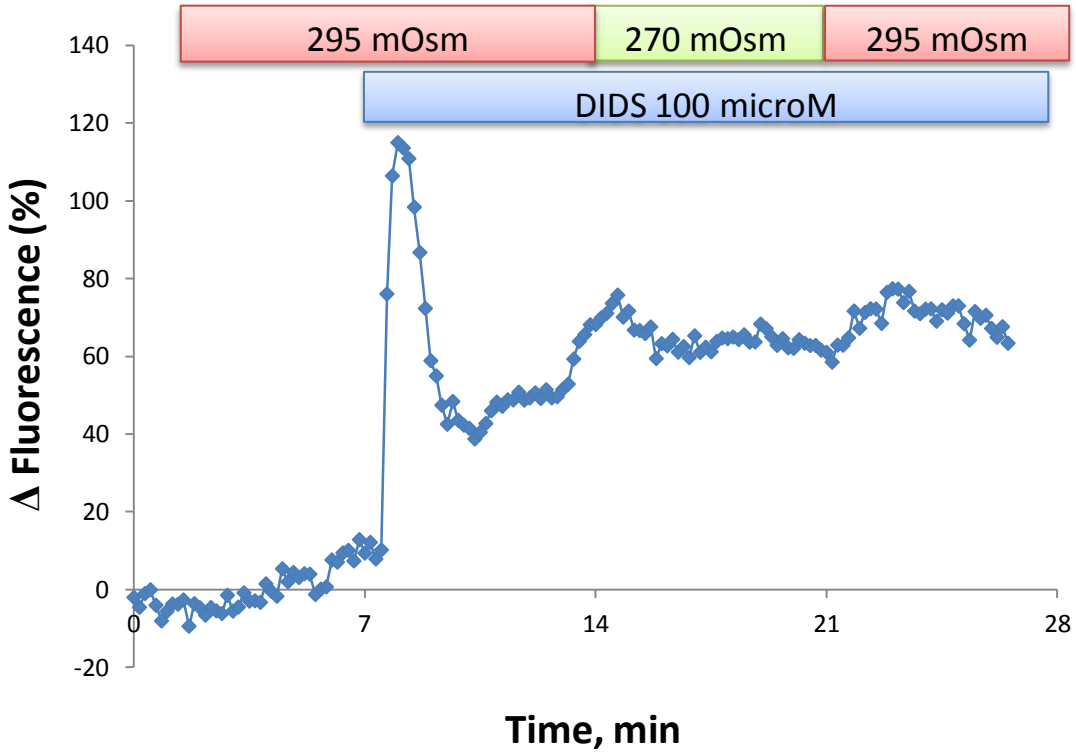

B

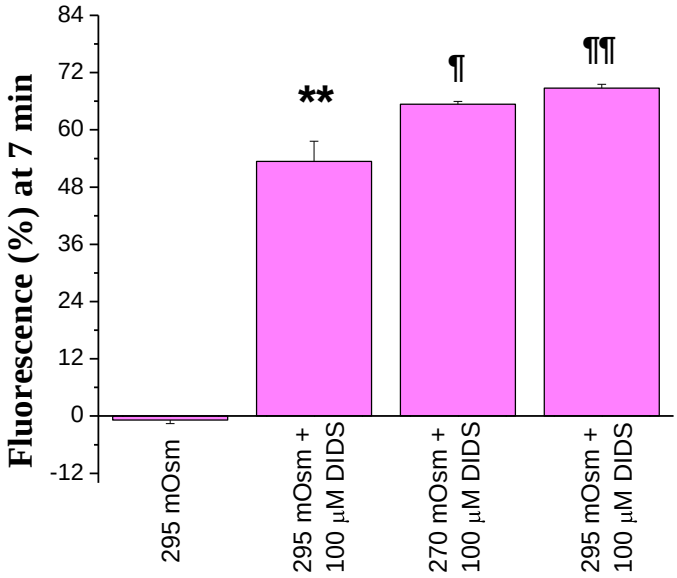

Figure 4.7: A. Effect of hyposmotic shock and 100 µM DIDS on $[Ca^{2+}]_i$ in human sperm bathed in capacitating conditions (sEBSS). Cell samples were perfused with sEBSS (295 mOsm) for 7 min, exposed to 270 mOsm for 7 min then returned to 295 mOsm. After the initial control period 100 µM DIDS was present in all the subsequent conditions of osmolality, as shown by the blue bar. The trace represents the average of the typical response obtained from 49 cells (out of 50) in one experiment (a total of four were performed). **B.** Mean $[Ca^{2+}]_i$ during the absence (295 mOsm), and the presence of 100 µM DIDS (295, 270 and 295 mOsm). Bar charts show the mean normalized increase in fluorescence of the same cells after 7 min of incubation in every condition. Values expressed as mean ± SEM (n= 49 cells).

** P < 0.001 vs control 295 mOsm

¶ P < 0.05 vs control 295 mOsm + DIDS

¶¶ P < 0.001 vs control 295 mOsm + DIDS

A

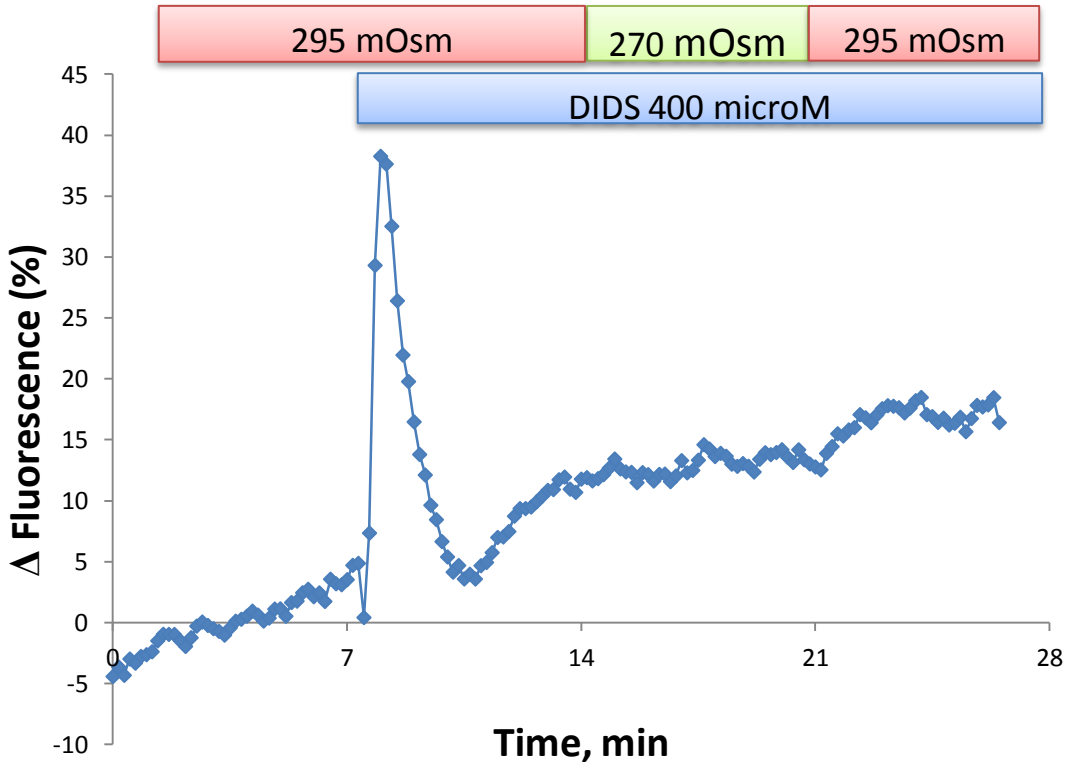

B

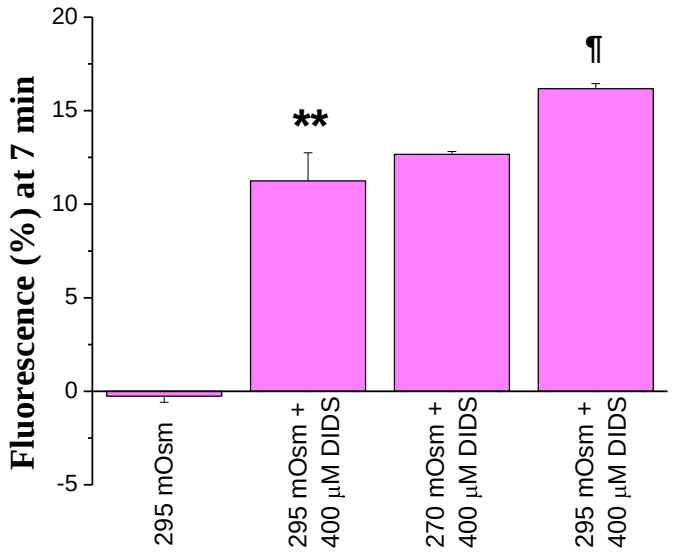

Figure 4.8: A. Effect of hyposmotic shock and 400 µM DIDS on $[Ca^{2+}]_i$ in human sperm bathed in capacitating conditions (sEBSS). Cell samples were perfused with sEBSS (295 mOsm) for 7 min, exposed to 270 mOsm for 7 min then returned to 295 mOsm. After the initial control period 400 µM DIDS was present in all the subsequent conditions of osmolality, as shown by the blue bar. The trace represents the average of the typical response obtained from 58 cells (out of 59) in one experiment (a total of four were performed). **B.** Mean $[Ca^{2+}]_i$ during the absence (295 mOsm) and the presence of 400 µM DIDS (295, 270 and 295 mOsm). Bar charts show the mean normalized increase in fluorescence of the same cells after 7 min of incubation in every condition. Values expressed as mean ± SEM (n= 58 cells).

** $P < 0.001$ vs control 295 mOsm

¶ $P < 0.05$ vs control 295 mOsm + DIDS

4.4.3 Effect of NPPB on the $[Ca^{2+}]_i$ response to hyposmotic shock in human sperm

NPPB is a well known blocker of chloride channels that are reported to be involved in volume regulation. In order to evaluate if NPPB had any effect in the $[Ca^{2+}]_i$ response during

osmotic stress, experiments were carried out to measure the effect of NPPB on human sperm exposed to hyposmotic shock. The same sequence of changes in osmolality was used, but this time 100 µM NPPB was present. The data shows that NPPB produced a immediate and substantial increase in $[Ca^{2+}]_i$ (figure 4.9: A), characterized by a high transient peak of fluorescence that fell rapidly before to stabilize at 5.1 ± 13.9% (figure 4.9: B). The rise in $[Ca^{2+}]_i$ occurred in 95% of the cells in this experiment and during the whole series 96% of the cells responded in similar way (119 out of 124 cells, n= 3 experiments). This increment in $[Ca^{2+}]_i$ was statistically significant ($P < 0.05$). When cells were challenged at 270 mOsm in presence of 100 µM NPPB the $[Ca^{2+}]_i$ exhibited a rise (figures 4.9: A and 4.9: B) that was also significant in comparison with its respective control ($P < 0.05$). The levels of fluorescence were stabilized at 13.6 ± 3.7% (figure 4.9: B). The response to 270 mOsm in the presence of NPPB was significantly smaller (8.4 ± 15.8%, which is the difference between 295 and 270 mOsm in presence of the drug) that when compared to the similar condition without it (12.1 ± 5.3%, $P < 0.001$). On the other hand, when the osmolality was restored to 295 mOsm there was a drop in the fluorescence (8 ± 3.5%) (figure 4.9: B). These results suggest that 100 µM NPPB mobilizes $[Ca^{2+}]_i$ in human sperm without attenuating the increment in $[Ca^{2+}]_i$ observed in response to osmotic stress.

A

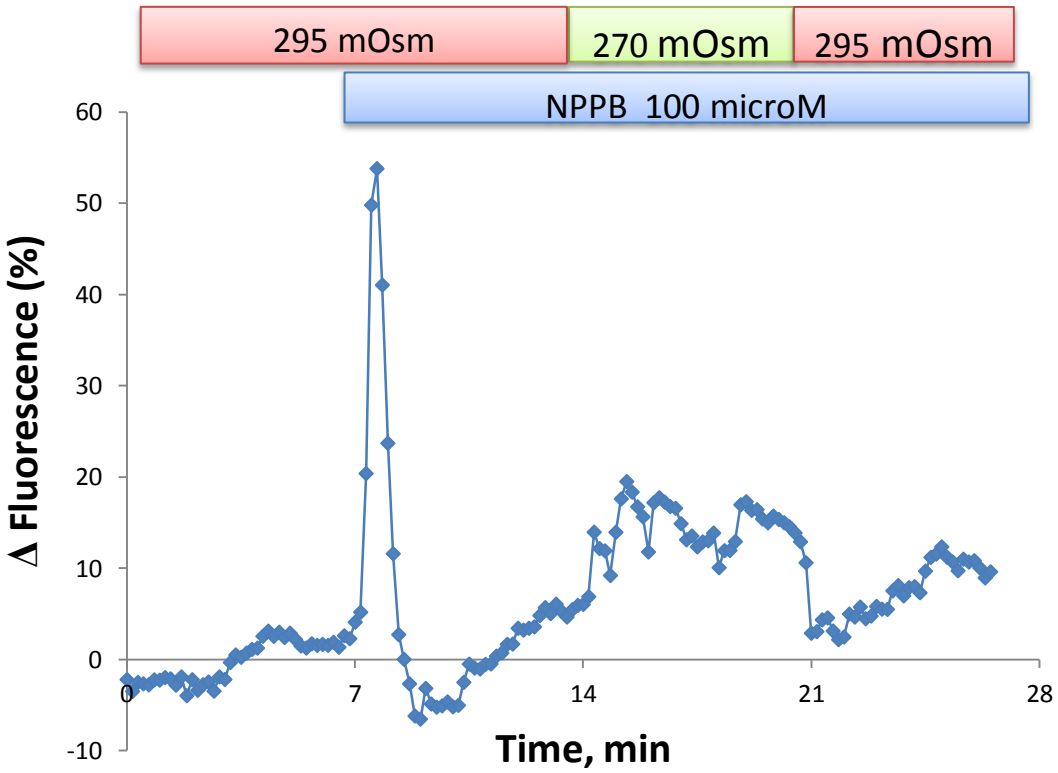
295 mOsm
270 mOsm
295 mOsm
NPPB 100 microM
Δ Fluorescence (%)
60
50
40
30
20
10
0
-10
0
7
14
21
28
Time, min

B

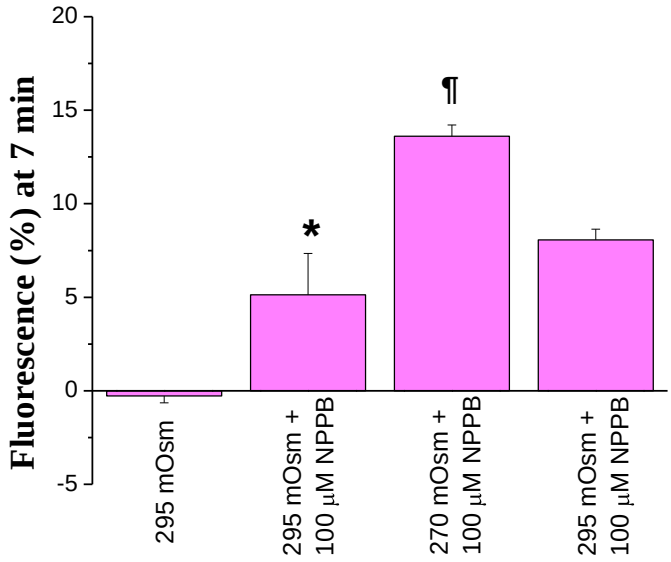
Fluorescence (%) at 7 min
20
15
10
5
0
-5
*
¶
295 mOsm
295 mOsm + 100 μM NPPB
270 mOsm + 100 μM NPPB
295 mOsm + 100 μM NPPB

Figure 4.9: A. Effect of hyposmotic shock and 100 µM NPPB on $[Ca^{2+}]_i$ in human sperm bathed in capacitating conditions (sEBSS). Cell samples were perfused with sEBSS (295 mOsm) for 7 min, exposed to 270 mOsm for 7 min then returned to 295 mOsm. After the initial control period 100 µM NPPB was present in all the subsequent conditions of osmolality, as shown by the blue bar. The trace represents the average of the typical response obtained from 41 cells (out of 43) in one experiment (a total of three were performed). **B.** Mean $[Ca^{2+}]_i$ during the absence (295 mOsm) and the presence of 100 µM NPPB (295, 270 and 295 mOsm). Bar charts show the mean normalized increase in fluorescence of the same cells after 7 min of incubation in every condition. Values expressed as mean ± SEM (n= 41 cells).

* $P < 0.05$ vs control 295 mOsm

¶ $P < 0.05$ vs control 295 mOsm + NPPB

4.4.4 Effect of Niflumic Acid on the $[Ca^{2+}]_i$ response to hyposmotic shock in human sperm

Niflumic acid is another well known blocker of chloride channels. In order to evaluate if niflumic acid had any effect in the $[Ca^{2+}]_i$ response during osmotic stress, experiments were carried out to measure the effect of 200 µM niflumic Acid on human sperm exposed to hyposmotic shock. The data shows that niflumic Acid produced an increase in $[Ca^{2+}]_i$ (figure 10.A), exhibiting a high transient peak of fluorescence that stabilized at 24.6 ± 11% (figure 10.B). The rise in $[Ca^{2+}]_i$ occurred in 97% of the cells in this experiment and during the whole series 92% of the cells responded in similar way (75 out of 81 cells n= 3 experiments). The increment in $[Ca^{2+}]_i$ was statistically significant ($P < 0.001$). When cells were challenged at 270 mOsm in presence of 200 µM niflumic acid the $[Ca^{2+}]_i$ exhibited a significant drop stabilizing at 15.7 ± 4% ($P < 0.001$) (figures 4.10: A and 4.10: B). When the osmolality is restored to 295 mOsm there was not significant change in the levels of fluorescence (Figure

10.B). These results suggest that 200 µM niflumic acid mobilizes $[Ca^{2+}]_i$ in human sperm and attenuates the levels of Ca^{2+} released in response to osmotic stress.

A

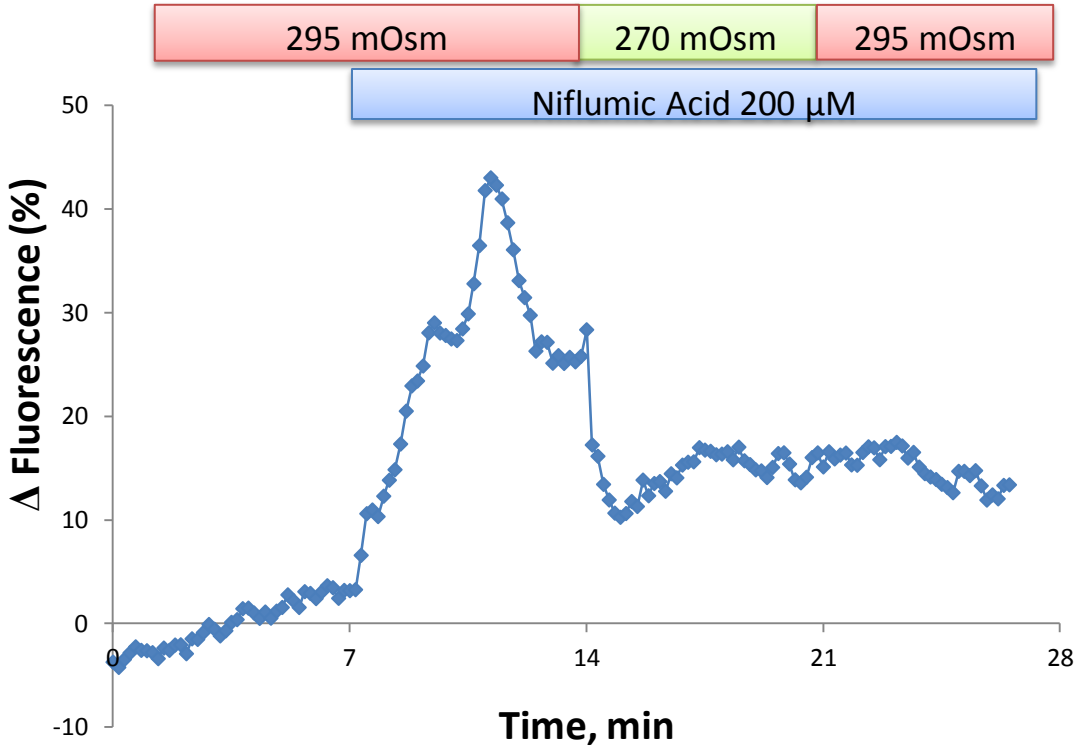

B

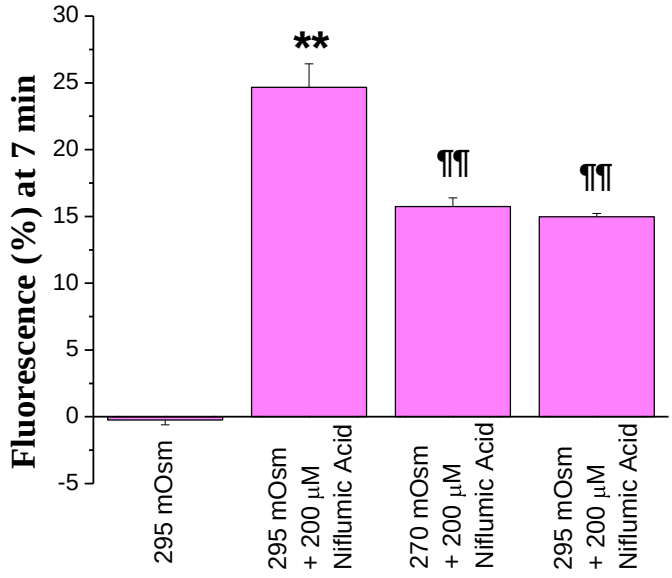

Figure 4.10: A. Effect of hyposmotic shock and 200 µM niflumic acid on $[Ca^{2+}]_i$ in human sperm bathed in capacitating conditions (sEBSS). Cell samples were perfused with sEBSS (295 mOsm) for 7 min, exposed to 270 mOsm for 7 min then returned to 295 mOsm. After the initial control period 200 µM niflumic acid was present in all the subsequent conditions of osmolality, as shown by the blue bar. The trace represents the average of the typical response obtained from 36 cells (out of 37) in one experiment (a total of three experiments were performed). **B.** Mean $[Ca^{2+}]_i$ during the absence (295 mOsm) and the presence of 200 µM niflumic acid (295, 270 and 295 mOsm). Bar charts show the mean normalized increase in fluorescence of the same cells after 7 min of incubation in every condition. Values expressed as mean ± SEM (n= 36 cells).

** $P < 0.001$ vs control 295 mOsm

¶¶ $P < 0.001$ vs control 295 mOsm + niflumic

4.5 Discussion

The role of Ca^{2+} in volume regulation has been established in other cell types previously, but had never been investigated in human spermatozoa. Indeed, when human sperm cells were exposed to the hyposmotic shock (270 mOsm) there was a significant rise in $[Ca^{2+}]_i$ in the majority of the cells (Figures 5.A and 5.B); this rise was characterized by an important and transient peak of fluorescence followed by a second phase with stabilization of levels that remained higher than during the control period (Figure 5.B). When the osmolality was restored to the previous condition (295 mOsm), little changes in $[Ca^{2+}]_i$ was observed. The rise in $[Ca^{2+}]_i$ when cells were exposed to 270 mOsm was statistically significant ($P < 0.001$). These results are of significant physiological importance due to the fact that the semen has osmolality of about 294 mOsm (Cooper et al., 2005), and once the ejaculation occurs the cells experience osmolalities of 280-294 mOsm (Casslen and Nilsson, 1984) in the cervical mucus and about 270 mOsm in the fallopian tubes (hydrosalpinx) (Ng et al., 2000) (Granot et al., 1998), requiring mechanisms to maintain the cell integrity and viability during

the passage of the sperm through these osmotic challenges. The data presented here suggest that $[Ca^{2+}]_i$ plays a pivotal role in volume regulation of human sperm under osmotic conditions that mimic the female tract. The mechanical and osmotic stress imposed by the hyposmolality might induce activation of Ca^{2+} channels at the plasma membrane that induce Ca^{2+} influx, which would trigger release of $[Ca^{2+}]$ from intracellular stores, hence contributing to the increase in $[Ca^{2+}]_i$. This could lead us to assume that the rise in $[Ca^{2+}]_i$ activates channels at the plasma membrane in charge of controlling the excess of volume entering to the cell.

Many cell types express Cl^- channels that are activated by cytosolic $[Ca^{2+}]_i$. Due to the importance of Cl^- channels in volume regulation I wanted to explore if the use of known blockers of Cl^- channels (DIDS, NPPB and niflumic acid) could modify the response of $[Ca^{2+}]_i$ during osmotic challenge. As evidenced here, 100 and 400 µM DIDS produced a significant increase in $[Ca^{2+}]_i$ when added to the preparation (figures 4.7: A and 4.8: A), followed by a plateau after the initial peak ($P < 0.001$) (figures 4.7: B and 4.8: B). However, the presence of DIDS prevented the rise of $[Ca^{2+}]_i$ in response to the hyposmotic stimuli. 400 µM DIDS has proven to impair volume regulation in human sperm (Yeung et al., 2005), therefore these results suggest that the effects of DIDS in volume regulation may have a relationship with $[Ca^{2+}]_i$ signalling. A possibility to explain the lack of response in $[Ca^{2+}]_i$ to osmotic stress might be that DIDS saturates specific mechanisms controlling $[Ca^{2+}]_i$ regulation that are also participating in volume regulation. However, we cannot discard that DIDS-induced swelling is due to Ca^{2+} - independent mechanisms (direct inhibition of anion channels or cell signalling pathways).

NPPB was also able to induce an increase in $[Ca^{2+}]_i$ in similar manner to DIDS but it did not

prevent the $[Ca^{2+}]_i$ rise in response to hypotonic conditions (Figures 9.A and B). Previous work indicate that 100 µM NPPB impairs volume regulation and therefore induces cell swelling in human sperm (Yeung et al., 2005). 10 µM NPPB is a potent agonist of TRP channels in mammalian HEK-293 cells, leading to a significant increase in $[Ca^{2+}]_i$ (Liu et al., 2010). In addition, 100 µM NPPB has been reported to inhibit 100% of T-Type Ca^{2+} currents (whole cell) in mouse spermatogenic cells (Espinosa et al., 1999). Finally, 200 µM niflumic acid increased basal $[Ca^{2+}]_i$ significantly (Figures 10.A and 10.B), but the $[Ca^{2+}]_i$ response to the osmotic stimuli was apparently reversed by pretreatment with the drug. With a concentration of 50 µM the drug increased basal $[Ca^{2+}]_i$ levels in rat pulmonary artery smooth muscle cells (Cruickshank et al., 2003), and 100 µM inhibited 100% of T-Type Ca^{2+} currents (whole cell) in mouse spermatogenic cells (Espinosa et al., 1999). The role of these ion channels and the possible involvement of intracellular stores need to be determined, in order to clarify the origin and the physiological implications of the Ca^{2+} signal during the osmotic stress.

In conclusion, the evidence suggest that $[Ca^{2+}]_i$ signals are induced in human sperm subject to hyposmotic challenge and that Ca^{2+} signaling may be involved in human sperm's RVD. The Cl^- channel blockers DIDS, NPPB and niflumic acid produced a substantial increase in basal $[Ca^{2+}]_i$ through mechanisms that, in the case of DIDS and niflumic acid, are able to attenuate the increase in $[Ca^{2+}]_i$ produced by hyposmotic stimuli. NPPB did not alter the $[Ca^{2+}]_i$ response to osmotic stress. In the following chapter more experiments are made in order to try to reveal what is the source of these $[Ca^{2+}]_i$ signals.

CHAPTER 5

EFFECT OF HYPOSMOTIC SHOCK AND CHLORIDE CHANNEL BLOCKERS IN CALCIUM SIGNALLING OF THE HUMAN SPERMATOZOON IN LOW CALCIUM sEBSS

5.1 Abstract

$[Ca^{2+}]_i$ might have an important role in Regulatory Volume Decrease (RVD) of human spermatozoa, but there is no information available regarding the source of mobilised Ca^{2+}, whether from outside or from intracellular stores. Human spermatozoa loaded with Oregon Green 488 BAPTA were superfused with low Ca^{2+} media (< 5 µM), and exposed to osmotic conditions that mimicked the hyposmotic shock experienced during the passage through the female tract. The effect of DIDS, NPPB and niflumic acid were tested in such conditions. The results show that the increase in $[Ca^{2+}]_i$ induced by the osmotic shocks is independent of extracellular Ca^{2+}. In addition, all the drugs produced a significant rise in $[Ca^{2+}]_i$, without affecting the increase in $[Ca^{2+}]_i$ produced by the osmotic challenges. These results suggest that release of Ca^{2+} from intracellular stores is the principal component of the $[Ca^{2+}]_i$ elevations observed in the human spermatozoa exposed to osmotic stress.

5.2 Introduction

Different theories to explain the role of intracellular Ca^{2+} stores in volume regulation have been proposed. Cell swelling and membrane stretch are able to induce IP_3 production by stimulation of phospholipase C and D (Dassouli et al., 1993, Jakab et al., 2002). Other reports propose that mobilization of $[Ca^{2+}]_i$ from intracellular stores may involve IP_3-independent processes such as prior entry of Ca^{2+} through stretch activated channels, with subsequent Ca^{2+} -induced Ca^{2+} release, or by a direct action of the cell stretching on the stores (Mohanty and Li, 2002, Galizia et al., 2008). $[Ca^{2+}]_i$ participates in RVD of rabbit TALH cells through release from intracellular stores induced by extracellular Ca^{2+} (Tinel et al., 2002). Thapsigargin prevents the hypotonic-induced $[Ca^{2+}]_i$ increase in rat cortical collecting duct line and abolishes rapid activation of RVD (Galizia et al., 2008). TMB8, an inhibitor of Ca^{2+} release from IP_3 sensitive stores, completely abolished RVD in eel intestine (Trischitta et al., 2005). The authors also postulate that Ca^{2+}-induced Ca^{2+} release is the fundamental mechanism for the response observed during hypotonicity (Trischitta et al., 2005). A similar trend showing the essential role of both extracellular Ca^{2+} and stores is reflected in other studies (Tinel et al., 1994, Mignen et al., 1999, Yellowley et al., 2002). In proliferating subpopulations of multicellular prostate cancer spheroids intracellular stores were the main source of Ca^{2+} signal in RVD (Sauer et al., 1998). Conversely, some groups have reported a lack of participation of intracellular stores in the Ca^{2+} response observed during RVD (Schlichter and Sakellaropoulos, 1994, Ross and Cahalan, 1995). In the previous chapter I presented data indicating that human spermatozoa exhibited an increase in $[Ca^{2+}]_i$ when exposed to hyposmotic conditions, and that different Cl^- channels blockers were able to induce a similar response. However, the origin (extracellular, intracellular or both) of these RVD-Ca^{2+} signals is still unknown.

The aims of this chapter were to investigate what the role of the extracellular Ca^{2+} in human sperm RVD is, and the possible role of intracellular stores. The effects of low Ca^{2+} conditions on the Ca^{2+} increase evoked by the treatment with Cl^- channel blockers are also evaluated. Please refer to the introduction of the chapter 4 (page 108) for more information about the role of Ca^{2+} in RVD.

5.3 Materials and methods

5.3.1 Materials

As described in chapter 4, page 109.

5.3.2 Preparation of spermatozoa

The nominal Ca^{2+} free sEBSS used in these assays was prepared according to a previous protocol from our lab (Harper et al., 2004). Basically Ca^{2+} free saline is normal sEBSS but with $CaCl_2$ left out and substituted with NaCl in order to maintain the correct osmolality. Because there is no EGTA in the saline there is a background "contaminating" level of Ca^{2+} (from water, glassware, etc) in the media. The protocol of Harper et al (Harper et al., 2004) used fluorimetry to quantify the exact amount of Ca^{2+} in media prepared in this way. The results determined that the Ca^{2+} concentration was less than 5 µM (Harper et al., 2004). The rest of the protocols were the same described in chapter 4, page 110.

5.3.3 Single cell imaging

As described in chapter 4, page 111.

5.3.4 Imaging data processing

As described in chapter 4, page 113.

5.3.5 Statistical analysis

Microsoft Excel© was used to produce the scatter charts and calculate the mean of fluorescence intensity of every cell at the specific point of time where the image was acquired; 40 images or points per condition, with an interval of 10 second between each one (equivalent to 7 min of recording under each condition examined). The data obtained were used for the statistical analysis. Bar charts and statistics were performed with the software OriginPro 8 Student Version (Origin Lab Corporation, Northampton, MA, USA). The results are expressed as mean ± standard error for the number of cells indicated in each case. The confidence interval was of 95%. Data analysis was performed with two sample Student's Test (unpaired data), with "*n"* being the number of repeated assays with different preparations. Only probabilities with values < 0.05 were accepted as significant. Though all experiments of a certain type clearly show a pattern of response, only the ones with stable control periods and steady responses were considered for further statistical analysis.

5.4 Results

5.4.1 Effect of hyposmotic shock on $[Ca^{2+}]_i$ of human sperm perfused with low extracellular Ca^{2+}

There are no reports about the effect of DIDS, NPPB and niflumic acid on $[Ca^{2+}]_i$ signalling of human sperm incubated in low extracellular $[Ca^{2+}]$ media. DIDS (100 and 400 µM), NPPB (100 µM) and niflumic acid (200 µM) were tested on cells exposed to media with osmolality

of 295 and 270 mOsm (200 mOsm couldn't be evaluated as the osmotic shoch was so strong that the cells were moved away from the lasso, which impeded any analysis). A previous work reported that 400 µM DIDS and 100 µM NPPB were able to induce cell swelling in human sperm (Yeung et al., 2005). In the same study 200 µM niflumic acid rather than increasing cell size produced cell shrinkage (Yeung et al., 2005). According to the authors the drugs only produced changes in cell size at these concentrations. I decided to use the same range of drug concentrations used in chapter 3 to evaluate any effect on $[Ca^{2+}]_i$. DIDS is an irreversible blocker in contrast with NPPB and niflumic acid wich are reversible (Jentsch et al., 2002). DMSO was used as a vehicle to prepare all the chemicals employed in the experiments.

In order to investigate if extracellular Ca^{2+} is important for the increment of $[Ca^{2+}]_i$ that occurs during osmotic stress, human sperm previously incubated with OGB-1AM were superfused with low Ca^{2+} (<5 µM) sEBSS for 5 min, before being exposed to the same sequence of osmotic challenges (chapter 4) using low Ca^{2+} sEBSS. Figure 11.A shows that a hyposmotic shock of 270 mOsm induced a rise in $[Ca^{2+}]_i$ in 68% of the cells in this particular experiment and during the whole series 55% of the cells studied responded in similar way (29 out of 53 cells, n= 3 experiments). The rest of the cells did not show any significant change in $[Ca^{2+}]_i$ at this stage. Fluorescence levels tended to stabilize at values of 24.5 ± 7% above the control period (vs 12.1 ± 5.3% in normal sEBSS, $P < 0.001$). This increment in $[Ca^{2+}]_i$ was statistically significant ($P < 0.001$) (figure 5.1: B). When cells were challenged again with medium at 295 mOsm, 55% (16 out of 29 cells, n= 3 experiments) of the "respondents" exhibited a further $[Ca^{2+}]_i$ increase that stayed up at levels of 44.7 ± 5.8% (figures 5.1: A and 5.1: B). However, the majority of the remaining 45% (13 out of 29 cells, n= 3 experiments) did not show any significant change in $[Ca^{2+}]_i$. The increment in $[Ca^{2+}]_i$ seen in cells that

responded to 295 mOsm was statistically significant ($P < 0.001$) (figure 5.1: B). These results suggest that the rise in $[Ca^{2+}]_i$ of human spermatozoa under osmotic stress depends mainly on intracellular stores.

A

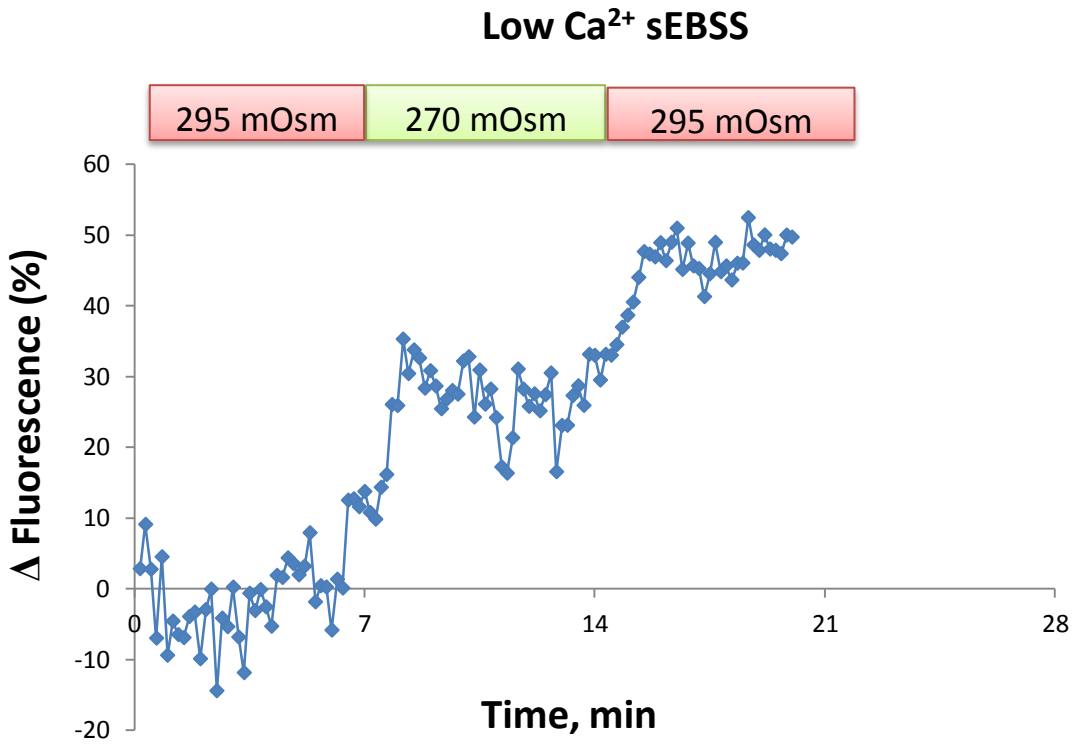

B

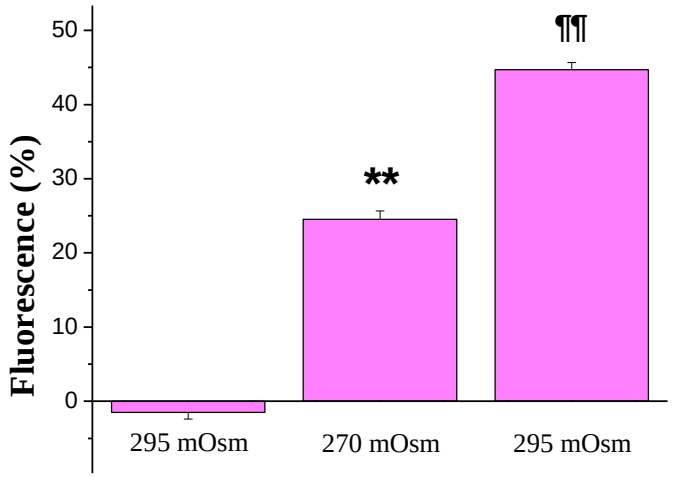

Figure 5.1: A. Effect of hyposmotic shock on $[Ca^{2+}]_i$ in human sperm perfused with low Ca^{2+} sEBSS (<5 µM). Cell samples were perfused with low Ca^{2+} sEBSS (295 mOsm) for 7 min, exposed to 270 mOsm for 7 min then returned to 295 mOsm. The trace represents the average of the typical response obtained from 12 cells (out of 22) in one experiment (a total of three were performed). **B.** Mean $[Ca^{2+}]_i$ during control conditions (295 mOsm) and hyposmotic (270 mOsm). Bar charts show the mean normalized increase in fluorescence of the same cells after 7 min of incubation in each condition except the last one, where the time taken was 3 min. Values expressed as mean ± standard error (n= 12 cells).

** $P < 0.001$ vs control

¶¶ $P < 0.001$ vs 270 mOsm

5.4.2 Effect of hyposmotic shock and DIDS on $[Ca^{2+}]_i$ in human sperm perfused with low extracellular Ca^{2+}

I investigated whether DIDS has effects on $[Ca^{2+}]_i$ and the response to osmotic shock when

sperm cells are in low Ca^{2+} media (<5 µM). The cells were prepared as described and the same sequence of changes of osmolality was used. The data show that 100 µM DIDS produced a significant increase in $[Ca^{2+}]_i$ (figures 5.2: A and 5.2: B). The rise in $[Ca^{2+}]_i$ occurred in 68% of the cells in this particular experiment and during the whole series 60% of the cells responded similarly (31 out of 52 cells, n= 2 experiments). The rest of the cells did not exhibit significant modifications in $[Ca^{2+}]_i$. This increment in $[Ca^{2+}]_i$ was statistically significant ($P < 0.001$) (figure 5.2: B) and the levels of fluorescence remained at 20.4 ± 11.3% (vs 53 ± 26.8% in normal sEBSS, $P < 0.001$). The fluorescence augmented (31.8 ± 4.6 % above control levels) during 270 mOsm ($P < 0.001$) but no appreciable peaks were observed (figure 5.2: A). The response to 270 mOsm in the presence of 100 µM DIDS was significantly smaller (11.4 ± 9.9%, which is the difference between 295 and 270 mOsm in presence of the drug) than that observed in the same condition without the drug (24.5 ± 7%, $P < 0.001$). When compared to similar conditions in normal sEBSS (65.3 ± 3.6% above control levels), the fluorescence levels were also significantly smaller ($P < 0.001$). No further changes were detected when the conditions were restored to 295 mOsm (figures 5.2: A and 5.2: B). When the effect of 400 µM DIDS was investigated a similar effect was observed (figures 5.3: A and 5.3: B), showing a significant ($P< 0.001$) increase in $[Ca^{2+}]_i$ in 83% of cells of the experiment shown and 76% of the entire population studied (42 out of 55 cells n= 3 experiments). The levels of fluorescence stabilized at 19.3 ± 11.2% (figure 5.3: B). When compared to similar conditions with normal sEBSS (11.2 ± 9.4%) there was an increment in the fluorescence ($P < 0.001$). Changing the osmolality to 270 mOsm produced an increase in the fluorescence (42.7 ± 5.3% above control levels) which was significant vs the control ($P < 0.001$). The response to 270 mOsm in the presence of 400 µM DIDS was significantly smaller (23.3 ± 12.1%, which is the difference between 295 and 270 mOsm in presence of the drug) than that observed in the same condition without the drug (24.5 ± 7%, $P < 0.001$).

When compared to similar conditions with normal sEBSS (12.6 ± 0.9% above control levels) there was a significant increase in fluorescence levels ($P < 0.001$). After exposition to 270 mOsm the fluorescence did not stabilize completely, instead showing a progressive increase in $[Ca^{2+}]_i$ that was higher than during 270 mOsm when the medium was restored at 295 mOsm ($P < 0.001$). These results suggest that DIDS induces an increase in $[Ca^{2+}]_i$ due to mobilization from intracellular stores and that this does not totally prevent the elevation in $[Ca^{2+}]_i$ caused by osmotic challenge.

A

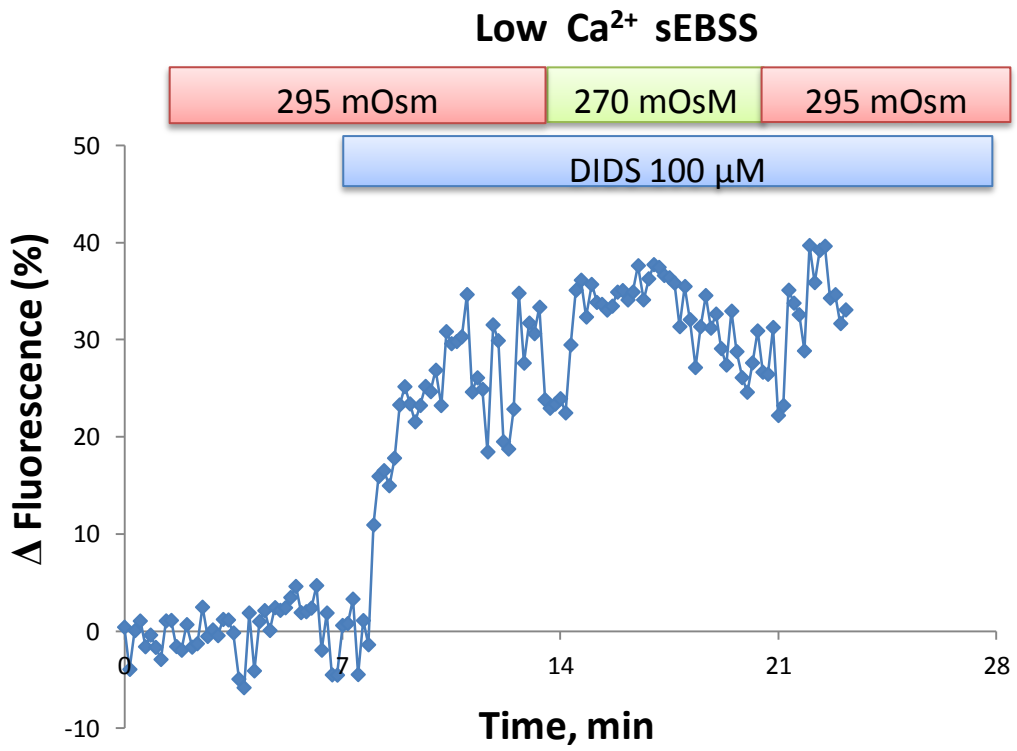

B

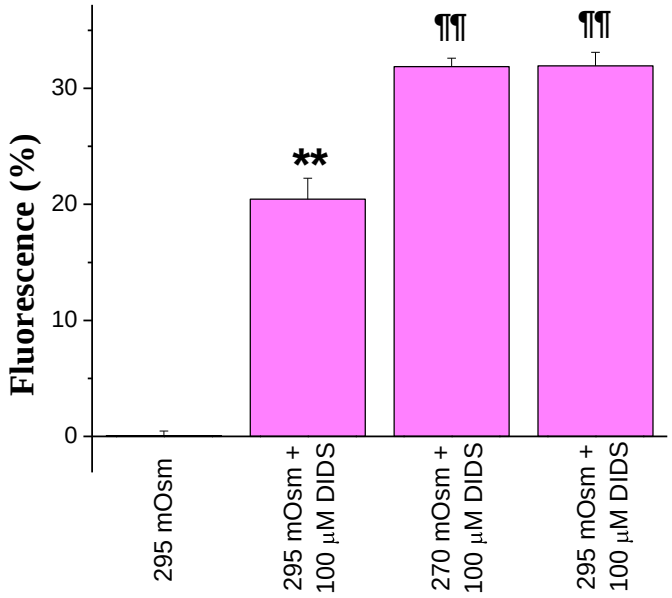

Figure 5.2: A. Effect of 100 μM DIDS and hyposmotic shock on $[Ca^{2+}]_i$ in human sperm perfused with low Ca^{2+} sEBSS (<5 μM). Cell samples were perfused with sEBSS (295 mOsm) for 7 min, exposed to 270 mOsm for 7 min then returned to 295 mOsm. After the initial control period 100 μM DIDS was present in all the subsequent conditions of osmolality, as shown by the blue bar. The trace represents the average of the typical response obtained from 15 cells (out of 22) in one experiment (a total of two were peformed). **B.** Mean $[Ca^{2+}]_i$ during the absence (295 mOsm) and the presence of 100 μM DIDS (295, 270 and 295 mOsm). Bar charts show the mean normalized increase in fluorescence of the same cells after 7 min of incubation in every condition except the last one, where the time taken was 3 min. Values expressed as mean ± SEM (n= 15 cells).

** $P < 0.001$ vs control 295 mOsm

¶¶ $P < 0.001$ vs control 295 mOsm + DIDS

A

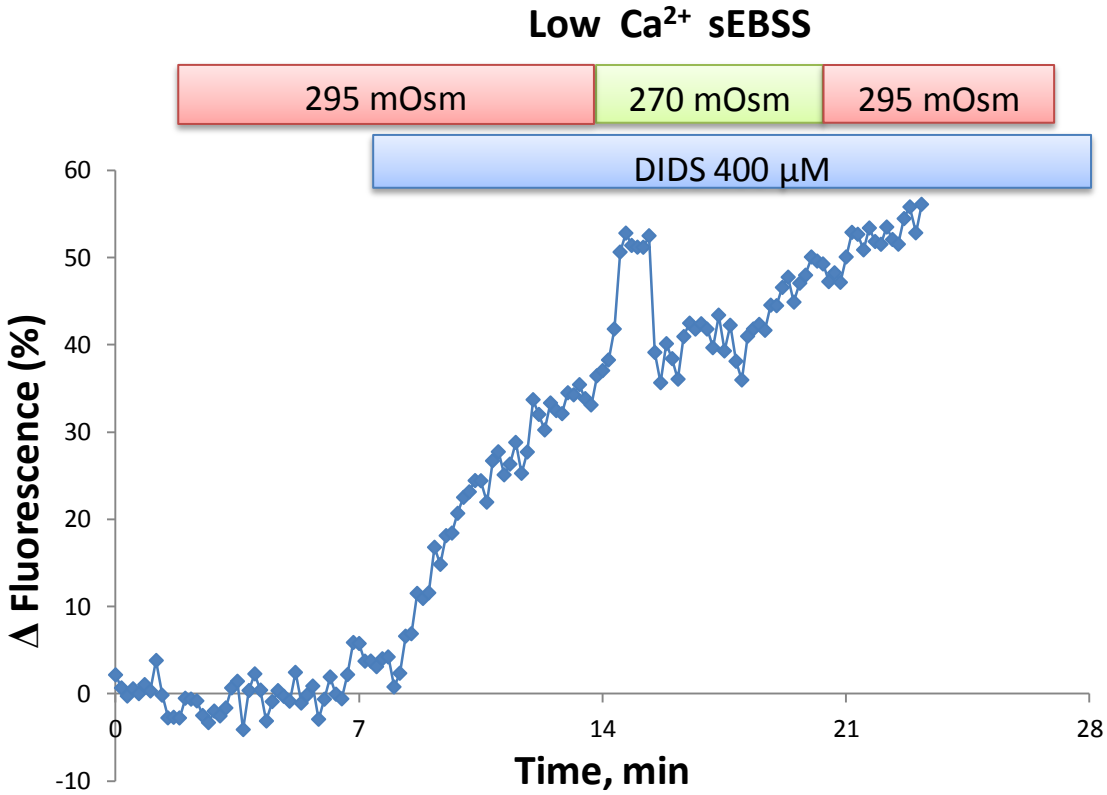
Low Ca2+ sEBSS
295 mOsm
270 mOsm
295 mOsm
DIDS 400 µM
Δ Fluorescence (%)
60
50
40
30
20
10
0
-10
0
7
14
21
28
Time, min

B

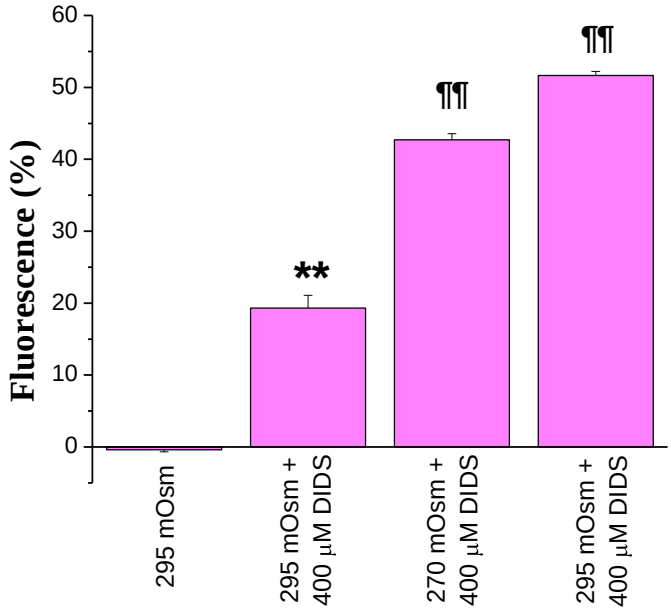
Fluorescence (%)
60
50
40
30
20
10
0
**
¶¶
¶¶
295 mOsm
295 mOsm + 400 µM DIDS
270 mOsm + 400 µM DIDS
295 mOsm + 400 µM DIDS

Figure 5.3: A. Effect of 400 µM DIDS and hyposmotic shock on $[Ca^{2+}]_i$ in human sperm perfused with low Ca^{2+} sEBSS (<5 µM). Cell samples were perfused with sEBSS (295 mOsm) for 7 min, exposed to 270 mOsm for 7 min then returned to 295 mOsm. After the initial control period 400 µM Niflumic Acid was present in all the subsequent conditions of osmolality, as shown by the blue bar. The trace represents the average of the typical response obtained from 24 cells (out of 29) in one experiment (a total of three were peformed). **B.** Mean $[Ca^{2+}]_i$ during the absence (295 mOsm) and the presence of 400 µM DIDS (295, 270 and 295 mOsm). Bar charts show the mean normalized increase in fluorescence of the same cells after 7 min of incubation in every condition except the last one, where the time taken was 3 min. Values expressed as mean ± SEM (n= 24 cells).

** $P < 0.001$ vs control 295 mOsm

¶¶ $P < 0.001$ vs control 295 mOsm + DIDS

5.4.3 Effect of NPPB and hyposmotic shock on $[Ca^{2+}]_i$ in human sperm perfused with low extracellular Ca^{2+}

The data show that 100 µM NPPB is able to produce a rise in $[Ca^{2+}]_i$ (figures 5.4: A and 5.4: B) in low Ca^{2+} media (<5 µM) immediately. The rise in $[Ca^{2+}]_i$ occurred in 74% of the cells in the experiment and 79% of the cells during the rest of the series (42 out of 62 cells, n= 3 experiments). The change in $[Ca^{2+}]_i$ was statistically significant ($P < 0.001$) and the levels of fluorescence remained at 35.5 ± 12.7% (figure 5.4: B). When compared to similar conditions with normal sEBSS (5.1 ± 13.9% above control levels) there was a significant increase in fluorescence ($P < 0.001$). When cells were challenged at 270 mOsm in presence of 100 µM NPPB there was no evident peak of $[Ca^{2+}]_i$. However, the fluorescence levels continued elevated reaching 45.8 ± 3.6% above control levels. The response to 270 mOsm in the presence of NPPB was significantly smaller (10.3 ± 11.7%, which is the difference between 295 and 270 mOsm in presence of the drug) that when compared to the similar condition without it (24.5 ± 7%, $P < 0.001$). When compared to similar conditions with normal sEBSS

(13.6 ± 3.7% above control levels), the levels of fluorescence are also significantly smaller ($P < 0.001$). No change occurred when the osmolality was restituted to 295 mOsm. These results suggest that NPPB is mobilizing Ca^{2+} from intracellular stores and that this does not totally prevent the elevation in $[Ca^{2+}]_i$ during osmotic stress.

A

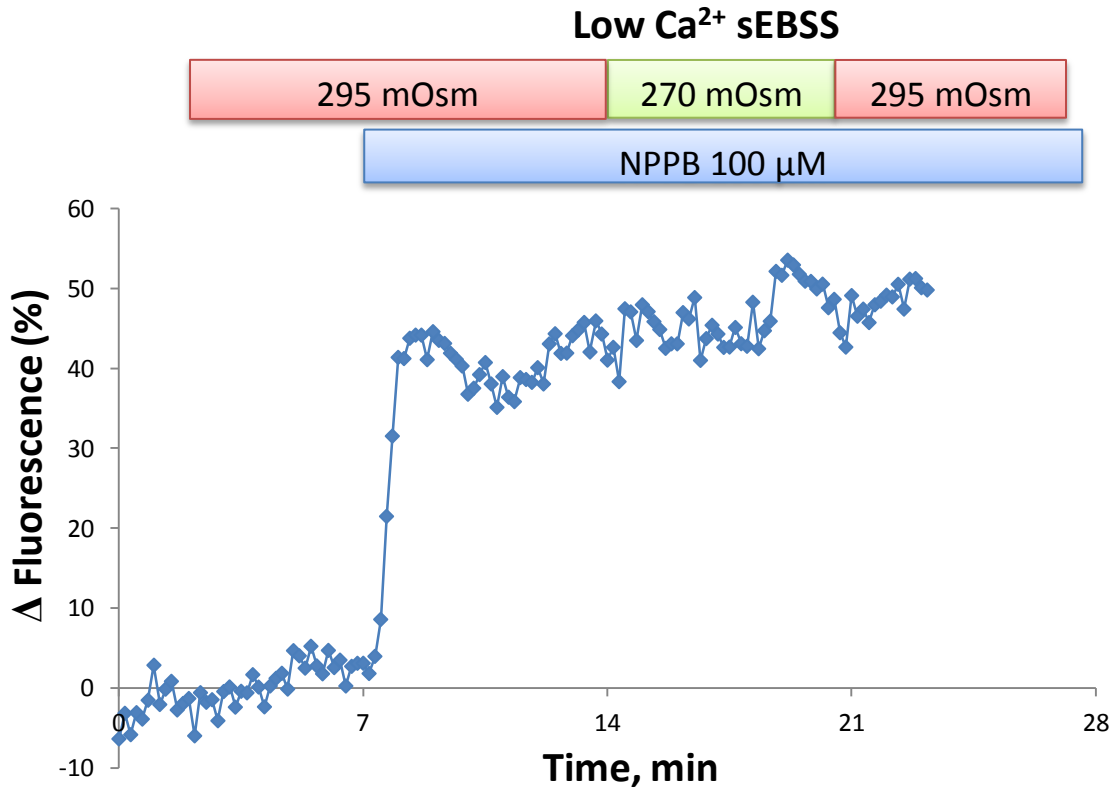

B

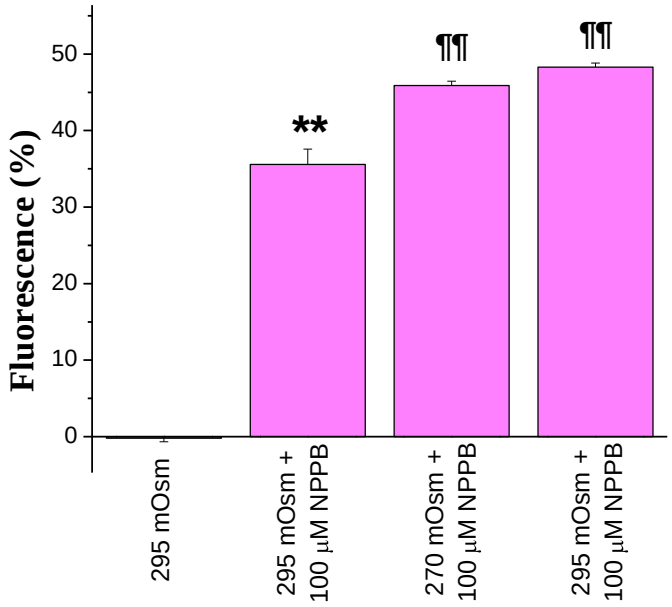

Figure 5.4: A. Effect of 100 μM NPPB and hyposmotic shock on $[Ca^{2+}]_i$ in human sperm perfused with low Ca^{2+} sEBSS (<5 μM). Cell samples were perfused with sEBSS (295 mOsm) for 7 min, exposed to 270 mOsm for 7 min then returned to 295 mOsm. After the initial control period 100 μM NPPB was present in all the subsequent conditions of osmolality, as shown by the blue bar. The trace represents the average of the typical response obtained from 26 cells (out of 27) in one experiment (a total of three were peformed). **B.** Mean $[Ca^{2+}]_i$ during the absence (295 mOsm) and the presence of 100 μM NPPB (295, 270 and 295 mOsm). Bar charts show the mean normalized increase in fluorescence of the same cells after 7 min of incubation in every condition except the last one, where the time taken was 3 min. Values expressed as mean ± SEM (n= 26 cells).

** $P < 0.001$ vs control 295 mOsm

¶¶ $P < 0.001$ vs control 295 mOsm + NPPB

5.4.4 Effect of Niflumic Acid and hyposmotic shock on $[Ca^{2+}]_i$ in human sperm perfused with low extracellular Ca^{2+}

The data shows that 200 µM niflumic acid increased $[Ca^{2+}]_i$ (figures 5.5: A and 5.5: B) in low Ca^{2+} media (<5 µM). The rise in $[Ca^{2+}]_i$ occurred in 55% of the cells in the experiment and 60% of the entire population of cells evaluated (35 out of 58 cells, n= 3 experiments). The rise in $[Ca^{2+}]_i$ was statistically significant ($P < 0.001$) and the levels of fluorescence were 15.7 ± 9.1 % (Figure 5.5: B). When compared to similar conditions with normal sEBSS (24.6 ± 11%) this was a significantly smaller response ($P < 0.001$). When cells were challenged at 270 mOsm in presence of 200 µM niflumic acid the $[Ca^{2+}]_i$ exhibited a rise that was also significant ($P < 0.001$). The fluorescence levels stabilized at 26.7 ± 4.7% (Figure 5.5: B). The response to 270 mOsm in the presence of niflumic acid was significantly smaller (11 ± 7%, which is the difference between 295 and 270 mOsm in presence of the drug) than that observed in the same condition without the drug (24.5 ± 7%, $P < 0.001$). When compared to similar conditions with normal sEBSS (15.7 ± 4%), the fluorescence levels were also significantly smaller ($P < 0.001$). There was no significant increase in $[Ca^{2+}]_i$ when osmolality is restored to 295 mOsm (figures 5.5: A and 5.5: B). These results suggest that the increase in $[Ca^{2+}]_i$ induced by niflumic acid probably is due to Ca^{2+} release from intracellular stores, and that this pretreatment partially inhibits elevation in $[Ca^{2+}]_i$ caused by osmotic stress.

A

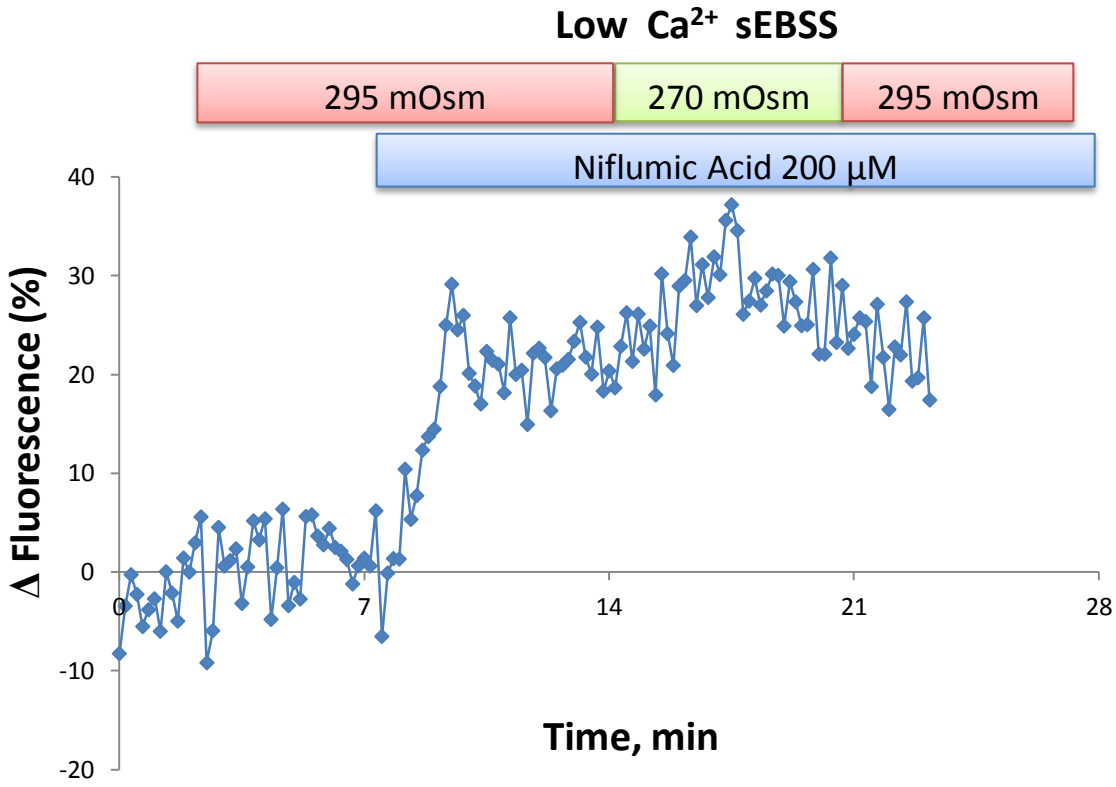
Low Ca2+ sEBSS
295 mOsm
270 mOsm
295 mOsm
Niflumic Acid 200 µM
Δ Fluorescence (%)
40
30
20
10
0
-10
-20
0
7
14
21
28
Time, min

B

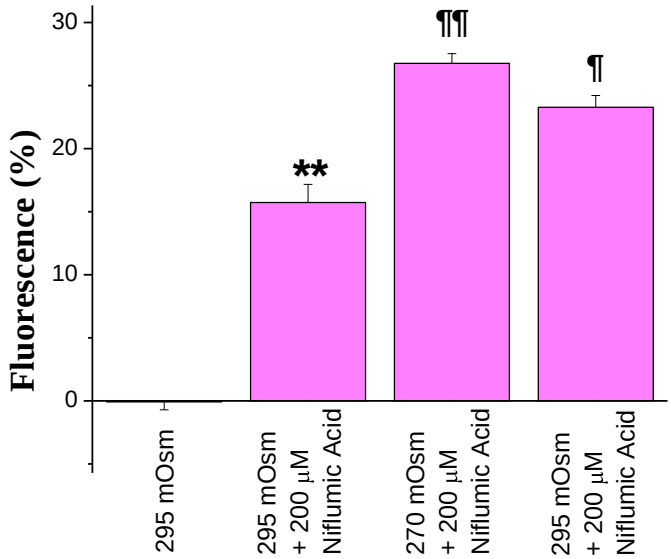
Fluorescence (%)
30
20
10
0
**
¶¶
¶
295 mOsm
295 mOsm + 200 µM Niflumic Acid
270 mOsm + 200 µM Niflumic Acid
295 mOsm + 200 µM Niflumic Acid

Figure 5.5: A. Effect of 200 µM Niflumic Acid and hyposmotic shock on $[Ca^{2+}]_i$ in human sperm perfused with low Ca^{2+} sEBSS (<5 µM). Cell samples were perfused with sEBSS (295 mOsm) for 7 min, exposed to 270 mOsm for 7 min then returned to 295 mOsm. After the initial control period 200 µM Niflumic Acid was present in all the subsequent conditions of osmolality, as shown by the blue bar. The trace represents the average of the typical response obtained from 12 cells (out of 22) in one experiment (a total of three were peformed). **B.** Mean $[Ca^{2+}]_i$ during the absence (295 mOsm) and the presence of 200 µM Niflumic Acid (295, 270 and 295 mOsm). Bar charts show the mean normalized increase in fluorescence of the same cells after 7 min of incubation in every condition except the last one, where the time taken was 3 min. Values expressed as mean ± SEM (n= 12 cells).

** $P < 0.001$ vs control 295 mOsm

¶ $P < 0.05$ vs control 295 mOsm + Niflumic

¶¶ $P < 0.001$ vs control 295 mOsm + Niflumic

5.5 Discussion

The data presented here provide evidence that in human spermatozoa, the increase in basal $[Ca^{2+}]_i$ induced by the osmotic stress is at least partly due to Ca^{2+} release from intracellular stores. The increase in $[Ca^{2+}]_i$ exhibited the same biphasic pattern observed when the cells are incubated in standard media with Ca^{2+}. When exposed at 270 mOsm the kinetics and amplitude of the Ca^{2+} response were similar to those detected with normal sEBSS. It is noteworthy to mention that when the cells were perfused again with 295 mOsm after being exposed to 270 mOsm, almost half of the cells had elevated levels of $[Ca^{2+}]_i$, whereas the majority of the other half did not show any increase (which is similar to the observed in normal sEBSS). This behavior might be due to loss of Ca^{2+} homeostasis in a percentage of cells when exposed to low extracellular Ca^{2+} media. Extracellular Ca^{2+} might be participating

in regulatory mechanisms that in its absence would make cells unable to control the Ca^{2+} responses to osmotic stress. Moreover, we cannot discard that the variability in quality and sperm characteristics among samples (and hence donors) might be having a role in the degree of responses observed. More experiments are needed to identify the exact pattern in sperm cells exposed to such condition.

Several hypotheses have been proposed regarding how hypotonic challenge may activate the intracellular stores for Ca^{2+} release. For instance, cell stretching may bring about a conformational change in intracellular stores, affecting IP_3, ryanodine receptors or NAADP channels (Mohanty and Li, 2002), with the subsequent Ca^{2+} release. It is also possible that the cytoskeletal network transmits mechanical force from the surface of the cells to the intracellular Ca^{2+} stores without a chemical mediator, resulting in a direct release of Ca^{2+} (Mohanty and Li, 2002). Another group working in vascular endothelial cells presented data indicating that the exposure of these cells to a hypotonic solution results in an influx of water, leading to dilution of cytoplasm and thus exposure of the intracellular stores to this hypotonic environment, which produces swelling of the intracellular stores (Jena et al., 1997). Human sperm posses a "toolkit" of intracellular stores that participate in the amplification of the Ca^{2+} signal needed for a range of activities like capacitation, motility, hyperactivation and acrosome reaction (Jimenez-Gonzalez et al., 2006, Costello et al., 2009). IP_3 receptors, RyRs, SERCA, SPCA, and mitochondria are present in human sperm and they are all located in the midpiece (Costello et al., 2009), though IP_3 receptors are also located in the acrosome (Costello et al., 2009). In addition our lab has recently identified the presence of Orai and STIM1 in the neck region and midpiece mainly (data not published). STIM1 is the putative sensor for detection of Ca^{2+} store status and Orai is thought to form Ca^{2+}- permeable membrane channels involved in "capacitative" Ca^{2+} entry (Costello et al., 2009). The

stimulation of Ca^{2+} release from stores in osmotic stress might be due to the lack of cytoplasm and the proximity of these intracellular organelles to the plasma membrane in the neck and midpiece. The mechanical force would be transmitted directly to the stores opening up the "gates" for releasing Ca^{2+} required for activation of channels (K^+ and Cl^-) controlling cell volume. Conformational changes induced by cell stretching and direct exposition to the hyposmotic solution are also attractive alternatives that need to be considered in order to explain this Ca^{2+} release. However, the role of a chemical mediator cannot be excluded completely. Further studies are required to discern which specific mechanisms apply in the case of human spermatozoa.

The different Cl^- channel blockers were effective in increasing the basal $[Ca^{2+}]_i$, indicating that they are producing Ca^{2+} mobilization from stores within the cell, although showing some differences in the amplitude when compared to experiments with normal sEBSS. The amplitude of the response to DIDS was lower at 100 µM and higher at 400 µM when compared to normal sEBSS. NPPB showed higher amplitude in the Ca^{2+} response in comparison with normal sEBSS. On the other hand, niflumic acid exhibited decreased amplitude when compared with normal sEBSS. The variability in the amplitude might be due to lack of regulatory mechanisms that are $[Ca^{2+}]_o$- dependent. This need to be further investigated with more replicates as well as with different experiments.

Though all three of the drugs clearly were able to mobilise stored Ca^{2+}, the drugs did not abolish the increment in Ca^{2+} levels that occurred when the osmotic shock was applied. This applies especially for 400 µM DIDS and niflumic acid (contrary to what was observed in normal sEBSS). Thus the ability of these Cl^- channel inhibitors to interfere with RVD, leading to changes in cell motility and morphology (chapters 1 and 2) probably cannot be

ascribed to interference with osmotically activated Ca^{2+} signalling. Reasons for such difference between the effect seen in normal sEBSS and low Ca^{2+} might be variability between sperm samples (donors), or activation of other Ca^{2+} signalling pathways due to the lack of extracellular Ca^{2+}. Further experiments are required to clarify the exact pattern of response.

A previous report (Cruickshank et al., 2003) showed that 100 µM DIDS increased basal $[Ca^{2+}]_i$ in rat pulmonary artery smooth cells. The authors cited a paper (Kawasaki and Kasai, 1989) stating that DIDS activates the ryanodine receptor and locks it in an open state without decreasing the single channel conductance. Another study has also showed an increase of ryanodine receptor-channel activity by DIDS (Sitsapesan, 1999). If this is the action exerted by the channel blockers used in this study then we must conclude that the ryanodine receptor-mobilised store is not the same Ca^{2+} storage compartment as that mobilized by osmotic challenge. The pharmacological evidence presented by Cruickshank et al (Cruickshank et al., 2003) indicates that niflumic acid-induced rise of $[Ca^{2+}]_i$ in rat pulmonary artery smooth muscle cells is due to release of Ca^{2+} from an intracellular store compatible with the ryanodine receptor. Moreover, the authors show that NPPB is also able to increase basal $[Ca^{2+}]_i$ levels, which was attributed to the sarcoplasmatic reticulum, and more specifically, to the ryanodine receptor (Cruickshank et al., 2003). However, Cruickshank et al postulate that it is improbable that DIDS enters into the cell, because is membrane impermeant, unless there is a specific transporter for getting the drug inside the cells, hence it would be unlikely to have an effect of DIDS on the ryanodine receptor in an intact cell (Cruickshank et al., 2003). On the other hand, DIDS is able to inhibit the PMCA (Plasma Membrane Calcium ATPase) (Niggli et al., 1982), which could explain the increase in $[Ca^{2+}]_i$.

Human spermatozoa possess different intracellular tools for Ca^{2+} homeostasis. These structures together, or separately, could be targeted by the drugs to induce the Ca^{2+} release. The results presented here provide a new insight about the functional role of intracellular Ca^{2+} stores in the physiology of RVD of human spermatozoa. More work is required to establish their exact involvement in RVD and Ca^{2+} homeostasis.

CHAPTER SIX

GENERAL DISCUSSION

The aim of this thesis was to evaluate the effect of osmotic challenges - that resembled the conditions found in the female tract - in the motility and Ca^{2+} homeostasis of human spermatozoa. Without RVD, hyposmotic challenge leads to cell swelling which in human sperm results in angulation of the flagellum and loss of motility (Yeung and Cooper, 2001). Particular emphasis was put in the role of Cl^- channels in these processes, as they are pivotal for the mechanisms involved in volume regulation of many cells.

A particular problem of studying Cl^- channels is the lack of specific inhibitors. The chemicals available have broad effects on other transport systems at the cell membrane. In this study, the Cl^- channel blockers DIDS, NPPB, and niflumic acid were used for evaluating the possible actions of Cl^- channels in the human sperm functions mentioned above. The results revealed that only DIDS was capable of impairing sperm motility (50 and 100 µM), and when the concentration of DIDS was augmented to 400 µM motility was abolished. NPPB and niflumic acid had no effects in overall motility despite the fact that they reduced, in some cases, parameters such as progressive velocity, track velocity, LIN, straightness and VAP. The different profiles of inhibition for the three chemicals remained consistent throughout the diverse osmotic conditions evaluated. However, because of the high variability exhibited in the kinematic parameters, it is difficult to establish patterns to discern which one is/are more important for overall motility. The only clear conclusion is that 400 µM DIDS is able to strongly reduce the overall motility and the subset of motility parameters in most of the osmotic conditions evaluated.

There are few reports available in the literature regarding the effect of DIDS on motility. 100

μM DIDS did not affect sperm motility in hamster, and although 1 mM DIDS reduced velocity and increased the curvature radius of the flagellum there was no modification on the percentage of motile cells (Visconti et al., 1990). Nonetheless, 25 μM DIDS + HCO_3^- was able to enhance motility, respiration rate and the cAMP content in pig sperm (Tajima and Okamura, 1990). The data presented here constitute the first report showing the detrimental effects of different concentrations of DIDS on human sperm motility. With regards to the effect of NPPB, the results are in agreement with a previous study reporting that NPPB (50 μM) did not impair motility in mouse sperm (Yeung et al., 1999). On the other hand, niflumic acid (10-20 μM) increased flagellar bending in response to speract (an egg-derived sperm-activating peptide) in sea urchin (Wood et al., 2007), but no such effect could be determined in this study.

DIDS (400 μM) and NPPB (100 μM) induced cell swelling by inhibition of RVD in human sperm, whereas niflumic acid (200 μM) induced cell shrinkage (Yeung et al., 2005). Sperm cell swelling due to loss of RVD induced by quinine has been linked to impairment of both migration and penetration through cervical mucus (Yeung and Cooper, 2001). Nonetheless, although the influence of cell volume in motility cannot be discarded, it seems that Cl^- channel blockers-induced inhibition of RVD is not the principal cause of low motility *per se* for several reasons: only 400 μM DIDS was able to induce sperm swelling measured by flow cytometry (Yeung et al., 2005) whereas 50 and 100 μM DIDS (and not only 400 μM) inhibited sperm motility significantly; NPPB did not impair motility despite the fact that was able to induce sperm swelling measured by flow cytometry (Yeung et al., 2005). Rather, the effect of DIDS might be a direct consequence of impairment of cell signaling pathways, such as cAMP regulation, phosphorylation of specific proteins and others, that are dependent of the transport of HCO_3^-; evidenced by the inhibition of the serine/threonine phosphorylation of

proteins produced by the presence of DIDS. It has been reported that DIDS inhibits the HCO_3^- transport (HCO_3^- / Cl^- exchanger) (Visconti et al., 1990). The diminution of HCO_3^- entry into the cell would lead to reduction of cAMP levels by inhibition of the soluble adenylate cyclase (that catalyses the production of cAMP). The reduction of cAMP levels would affect PKA activity, and hence, the levels of serine/threonine and tyrosine phosphorylation of some proteins critical for sperm motility. Moreover, reduction of intracellular HCO_3^- may produce acidification within the cells. This will affect the activity of different mechanisms such as human sperm dynein ATPases, which are responsible of the movement of sperm flagella (Vivenes et al., 2009), the pH-dependent CatSper channels in the flagellar membrane, causing a fall in resting $[Ca^{2+}]_i$ (Ren et al., 2001), and many others enzymatic and non enzymatic systems that could participate in motility (such as ATPases, exchangers, calcium channels, anion channels, etc), including the adenylate cyclase.

With regards to the morphological alterations that might occur after treatment with the chemicals, 400 µM DIDS was able to increase the percentage of coiled sperm. No significant changes were observed with 50 and 100 µM DIDS (in contrast with the results in motility). On the other hand, NPPB incremented the percentage of coiled sperm during the extreme condition of 200 mOsm, and niflumic acid did the same at 270 mOsm only. In light of the observation that 400 µM DIDS produced a drastic reduction in sperm motility, it might be the case that this concentration is also affecting the cell in such a way, that coiling of the flagella becomes necessary due to the increase in volume. However, it is obvious that most accurate techniques for measuring cell size (e.g. flow cytometry) are needed before to draw any conclusion, as changes in volume that might not be detectable with the conventional microscope might be able to produce significant disturbance of cell homeostasis, i.e. sperm motility.

This is the first observation of the effect of hyposmotic challenge in $[Ca^{2+}]_i$ levels of human spermatozoa. There was a significant increase in $[Ca^{2+}]_i$ in response to osmotic challenge (270 mOsm), characterized by an important and transient peak of fluorescence followed by a second phase with stabilization of levels that remained higher than during the control period. The data also show that an important component of the $[Ca^{2+}]_i$ response to osmotic stress is due to intracellular stores. Further studies are necessary to establish the functional significance of these $[Ca^{2+}]_i$ signals, but these findings suggest that Ca^{2+} plays a significant role in volume regulation of human spermatozoa exposed to osmotic changes that mimic the female tract.

The Cl^- channel blockers used for the assessment of motility and morphology were assessed for their effects on the osmotically-induced $[Ca^{2+}]_i$ response and the possible participation of the Ca^{2+}-activated Cl^- channels in the RVD process. The results show that DIDS (100 and 400 µM), NPPB (100 µM) and niflumic acid (200 µM) induced a substantial and immediate rise in $[Ca^{2+}]_i$ followed by a plateau in the fluorescence levels. Moreover, DIDS and niflumic acid seem to attenuate the $[Ca^{2+}]_i$ response to osmotic stress. These results are in agreement with reports describing that DIDS, NPPB and niflumic acid are able to mobilize $[Ca^{2+}]_i$ due to release from the ryanodine receptors (Kawasaki and Kasai, 1989, Sitsapesan, 1999, Cruickshank et al., 2003). Although DIDS is also able to inhibit the PMCA activity (Niggli et al., 1982). Thus effects of Cl^- channel blockers on RVD and consequent effects on morphology and motility may reflect impairement of cellular Ca^{2+} signals induced by osmotic challenge.

In conclusion, the results suggest that pharmacological blockade of Cl^- channels to investigate impairment of RVD and downstream effects on cell function must be interpreted cautiously. The effect of DIDS on motility is probably due to failure of the HCO_3^- transport by means of inhibition of the HCO_3^- / Cl^- exchanger, which leads to reduced serine/threonine phosphorylation of proteins. $[Ca^{2+}]_i$ is probably important for human sperm homeostasis in response to osmotic stress, and the principal source of this Ca^{2+} are intracellular stores. DIDS, NPPB and niflumic acid induce mobilisation of $[Ca^{2+}]_i$ in human spermatozoa that may interfere with the usual $[Ca^{2+}]_i$ response to hyposmotic shock.

6.1 Future Research

The importance of Ca^{2+} in RVD of human spermatozoa must be establish with experiments using flow cytometry, or a similar system, for measuring cell size under low extracellular Ca^{2+}. Another line of research would be to study the effect of gadolinium (which can block stretch-activated ion channels) in cell volume and $[Ca^{2+}]_i$ of human sperm cells. The role of CFTR channels (which possess a specific pharmacological inhibitor) in RVD must be further studied. The specific origin of the $[Ca^{2+}]_i$ signal in response to osmotic stress and the exact role of ryanodine receptors, Orai, STIM, SPCA, must be elucidated. It becomes clear that intracellular pH measurements in cells treated with DIDS should be performed. Finally, patch clamp studies to characterize the hyposmotic-induced ionic currents are vital to understand the physiology of RVD in human spermatozoa.

APPENDIX I: PATCH CLAMP

A substantial component of the original project involved patch clamp of human sperm in order to study the activity of anion channels under osmotic challenge. Our lab had been successful in patch clamp of human sperm in the past (Jimenez-Gonzalez et al., 2007), therefore I was given the opportunity to continue with this research. I had no experience with electrophysiology; nonetheless I found the project very interesting and tried to learn as quickly as possible.

I spent the first one and a half years based exclusively at the Medical School trying to get recordings from the cells. Unfortunately, due to technical reasons that included problems with the software and noise from unknown origin, it was impossible to obtain any data of value. Therefore my supervisor and I agreed to abandon the patch clamp and focus in the Ca^{2+} imaging under osmotic stress.

Patch clamp of human sperm has proven to be very difficult, but significant progress has been made recently with the first report of whole cell recordings (Lishko et al., 2010). I still think that with the right conditions, this technique can give us extraordinary insights into the human sperm physiology.

APPENDIX II: MEDIA

Supplemented Earle's Balanced Salt Solution (sEBSS)

Sodium Dihyd. Phosphate 0.122g/l (1.0167 mM)

Potassium Chloride 0.4g/l (5.4 mM)

Magnesium Sulphate.7H_2O 0.2g/l (0.811 mM)

Dextrose Anhydrous 1.0g/l (5.5 mM)

Sodium Pyruvate 0.3g/l (2.5 mM)

DL-Lactic Acid, Sodium 4.68g/l (19.0 mM)

Calcium Chloride.2H_2O 0.264g/l (1.8 mM)

Sodium Bicarbonate 2.2g/l (25.0 mM)

Sodium Chloride _6.8g/l (116.4 mM)

sEBSS recipe was based upon Supplemented Earle's Balanced Salt Solution w/o Phenol Red recipe. Sodium chloride was added until the osmolality desired was achieved (295, 270 and 200 mOsm). Media osmolality was checked using an Osmometer 3MO Plus (Advanced Instruments, Norwood, MA, USA), which was pre-calibrated using a 50 mOsm/Kg H_2O and a 850 mOsm/Kg H_2O calibration standards. sEBSS pH was adjusted to 7.3-7.4 with 1M HCl and 1M NaOH and subsequently stored as 100 ml volumes in glass beakers at 4°C until use. 0.3% Bovine serum albumin (BSA) was added on experimental day. Media were pre-warmed at 37 °C before starting the experiment.

Ca^{2+}-free sEBSS

Sodium Dihyd. Phosphate 0.122g/l (1.0167 mM)

Potassium Chloride 0.4g/l (5.4 mM)

Magnesium Sulphate.7H_2O 0.2g/l (0.811 mM)

Dextrose Anhydrous 1.0g/l (5.5 mM)

Sodium Pyruvate 0.3g/l (2.5 mM)

DL-Lactic Acid, Sodium 4.68g/l (19.0 mM)

Sodium Bicarbonate 2.2g/l (25.0 mM)

Sodium Chloride _6.8g/l (118.4 mM)

Prepared as for standard sEBSS and stored as 100 ml volumes glass beakers at 4°C until use. 0.3% BSA was added on experimental day. Media were pre-warmed at 37 °C before starting the experiment.

HCO_3^--free sEBSS

Sodium Dihyd. Phosphate 0.122g/l (1.0167 mM)

Potassium Chloride 0.4g/l (5.4 mM)

Magnesium Sulphate.7H_2O 0.2g/l (0.811 mM)

Dextrose Anhydrous 1.0g/l (5.5 mM)

Sodium Pyruvate 0.3g/l (2.5 mM)

DL-Lactic Acid, Sodium 4.68g/l (19.0 mM)

Calcium Chloride.2H_2O 0.264g/l (1.8 mM)

Sodium Chloride _6.8g/l (118.4 mM)

Prepared as for standard sEBSS and stored as 100 ml volumes glass beakers at 4°C until use. 0.3% BSA was added on experimental day. Media were pre-warmed at 37 °C before starting the experiment.

M medium

137 mM Sodium Chloride

2.5 mM Potassium Chloride

20 mM 4-(2-hydroxyethyl)-1-piperazineethanesulfonic acid (Hepes)

10 mM Glucose

Percoll

Percoll was obtained from Sigma-Aldrich (Dorset, UK) and the gradients were prepared as follows:

- 80% Percoll = 8ml Percoll + 2ml M medium
- 40% Percoll = 4ml Percoll + 6ml M medium

Media osmolality was checked using an Osmometer 3MO Plus (Advanced Instruments, Norwood, MA, USA), and stored as 50 ml volumes in falcon tubes (Becton Dickinson, USA) at 4°C until use. Media were pre-warmed at 37 °C before starting the experiment.

Sodium dodecyl sulphate polyacrylamide gel electrophoresis (SDS-PAGE) loading buffer

2% SDS

10% Glycerol

62.5 mM Tris-HCl

(pH 6.8)

TBS

0.9% Sodium Chloride

20 mM Tris-HCl

(pH 7.8)

APPENDIX III: PUBLICATIONS AND PRESENTATIONS OF RESEARCH

Reviews:

NASH, K., LEFIEVRE, L., **PERALTA-ARIAS, R**., MORRIS, J., MORALES-GARCIA, A., CONNOLLY, T., COSTELLO, S., KIRKMAN-BROWN, J. C. & PUBLICOVER, S. J. 2010. Techniques for imaging Ca2+ signaling in human sperm. *J Vis Exp*.

Abstracts:

"The influence of chloride channels in human sperm motility" Annual Meeting of the Society of Reproduction and Fertility. July 2008. Edinburgh, UK.

"The influence of chloride channels in the morphology and motility of the human spermatozoon" Proceedings of the 9th International Congress of Andrology, Journal of Andrology. March 2009. Barcelona, Spain.

REFERENCES

AFZELIUS, B. 1959. Electron microscopy of the sperm tail; results obtained with a new fixative. *J Biophys Biochem Cytol,* 5**,** 269-78.

AFZELIUS, B. A. & ELIASSON, R. 1979. Flagellar mutants in man: on the heterogeneity of the immotile-cilia syndrome. *J Ultrastruct Res,* 69**,** 43-52.

AFZELIUS, B. A. & ELIASSON, R. 1983. Male and female infertility problems in the immotile-cilia syndrome. *Eur J Respir Dis Suppl,* 127**,** 144-7.

AUGER, J., EUSTACHE, F., ANDERSEN, A. G., IRVINE, D. S., JORGENSEN, N., SKAKKEBAEK, N. E., SUOMINEN, J., TOPPARI, J., VIERULA, M. & JOUANNET, P. 2001. Sperm morphological defects related to environment, lifestyle and medical history of 1001 male partners of pregnant women from four European cities. *Hum Reprod,* 16**,** 2710-7.

AUZANNEAU, C., NOREZ, C., NOEL, S., JOUGLA, C., BECQ, F. & VANDEBROUCK, C. 2006. Pharmacological profile of inhibition of the chloride channels activated by extracellular acid in cultured rat Sertoli cells. *Reprod Nutr Dev,* 46**,** 241-55.

BALDI, E., CASANO, R., FALSETTI, C., KRAUSZ, C. S. & MAGGI, M. 1991. Intracellular calcium accumulation and responsiveness to progesterone in capacitating human spermatozoa. *J Androl,* 12**,** 323-330.

BALDI, E., LUCONI, M., BONACCORSI, L. & FORTI, G. 2002. Signal transduction pathways in human spermatozoa. *J Reprod Immunol,* 53**,** 121-31.

BARFIELD, J. P., YEUNG, C. H. & COOPER, T. G. 2005. Characterization of potassium channels involved in volume regulation of human spermatozoa. *Mol Hum Reprod,* 11**,** 891-7.

BARON, A., PACAUD, P., LOIRAND, G., MIRONNEAU, C. & MIRONNEAU, J. 1991. Pharmacological block of Ca(2+)-activated Cl- current in rat vascular smooth muscle cells in short-term primary culture. *Pflugers Arch,* 419**,** 553-8.

BECK, J. S., BRETON, S., LAPRADE, R. & GIEBISCH, G. 1991. Volume regulation and intracellular calcium in the rabbit proximal convoluted tubule. *Am J Physiol,* 260**,** F861-7.

BEDU-ADDO, K., BARRATT, C. L., KIRKMAN-BROWN, J. C. & PUBLICOVER, S. J. 2007. Patterns of [Ca2+](i) mobilization and cell response in human spermatozoa exposed to progesterone. *Dev Biol,* 302**,** 324-32.

BEDU-ADDO, K., COSTELLO, S., HARPER, C., MACHADO-OLIVEIRA, G., LEFIEVRE, L., FORD, C., BARRATT, C. & PUBLICOVER, S. 2008. Mobilisation of stored calcium in the neck region of human sperm--a mechanism for regulation of flagellar activity. *Int J Dev Biol,* 52**,** 615-26.

BEDU-ADDO, K., LEFIEVRE, L., MOSELEY, F. L., BARRATT, C. L. & PUBLICOVER, S. J. 2005. Bicarbonate and bovine serum albumin reversibly 'switch' capacitation-induced events in human spermatozoa. *Mol Hum Reprod,* 11**,** 683-91.

BERNARDI, P. 1999. Mitochondrial transport of cations: channels, exchangers, and permeability transition. *Physiol Rev,* 79**,** 1127-55.

BERRIDGE, M. J. 2004. Calcium signal transduction and cellular control mechanisms. *Biochim Biophys Acta,* 1742**,** 3-7.

BLACKMORE, P. F. 1993. Thapsigargin elevates and potentiates the ability of progesterone to increase intracellular free calcium in human sperm: possible role of

perinuclear calcium. *Cell Calcium,* 14**,** 53-60.

BLACKMORE, P. F., BEEBE, S. J., DANFORTH, D. R. & ALEXANDER, N. 1990. Progesterone and 17 alpha-hydroxyprogesterone. Novel stimulators of calcium influx in human sperm. *J Biol Chem,* 265**,** 1376-80.

BOATMAN, D. E. & ROBBINS, R. S. 1991. Bicarbonate: carbon-dioxide regulation of sperm capacitation, hyperactivated motility, and acrosome reactions. *Biol Reprod,* 44**,** 806-13.

BONACCORSI, L., FORTI, G. & BALDI, E. 2001. Low-voltage-activated calcium channels are not involved in capacitation and biological response to progesterone in human sperm. *Int J Androl,* 24**,** 341-351.

BOND, T. D., AMBIKAPATHY, S., MOHAMMAD, S. & VALVERDE, M. A. 1998. Osmosensitive C1- currents and their relevance to regulatory volume decrease in human intestinal T84 cells: outwardly vs. inwardly rectifying currents. *J Physiol,* 511 (Pt 1)**,** 45-54.

BONIGK, W., LOOGEN, A., SEIFERT, R., KASHIKAR, N., KLEMM, C., KRAUSE, E., HAGEN, V., KREMMER, E., STRUNKER, T. & KAUPP, U. B. 2009. An atypical CNG channel activated by a single cGMP molecule controls sperm chemotaxis. *Sci Signal,* 2**,** ra68.

BRADLEY, M. P. & FORRESTER, I. T. 1980. A sodium-calcium exchange mechanism in plasma membrane vesicles isolated from ram sperm flagella. *FEBS Lett,* 121**,** 15-8.

BRANHAM, M. T., MAYORGA, L. S. & TOMES, C. N. 2006. Calcium-induced Acrosomal Exocytosis Requires cAMP Acting through a Protein Kinase A-independent, Epac-mediated Pathway. *J Biol Chem,* 281, No. 13**,** 8656-8666.

BRAY, C., SON, J. H., KUMAR, P., HARRIS, J. D. & MEIZEL, S. 2002. A role for the human sperm glycine receptor/Cl(-) channel in the acrosome reaction initiated by recombinant ZP3. *Biol Reprod,* 66(1)**,** 91-97.

BREWER, L., CORZETT, M. & BALHORN, R. 2002. Condensation of DNA by spermatid basic nuclear proteins. *J Biol Chem,* 277**,** 38895-900.

BREWER, L. R., CORZETT, M. & BALHORN, R. 1999. Protamine-induced condensation and decondensation of the same DNA molecule. *Science,* 286**,** 120-3.

BREWIS, I. A., MORTON, I. E., MOHAMMAD, S. N., BROWES, C. E. & MOORE, H. D. M. 2000. Measurement of intracellular calcium concentration and plasma membrane potential in human spermatozoa using flow cytometry. *J Androl,* 21**,** 238-249.

BRIEL, M., GREGER, R. & KUNZELMANN, K. 1998. Cl^- transport by cystic fibrosis transmembrane conductance regulator (CFTR) contributes to the inhibition of epithelial Na^+ channels (ENaCs) in *Xenopus* oocytes co-expressing CFTR and ENaC. *J Physiol,* 508(3)**,** 825-836.

BROCHIERO, E., BANDERALI, U., LINDENTHAL, S., RASCHI, C. & EHRENFELD, J. 1995. Basolateral membrane chloride permeability of A6 cells: implication in cell volume regulation. *Pflugers Arch,* 431**,** 32-45.

BUJAN, L., MIEUSSET, R., MONDINAT, C., MANSAT, A. & PONTONNIER, F. 1988. Sperm morphology in fertile men and its age related variation. *Andrologia,* 20**,** 121-8.

BUSSO, D., COHEN, D. J., HAYASHI, M., KASAHARA, M. & CUASNICU, P. S. 2005. Human testicular protein TPX1/CRISP-2: localization in spermatozoa, fate after capacitation and relevance for gamete interaction. *Mol Hum Reprod,* 11**,** 299-305.

CARAFOLI, E. & BRINI, M. 2000. Calcium pumps: structural basis for and mechanism of calcium transmembrane transport. *Curr Opin Chem Biol,* 4**,** 152-161.

CARRERA, A., MOOS, J., NING, X. P., GERTON, G. L., TESARIK, J., KOPF, G. S.

& MOSS, S. B. 1996. Regulation of protein tyrosine phosphorylation in human sperm by a calcium/calmodulin-dependent mechanism: identification of A kinase anchor proteins as major substrates for tyrosine phosphorylation. *Dev Biol,* 180**,** 284-96.

CASEY, J. R., SLY, W. S., SHAH, G. N. & ALVAREZ, B. V. 2009. Bicarbonate homeostasis in excitable tissues: role of AE3 Cl-/HCO3- exchanger and carbonic anhydrase XIV interaction. *Am J Physiol Cell Physiol,* 297**,** C1091-102.

CASSLEN, B. & NILSSON, B. 1984. Human uterine fluid, examined in undiluted samples for osmolarity and the concentrations of inorganic ions, albumin, glucose, and urea. *Am J Obstet Gynecol,* 150**,** 877-81.

CHAN, H. C., SHI, Q. X., ZHOU, C. X., WANG, X. F., XU, W. M., CHEN, W. Y., CHEN, A. J., NI, Y. & YUAN, Y. Y. 2006. Critical role of CFTR in uterine bicarbonate secretion and the fertilizing capacity of sperm. *Mol Cell Endocrinol,* 250(1-2)**,** 106-113.

CHENG, C. Y., WONG, E. W., YAN, H. H. & MRUK, D. D. 2010. Regulation of spermatogenesis in the microenvironment of the seminiferous epithelium: new insights and advances. *Mol Cell Endocrinol,* 315**,** 49-56.

CHIEN, L. T. & HARTZELL, H. C. 2007. Drosophila bestrophin-1 chloride current is dually regulated by calcium and cell volume. *J Gen Physiol,* 130**,** 513-24.

CHIPPERFIELD, A. R. & HARPER, A. A. 2000. Chloride in smooth muscle. *Prog Biophys Mol Biol,* 74**,** 175-221.

CHO, C., BUNCH, D. O., FAURE, J. E., GOULDING, E. H., EDDY, E. M., PRIMAKOFF, P. & MYLES, D. G. 1998. Fertilization defects in sperm from mice lacking fertilin beta. *Science,* 281**,** 1857-9.

COHEN, D. J., BUSSO, D., DA ROS, V., ELLERMAN, D. A., MALDERA, J. A., GOLDWEIC, N. & CUASNICU, P. S. 2008. Participation of cysteine-rich secretory proteins (CRISP) in mammalian sperm-egg interaction. *Int J Dev Biol,* 52**,** 737-42.

COHEN, D. J., ELLERMAN, D. A., BUSSO, D., MORGENFELD, M. M., PIAZZA, A. D., HAYASHI, M., YOUNG, E. T., KASAHARA, M. & CUASNICU, P. S. 2001. Evidence that human epididymal protein ARP plays a role in gamete fusion through complementary sites on the surface of the human egg. *Biol Reprod,* 65**,** 1000-5.

COOPER, T. & YEUNG, C. 2000. Physiology of Sperm Maturation and Fertilization. *In:* NIESCHLAG, E. & BEHRE, H. (eds.) *Andrology.* Berlin: Springer.

COOPER, T. G. 1996. Epididymis and sperm function. *Andrologia,* 28 Suppl 1**,** 57-9.

COOPER, T. G. & BARFIELD, J. P. 2006. Utility of infertile male models for contraception and conservation. *Mol Cell Endocrinol,* 250(1-2)**,** 206-211.

COOPER, T. G., BARFIELD, J. P. & YEUNG, C. H. 2005. Changes in osmolality during liquefaction of human semen. *Int J Androl,* 28**,** 58-60.

COOPER, T. G., RACZEK, S., YEUNG, C. H., SCHWAB, E., SCHULZE, H. & HERTLE, L. 1992. Composition of fluids obtained from human epididymal cysts. *Urol Res,* 20**,** 275-80.

COOPER, T. G. & YEUNG, C. 2006. Sperm maturation in the human epididymis. *In:* DE JONGE, C. & BARRAT, C. L. R. (eds.) *The Sperm Cell.* Cambridge: Cambridge University Press.

COOPER, T. G. & YEUNG, C. H. 2003. Acquisition of volume regulatory response of sperm upon maturation in the epididymis and the role of the cytoplasmic droplet. *Microsc Res Tech,* 61**,** 28-38.

COOPER, T. G. & YEUNG, C. H. 2007. Involvement of potassium and chloride channels and other transporters in volume regulation by spermatozoa. *Curr Pharm Des,* 13**,** 3222-30.

CORREIA, J. N., CONNER, S. J. & KIRKMAN-BROWN, J. C. 2007. Non-genomic steroid actions in human spermatozoa. "Persistent tickling from a laden environment". *Semin Reprod Med,* 25**,** 208-19.

COSTELLO, S., MICHELANGELI, F., NASH, K., LEFIEVRE, L., MORRIS, J., MACHADO-OLIVEIRA, G., BARRATT, C., KIRKMAN-BROWN, J. & PUBLICOVER, S. 2009. Ca2+-stores in sperm: their identities and functions. *Reproduction,* 138**,** 425-37.

COTTON, K. D., HOLLYWOOD, M. A., MCHALE, N. G. & THORNBURY, K. D. 1997. Ca2+ current and Ca(2+)-activated chloride current in isolated smooth muscle cells of the sheep urethra. *J Physiol,* 505 (Pt 1)**,** 121-31.

CROSS, N. L. 1998. Role of cholesterol in sperm capacitation. *Biol Reprod,* 59**,** 7-11.

CROWE, W. E., EHRENFELD, J., BROCHIERO, E. & WILLS, N. K. 1995. Apical membrane sodium and chloride entry during osmotic swelling of renal (A6) epithelial cells. *J Membr Biol,* 144**,** 81-91.

CRUICKSHANK, S. F., BAXTER, L. M. & DRUMMOND, R. M. 2003. The Cl(-) channel blocker niflumic acid releases Ca(2+) from an intracellular store in rat pulmonary artery smooth muscle cells. *Br J Pharmacol,* 140**,** 1442-50.

DADOUNE, J. P. 2003. Expression of mammalian spermatozoal nucleoproteins. *Microsc Res Tech,* 61**,** 56-75.

DANSHINA, P. V., GEYER, C. B., DAI, Q., GOULDING, E. H., WILLIS, W. D., KITTO, G. B., MCCARREY, J. R., EDDY, E. M. & O'BRIEN, D. A. 2010. Phosphoglycerate kinase 2 (PGK2) is essential for sperm function and male fertility in mice. *Biol Reprod,* 82**,** 136-45.

DARSZON, A., ACEVEDO, J. J., GALINDO, B. E., HERNÁNDEZ-GONZÁLEZ, E. O., NISHIGAKI, T., TREVIÑO, C. L., WOOD, C. & BELTRÁN, C. 2006. Sperm channel diversity and functional multiplicity. *Reproduction,* 131**,** 977-988.

DARSZON, A., LABARCA, P., NISHIGAKI, T. & ESPINOSA, F. 1999. Ion channels in sperm physiology. *Physiol Rev,* 79**,** 481-510.

DASSOULI, A., SULPICE, J. C., ROUX, S. & CROZATIER, B. 1993. Stretch-induced inositol trisphosphate and tetrakisphosphate production in rat cardiomyocytes. *J Mol Cell Cardiol,* 25**,** 973-82.

DE LAMIRANDE, E., LAMOTHE, G. & VILLEMURE, M. 2009. Control of superoxide and nitric oxide formation during human sperm capacitation. *Free Radic Biol Med,* 46**,** 1420-7.

DE MOUZON, J., GOOSSENS, V., BHATTACHARYA, S., CASTILLA, J. A., FERRARETTI, A. P., KORSAK, V., KUPKA, M., NYGREN, K. G. & NYBOE ANDERSEN, A. 2010. Assisted reproductive technology in Europe, 2006: results generated from European registers by ESHRE. *Hum Reprod,* 25**,** 1851-62.

DE SMET, P., SIMAELS, J. & VAN DRIESSCHE, W. 1995. Regulatory volume decrease in a renal distal tubular cell line (A6). II. Effect of Na+ transport rate. *Pflugers Arch,* 430**,** 945-53.

DEMARCO, I. A., ESPINOSA, F., EDWARDS, J., SOSNIK, J., DE LA VEGA-BELTRAN, J. L., HOCKENSMITH, J. W., KOPF, G. S., DARSZON, A. & VISCONTI, P. E. 2003. Involvement of a Na+/HCO-3 cotransporter in mouse sperm capacitation. *J Biol Chem,* 278(9)**,** 7001-7009.

DIPOLO, R. & BEAUGÉ, L. 2006. Sodium/Calcium Exchanger : influence of metabolic regulation on ion carrier interactions. . *Physiol Rev,* 86**,** 155-203.

DO, C. W. & CIVAN, M. M. 2006. Swelling-activated chloride channels in aqueous humour formation: on the one side and the other. *Acta Physiol (Oxf),* 187**,** 345-52.

DOROSHENKO, P., SABANOV, V. & DOROSHENKO, N. 2001. Cell cycle-related

changes in regulatory volume decrease and volume-sensitive chloride conductance in mouse fibroblasts. *J Cell Physiol,* 187**,** 65-72.

DRAGILEVA, E., RUBINSTEIN, S. & BREITBART, H. 1999. Intracellular $Ca(^{2+})$-$Mg(^{2+})$-ATPase regulates calcium influx and acrosomal exocytosis in bull and ram spermatozoa. *Biol Reprod,* 61**,** 1226-1234.

DREVIUS, L. O. & ERIKSSON, H. 1966. Osmotic swelling of mammalian spermatozoa. *Exp Cell Res,* 42**,** 136-56.

DUNHAM, P. B. 1995. Effects of urea on K-Cl cotransport in sheep red blood cells: evidence for two signals of swelling. *Am J Physiol,* 268**,** C1026-32.

DUTZLER, R. 2004. Structural basis for ion conduction and gating in ClC chloride channels. *FEBS Lett,* 564**,** 229-33.

DUTZLER, R. 2007. A structural perspective on ClC channel and transporter function. *FEBS Lett,* 581**,** 2839-2844.

DUTZLER, R., CAMPBELL, E. B., CADENE, M., CHAIT, B. T. & MACKINNON, R. 2002. X-ray structure of a ClC chloride channel at 3.0 A reveals the molecular basis of anion selectivity. *Nature,* 415(6869)**,** 287-294.

EDDY, E. M., TOSHIMORI, K. & O'BRIEN, D. A. 2003. Fibrous sheath of mammalian spermatozoa. *Microsc Res Tech,* 61**,** 103-15.

EGGERMONT, J., TROUET, D., CARTON, I. & NILIUS, B. 2001. Cellular function and control of volume-regulated anion channels. *Cell Biochem Biophys,* 35**,** 263-74.

EL HIANI, Y. & LINSDELL, P. 2010. Changes in accessibility of cytoplasmic substances to the pore associated with activation of the cystic fibrosis transmembrane conductance regulator chloride channel. *J Biol Chem,* 285**,** 32126-40.

ELLERMAN, D. A., COHEN, D. J., WEIGEL MUNOZ, M., DA ROS, V. G., ERNESTO, J. I., TOLLNER, T. L. & CUASNICU, P. S. 2010. Immunologic behavior of human cysteine-rich secretory protein 1 (hCRISP1) in primates: prospects for immunocontraception. *Fertil Steril,* 93**,** 2551-6.

ERTEL, E. A., CAMPBELL, K. P., HARPOLD, M. M., HOFMANN, F., MORI, Y., PEREZ-REYES, E., SCHWARTZ, A., SNUTCH, T. P., TANABE, T., BIRNBAUMER, L., TSIEN, R. W. & CATTERALL, W. A. 2000. Nomenclature of voltage-gated calcium channels. *Neuron,* 25**,** 533-5.

ESPINOSA, F., LOPEZ-GONZALEZ, I., SERRANO, C. J., GASQUE, G., DE LA VEGA-BELTRAN, J. L., TREVINO, C. L. & DARSZON, A. 1999. Anion channel blockers differentially affect T-type Ca(2+) currents of mouse spermatogenic cells, alpha1E currents expressed in Xenopus oocytes and the sperm acrosome reaction. *Dev Genet,* 25**,** 103-14.

ETO, K., HUET, C., TARUI, T., KUPRIYANOV, S., LIU, H. Z., PUZON-MCLAUGHLIN, W., ZHANG, X. P., SHEPPARD, D., ENGVALL, E. & TAKADA, Y. 2002. Functional classification of ADAMs based on a conserved motif for binding to integrin alpha 9beta 1: implications for sperm-egg binding and other cell interactions. *J Biol Chem,* 277**,** 17804-10.

EVANS, J. P. 1999. Sperm disintegrins, egg integrins, and other cell adhesion molecules of mammalian gamete plasma membrane interactions. *Front Biosci,* 4**,** D114-31.

EVANS, J. P. & FLORMAN, H. M. 2002. The state of the union: the cell biology of fertilization. *Nat Cell Biol,* 4 Suppl**,** s57-63.

FLORMAN, H. M., CORRON, M. E., KIM, T. D. & BABCOCK, D. F. 1992. Activation of voltage-dependent calcium channels of mammalian sperm is required for zona pellucida-induced acrosomal exocytosis. *Dev Biol,* 152**,** 304-314.

FORESTA, C., ROSSATO, M. & DI VIRGILIO, F. 1995. Differential modulation by protein kinase C of progesterone-activated responses in human sperm. *Biochem*

Biophys Res Commun, 206**,** 408-13.

FRASER, L. R. 2010. The "switching on" of mammalian spermatozoa: molecular events involved in promotion and regulation of capacitation. *Mol Reprod Dev,* 77**,** 197-208.

GAGNON, C. & DE LAMIRANDE, E. 2006. Controls of Sperm Motility. *In:* DE JONGE, C. & BARRAT, C. L. R. (eds.) *The Sperm Cell.* Cambridge: Cambridge University Press.

GALIZIA, L., FLAMENCO, M. P., RIVAROLA, V., CAPURRO, C. & FORD, P. 2008. Role of AQP2 in activation of calcium entry by hypotonicity: implications in cell volume regulation. *Am J Physiol Renal Physiol,* 294**,** F582-90.

GARCIA, M. A. & MEIZEL, S. 1999. Progesterone-mediated calcium influx and acrosome reaction of human spermatozoa: pharmacological investigation of T-type calcium channels. *Biol Reprod,* 60(1)**,** 102-109.

GEIGER, D., SCHERZER, S., MUMM, P., STANGE, A., MARTEN, I., BAUER, H., ACHE, P., MATSCHI, S., LIESE, A., AL-RASHEID, K. A., ROMEIS, T. & HEDRICH, R. 2009. Activity of guard cell anion channel SLAC1 is controlled by drought-stress signaling kinase-phosphatase pair. *Proc Natl Acad Sci U S A,* 106**,** 21425-30.

GONZALÈS, J. 2006. [History of spermatozoon and changing views]. *Gynecol Obstet Fertil,* 34**,** 819-26.

GONZÁLEZ-MARTÍNEZ, M. T., BONILLA-HERNÁNDEZ, M. A. & GUZMÁN-GRENFELL, A. M. 2002. Stimulation of voltage-dependent calcium channels during capacitation and by progesterone in human sperm. *Arch Biochem Biophys,* 408(2)**,** 205-210.

GONZALEZ-MARTINEZ, M. T., GALINDO, B. E., DE DE LA TORRE, L., ZAPATA, O., RODRIGUEZ, E., FLORMAN, H. M. & DARSZON, A. 2001. A sustained increase in intracellular Ca(2+) is required for the acrosome reaction in sea urchin sperm. *Dev Biol,* 236**,** 220-9.

GOTO, N. & HARAYAMA, H. 2009. Calyculin A-sensitive protein phosphatases are involved in maintenance of progressive movement in mouse spermatozoa in vitro by suppression of autophosphorylation of protein kinase A. *J Reprod Dev,* 55**,** 327-34.

GRANOT, I., DEKEL, N., SEGAL, I., FIELDUST, S., SHOHAM, Z. & BARASH, A. 1998. Is hydrosalpinx fluid cytotoxic? *Hum Reprod,* 13**,** 1620-4.

GU, Y., KIRKMAN-BROWN, J. C., KORCHEV, Y., BARRAT, C. L. R. & PUBLICOVER, S. J. 2004. Multi-state, 4-aminopyridine-sensitive ion channels in human spermatozoa. *Dev Biol,* 274**,** 308-317.

GUGGINO, W. B. & STANTON, B. A. 2006. Mechanisms of disease: New insights into cystic fibrosis: molecular switches that regulate CFTR. *Nat Rev Mol Cell Biol,* 7**,** 426-436.

HAMMAMI, S., WILLUMSEN, N. J., OLSEN, H. L., MORERA, F. J., LATORRE, R. & KLAERKE, D. A. 2009. Cell volume and membrane stretch independently control K+ channel activity. *J Physiol,* 587**,** 2225-31.

HAMMOUD, S. S., NIX, D. A., ZHANG, H., PURWAR, J., CARRELL, D. T. & CAIRNS, B. R. 2009. Distinctive chromatin in human sperm packages genes for embryo development. *Nature,* 460**,** 473-8.

HARPER, C. V., BARRAT, C. L. R. & PUBLICOVER, S. J. 2004. Stimulation of human spermatozoa with progesterone gradients to stimulate approach to the oocyte. *J Biol Chem,* 279, No. 44**,** 46315-46325.

HARPER, C. V., WOOTTON, L., MICHELANGELI, F., LEFIÈVRE, L., BARRAT, C. L. R. & PUBLICOVER, S. J. 2005. Secretory pathway Ca^{2+} -ATPase (SPCA1) Ca^{2+} pumps, not SERCAs, regulate complex $[Ca^{2+}]_i$ signals in human spermatozoa. *J Cell*

Sci 118**,** 1673-1685.

HELLER, C. & CLERMONT, Y. 1966. Spermatogenesis in man : an estimate of its duration. *Science***,** 184-186.

HERNÁNDEZ-GONZÁLEZ, E. O., SOSNIK, J., EDWARDS, J., ACEVEDO, J. J., MENDOZA-LUJAMBIO, I., LÓPEZ-GONZÁLEZ, I., DEMARCO, I., WERTHEIMER, E., DARSZON, A. & VISCONTI, P. E. 2006. Sodium and epithelial sodium channels participate in the regulation of the capacitation-associated hyperpolarization in mouse sperm. *J Biol Chem,* 281, No. 9**,** 5623-5633.

HERNÁNDEZ-GONZÁLEZ, E. O., TREVIÑO, C. L., CASTELLANO, L. E., DE LA VEGA-BELTRAN, J. L., OCAMPO, A. Y., WERTHEIMER, E., VISCONTI, P. E. & DARSZON, A. 2007. Involvement of cystic fibrosis transmembrane conductance regulator in mouse sperm capacitation. *J Biol Chem,* 282(33)**,** 24397-24406.

HFEA 2008. A long term analysis of the HFEA Register data (1991-2006). *In:* HFEA (ed.). London: Human Fertilisation and Embryology Authority.

HINTON, B. T., PRYOR, J. P., HIRSH, A. V. & SETCHELL, B. P. 1981. The concentration of some inorganic ions and organic compounds in the luminal fluid of the human ductus deferens. *Int J Androl,* 4**,** 457-461.

HIRANO, Y., SHIBAHARA, H., OBARA, H., SUZUKI, T., TAKAMIZAWA, S., YAMAGUCHI, C., TSUNODA, H. & SATO, I. 2001. Relationships between sperm motility characteristics assessed by the computer-aided sperm analysis (CASA) and fertilization rates in vitro. *J Assist Reprod Genet,* 18**,** 213-8.

HO, H. C., GRANISH, K. A. & SUAREZ, S. S. 2002. Hyperactivated motility of bull sperm is triggered at the axoneme by Ca2+ and not cAMP. *Dev Biol,* 250**,** 208-17.

HO, H. C. & SUAREZ, S. S. 2001. An inositol 1,4,5-trisphosphate receptor-gated intracellular Ca(2+) store is involved in regulating sperm hyperactivated motility. *Biol Reprod,* 65**,** 1606-15.

HOFFMANN, E. K., LAMBERT, I. H. & PEDERSEN, S. F. 2009. Physiology of cell volume regulation in vertebrates. *Physiol Rev,* 89**,** 193-277.

HOGG, R. C., WANG, Q. & LARGE, W. A. 1994. Effects of Cl channel blockers on Ca-activated chloride and potassium currents in smooth muscle cells from rabbit portal vein. *Br J Pharmacol,* 111**,** 1333-41.

HOLSTEIN, A. F., SCHULZE, W. & DAVIDOFF, M. 2003. Understanding spermatogenesis is a prerequisite for treatment. *Reprod Biol Endocrinol,* 1**,** 107.

ISOYA, E., TOYODA, F., IMAI, S., OKUMURA, N., KUMAGAI, K., OMATSU-KANBE, M., KUBO, M., MATSUURA, H. & MATSUSUE, Y. 2009. Swelling-activated Cl(-) current in isolated rabbit articular chondrocytes: inhibition by arachidonic Acid. *J Pharmacol Sci,* 109**,** 293-304.

IVELL, R. 2007. Lifestyle impact and the biology of the human scrotum. *Reprod Biol Endocrinol,* 5**,** 15.

JACOBSON, G. & KARSNAS, P. 1990. Important parameters in semi-dry electrophoretic transfer. *Electrophoresis,* 11**,** 46-52.

JAGANNATHAN, S., PUNT, E. L., GU, Y., ARNOULT, C., SAKKAS, D., BARRATT, C. L. & PUBLICOVER, S. J. 2002. Identification and localization of T-type voltage-operated calcium channel subunits in human male germ cells. Expression of multiple isoforms. *J Biol Chem,* 277**,** 8449-56.

JAKAB, M., FURST, J., GSCHWENTNER, M., BOTTA, G., GARAVAGLIA, M. L., BAZZINI, C., RODIGHIERO, S., MEYER, G., EICHMUELLER, S., WOLL, E., CHWATAL, S., RITTER, M. & PAULMICHL, M. 2002. Mechanisms sensing and modulating signals arising from cell swelling. *Cell Physiol Biochem,* 12**,** 235-58.

JENA, M., MINORE, J. F. & O'NEILL, W. C. 1997. A volume-sensitive, IP3-insensitive Ca2+ store in vascular endothelial cells. *Am J Physiol,* 273**,** C316-22.

JENTSCH, T. J., STEIN, V., WEINREICH, F. & ZDEBIK, A. A. 2002. Molecular structure and physiological function of chloride channels. *Physiol Rev,* 82**,** 503-68.

JEYENDRAN, R. S., VAN DER VEN, H. H., PEREZ-PELAEZ, M., CRABO, B. G. & ZANEVELD, L. J. 1984. Development of an assay to assess the functional integrity of the human sperm membrane and its relationship to other semen characteristics. *J Reprod Fertil,* 70**,** 219-28.

JIMENEZ-GONZALEZ, M. C., GU, Y., KIRKMAN-BROWN, J. C., BARRAT, C. L. R. & PUBLICOVER, S. 2007. Patch-clamp "mapping" of ion channel activity in human sperm reveals regionalisation and co-localisation into mixed clusters. *J Cell Physiol,* 213**,** 801-808.

JIMENEZ-GONZALEZ, M. C., MICHELANGELI, F., HARPER, C. V., BARRAT, C. L. R. & PUBLICOVER, S. J. 2006. Calcium signalling in human spermatozoa: a specialized "toolkit" of channels, transporters and stores. *Hum Reprod Update,* 12(3)**,** 253-267.

JOHNSON, L. & VARNER, D. 1988. Effect of daily sperm production but no age on transit time of spermatozoa through the human epididymis. *Biol Reprod***,** 812-817.

JONES, R. 2004. Sperm survival versus degradation in the mammalian epididymis: A hypothesis. *Biol Reprod,* 71**,** 1405-1411.

JORGENSEN, N. K., CHRISTENSEN, S., HARBAK, H., BROWN, A. M., LAMBERT, I. H., HOFFMANN, E. K. & SIMONSEN, L. O. 1997. On the role of calcium in the regulatory volume decrease (RVD) response in Ehrlich mouse ascites tumor cells. *J Membr Biol,* 157**,** 281-99.

JOUANNET, P., DUCOT, B., FENEUX, D. & SPIRA, A. 1988. Male factors and the likelihood of pregnancy in infertile couples. I. Study of sperm characteristics. *Int J Androl,* 11**,** 379-94.

JUNGNICKEL, M. K., MARRERO, H., BIRNBAUMER, L., LEMOS, J. R. & FLORMAN, H. M. 2001. Trp2 regulates entry of Ca2+ into mouse sperm triggered by egg ZP3. *Nat Cell Biol,* 3**,** 499-502.

JUUL, S., KARMAUS, W. & OLSEN, J. 1999. Regional differences in waiting time to pregnancy: pregnancy-based surveys from Denmark, France, Germany, Italy and Sweden. The European Infertility and Subfecundity Study Group. *Hum Reprod,* 14**,** 1250-4.

KAWASAKI, T. & KASAI, M. 1989. Disulfonic stilbene derivatives open the Ca2+ release channel of sarcoplasmic reticulum. *J Biochem,* 106**,** 401-5.

KIM, S. J., SHIN, S. Y., LEE, J. E., KIM, J. H. & UHM, D. Y. 2003. Ca2+-activated Cl- channel currents in rat ventral prostate epithelial cells. *Prostate,* 55**,** 118-27.

KIRKMAN-BROWN, J. C., BRAY, C., STEWART, P. M., BARRAT, C. L. R. & PUBLICOVER, S. J. 2000. Biphasic elevation of $[Ca^{2+}]_i$ in individual human spermatozoa exposed to progesterone. *Dev Biol,* 222**,** 326-335.

KIRKMAN-BROWN, J. C., PUNT, E. L., BARRAT, C. L. R. & PUBLICOVER, S. J. 2002. Zona pellucida and progesterone-induced Ca^{2+} signaling and acrosome reaction in human spermatozoa. *J Androl,* 23, No. 3**,** 306-315.

KLEIN, J. D., PERRY, P. B. & O'NEILL, W. C. 1993. Regulation by cell volume of Na(+)-K(+)-2Cl- cotransport in vascular endothelial cells: role of protein phosphorylation. *J Membr Biol,* 132**,** 243-52.

KLEIN, T., COOPER, T. G. & YEUNG, C. H. 2006. The role of potassium chloride cotransporters in murine and human sperm volume regulation. *Biol Reprod,* 75**,** 853-8.

KOBORI, H., MIYAZAKI, S. & KUWABARA, Y. 2000. Characterization of intracellular Ca(2+) increase in response to progesterone and cyclic nucleotides in mouse spermatozoa. *Biol Reprod,* 63**,** 113-20.

KOHANE, A. C., CAMEO, M. S., PINEIRO, L., GARBERI, J. C. & BLAQUIER, J. A. 1980a. Distribution and site of production of specific proteins in the rat epididymis. *Biol Reprod,* 23**,** 181-7.

KOHANE, A. C., GONZALEZ ECHEVERRIA, F. M., PINEIRO, L. & BLAQUIER, J. A. 1980b. Interaction of proteins of epididymal origin with spermatozoa. *Biol Reprod,* 23**,** 737-42.

KOPF, G. 1999. Acrosome Reaction. *Encyclopedia of Reproduction.* Academic Press.

KOSOWER, N. S., KATAYOSE, H. & YANAGIMACHI, R. 1992. Thiol-disulfide status and acridine orange fluorescence of mammalian sperm nuclei. *J Androl,* 13**,** 342-8.

KRASZNAI, Z., KRASZNAI, Z., MORISAWA, M., BAZSÁNÉ, Z., HERNÁDI, Z., FAZEKAS, Z., TRÓN, L., GODA, K. & MÁRIÁN, T. 2006. Role of the Na^{+}/Ca^{2+} exchanger in calcium homeostasis and human sperm motility regulation. *Cell Motil Cytoskeleton* 63**,** 66-76.

KUBO-IRIE, M., MATSUMIYA, K., IWAMOTO, T., KANEKO, S. & ISHIJIMA, S. 2005. Morphological abnormalities in the spermatozoa of fertile and infertile men. *Mol Reprod Dev,* 70**,** 70-81.

KUNZELMANN, K. & SCHREIBER, R. 1999. CFTR, a regulator of channels. *J Membr Biol,* 168(1)**,** 1-8.

LAEMMLI, U. K. 1970. Cleavage of structural proteins during the assembly of the head of bacteriophage T4. *Nature,* 227**,** 680-5.

LEAF, A. 1959. Maintenance of concentration gradients and regulation of cell volume. *Ann N Y Acad Sci,* 72**,** 396-404.

LEFIEVRE, L., BEDU-ADDO, K., CONNER, S. J., MACHADO-OLIVEIRA, G. S., CHEN, Y., KIRKMAN-BROWN, J. C., AFNAN, M. A., PUBLICOVER, S. J., FORD, W. C. & BARRATT, C. L. 2007a. Counting sperm does not add up any more: time for a new equation? *Reproduction,* 133**,** 675-84.

LEFIEVRE, L., CHEN, Y., CONNER, S. J., SCOTT, J. L., PUBLICOVER, S. J., FORD, W. C. & BARRATT, C. L. 2007b. Human spermatozoa contain multiple targets for protein S-nitrosylation: an alternative mechanism of the modulation of sperm function by nitric oxide? *Proteomics,* 7**,** 3066-84.

LINARES-HERNÁNDEZ, L., GUZMÁN-GRENFELL, A. M., HICKS-GOMEZ, J. J. & GONZÁLEZ-MARTÍNEZ, M. T. 1998. Voltage-dependent calcium influx in human sperm assessed by simultaneous optical detection of intracellular calcium and membrane potential. *Biochim Biophys Acta,* 1372(1)**,** 1-12.

LINDEMANN, C. & GOLTZ, J. 1988. Calcium regulation of flagellar curvature and swimming pattern in Triton-X100 extracted rat sperm. *Cell Motil Cytoskeleton,* 10**,** 420-431.

LINSDELL, P. 2005. Mechanism of chloride permeation in the cystic fibrosis conductance regulator chloride channel. *Exp Physiol,* 91(1)**,** 123-129.

LISHKO, P. V., BOTCHKINA, I. L., FEDORENKO, A. & KIRICHOK, Y. 2010. Acid extrusion from human spermatozoa is mediated by flagellar voltage-gated proton channel. *Cell,* 140**,** 327-37.

LIU, D. Y., CLARKE, G. N. & BAKER, H. W. 1991. Relationship between sperm motility assessed with the Hamilton-Thorn motility analyzer and fertilization rates in vitro. *J Androl,* 12**,** 231-9.

LIU, K., SAMUEL, M., HO, M., HARRISON, R. K. & PASLAY, J. W. 2010. NPPB structure-specifically activates TRPA1 channels. *Biochem Pharmacol,* 80**,** 113-21.

LIU, X., SINGH, B. B. & AMBUDKAR, I. S. 1999. ATP-dependent activation of K_{Ca} and ROMK-type K_{ATP} channels in human submandibular gland ductal cells. *J Biol Chem,* 274(35)**,** 25121-25129.

LOBET, S. & DUTZLER, R. 2006. Ion-binding properties of the ClC chloride selectivity filter. *EMBO J,* 25(1)**,** 24-33.

LOSEL, R., BREITER, S., SEYFERT, M., WEHLING, M. & FALKENSTEIN, E. 2005. Classic and non-classic progesterone receptors are both expressed in human spermatozoa. *Horm Metab Res,* 37**,** 10-4.

LUCONI, M., PORAZZI, I., FERRUZZI, P., MARCHIANI, S., FORTI, G. & BALDI, E. 2005. Tyrosine phosphorylation of the a kinase anchoring protein 3 (AKAP3) and soluble adenylate cyclase are involved in the increase of human sperm motility by bicarbonate. *Biol Reprod,* 72**,** 22-32.

LÜSCHER, B. & KELLER, C. A. 2004. Regulation of $GABA_A$ receptor trafficking, channel activity, and functional plasticity of inhibitory synapses. *Pharmacol Ther,* 102(3)**,** 195-221.

LYNCH, J. W. 2004. Molecular structure and function of the glycine receptor chloride channel. *Physiol Rev,* 84**,** 1051-1095.

MACHADO-OLIVEIRA, G., LEFIEVRE, L., FORD, C., HERRERO, M. B., BARRATT, C., CONNOLLY, T. J., NASH, K., MORALES-GARCIA, A., KIRKMAN-BROWN, J. & PUBLICOVER, S. 2008. Mobilisation of Ca2+ stores and flagellar regulation in human sperm by S-nitrosylation: a role for NO synthesised in the female reproductive tract. *Development,* 135**,** 3677-86.

MACIAS, M. J., TEIJIDO, O., ZIFARELLI, G., MARTIN, P., RAMIREZ-ESPAIN, X., ZORZANO, A., PALACIN, M., PUSCH, M. & ESTEVEZ, R. 2007. Myotonia-related mutations in the distal C-terminus of ClC-1 and ClC-0 chloride channels affect the structure of a poly-proline helix. *Biochem J,* 403**,** 79-87.

MANOURY, B., TAMULEVICIUTE, A. & TAMMARO, P. 2010. TMEM16A/anoctamin 1 protein mediates calcium-activated chloride currents in pulmonary arterial smooth muscle cells. *J Physiol,* 588**,** 2305-14.

MATSUDA, J. J., FILALI, M. S., MORELAND, J. G., MILLER, F. J. & LAMB, F. S. 2010. Activation of swelling-activated chloride current by tumor necrosis factor-alpha requires ClC-3-dependent endosomal reactive oxygen production. *J Biol Chem,* 285**,** 22864-73.

MCCARTY, N. A. & O'NEIL, R. G. 1992. Calcium signaling in cell volume regulation. *Physiol Rev,* 72**,** 1037-61.

MEISTRICH, M. L., MOHAPATRA, B., SHIRLEY, C. R. & ZHAO, M. 2003. Roles of transition nuclear proteins in spermiogenesis. *Chromosoma,* 111**,** 483-8.

MEIZEL, S. 1997. Amino acid neurotransmitter receptor/chloride channels of mammalian sperm and the acrosome reaction. *Biol Reprod,* 56(3)**,** 569-574.

MIGNEN, O., LE GALL, C., HARVEY, B. J. & THOMAS, S. 1999. Volume regulation following hypotonic shock in isolated crypts of mouse distal colon. *J Physiol,* 515 (Pt 2)**,** 501-10.

MIKI, K., QU, W., GOULDING, E. H., WILLIS, W. D., BUNCH, D. O., STRADER, L. F., PERREAULT, S. D., EDDY, E. M. & O'BRIEN, D. A. 2004. Glyceraldehyde 3-phosphate dehydrogenase-S, a sperm-specific glycolytic enzyme, is required for sperm motility and male fertility. *Proc Natl Acad Sci U S A,* 101**,** 16501-6.

MINTON, A. P., COLCLASURE, G. C. & PARKER, J. C. 1992. Model for the role of macromolecular crowding in regulation of cellular volume. *Proc Natl Acad Sci U S A,* 89**,** 10504-6.

MITCHISON, T. J. & MITCHISON, H. M. 2010. Cell biology: How cilia beat. *Nature,*

463**,** 308-9.

MIYADO, K., YAMADA, G., YAMADA, S., HASUWA, H., NAKAMURA, Y., RYU, F., SUZUKI, K., KOSAI, K., INOUE, K., OGURA, A., OKABE, M. & MEKADA, E. 2000. Requirement of CD9 on the egg plasma membrane for fertilization. *Science,* 287**,** 321-4.

MOCZ, G. & GIBBONS, I. R. 2001. Model for the motor component of dynein heavy chain based on homology to the AAA family of oligomeric ATPases. *Structure,* 9**,** 93-103.

MOHANTY, M. J. & LI, X. 2002. Stretch-induced Ca(2+) release via an IP(3)-insensitive Ca(2+) channel. *Am J Physiol Cell Physiol,* 283**,** C456-62.

MOORE, H. D. & AKHONDI, M. A. 1996. Fertilizing capacity of rat spermatozoa is correlated with decline in straight-line velocity measured by continuous computer-aided sperm analysis: epididymal rat spermatozoa from the proximal cauda have a greater fertilizing capacity in vitro than those from the distal cauda or vas deferens. *J Androl,* 17**,** 50-60.

MORALES, P., VIGIL, P., FRANKEN, D. R., KASKAR, K., COETZEE, K. & KRUGER, T. F. 1994. Sperm-oocyte interaction: studies on the kinetics of zona pellucida binding and acrosome reaction of human spermatozoa. *Andrologia,* 26**,** 131-7.

MORENO, R. D., RAMALHO-SANTOS, J., SUTOVSKY, P., CHAN, E. K. & SCHATTEN, G. 2000. Vesicular traffic and golgi apparatus dynamics during mammalian spermatogenesis: implications for acrosome architecture. *Biol Reprod,* 63**,** 89-98.

MORTIMER, S. T. & MORTIMER, D. 1990. Kinematics of human spermatozoa incubated under capacitating conditions. *J Androl,* 11**,** 195-203.

MOSELEY, F. L., JHA, K. N., BJORNDAHL, L., BREWIS, I. A., PUBLICOVER, S. J., BARRATT, C. L. & LEFIEVRE, L. 2005. Protein tyrosine phosphorylation, hyperactivation and progesterone-induced acrosome reaction are enhanced in IVF media: an effect that is not associated with an increase in protein kinase A activation. *Mol Hum Reprod,* 11**,** 523-9.

MUÑOZ-GARAY, C., DE LA VEGA-BELTRAN, J. L., DELGADO, R., LABARCA, P., FELIX, R. & DARSZON, A. 2001. Inwardly rectifying K(+) channels in spermatogenic cells: Functional expression and implication in sperm capacitation. *Dev Biol,* 234**,** 261-274.

MURDOCH, R. N. & DAVIS, W. D. 1978. Effects of bicarbonate on the respiration and glycolytic activity of boar spermatozoa. *Aust J Biol Sci,* 31**,** 385-94.

NAABY-HANSEN, S., WOLKOWICZ, M. J., KLOTZ, K., BUSH, L. A., WESTBROOK, V. A., SHIBAHARA, H., SHETTY, J., COONROD, S. A., REDDI, P. P., SHANNON, J., KINTER, M., SHERMAN, N. E., FOX, J., FLICKINGER, C. J. & HERR, J. C. 2001. Co-localization of the inositol 1,4,5-trisphosphate receptor and calreticulin in the equatorial segment and in membrane bounded vesicles in the cytoplasmic droplet of human spermatozoa. *Mol Hum Reprod,* 7**,** 923-33.

NAKAZAWA, H., HORI, M., MURATA, T., OZAKI, H. & KARAKI, H. 2001. Contribution of chloride channel activation to the elevated muscular tone of the pulmonary artery in monocrotaline-induced pulmonary hypertensive rats. *Jpn J Pharmacol,* 86**,** 310-5.

NASH, K., LEFIEVRE, L., PERALTA-ARIAS, R., MORRIS, J., MORALES-GARCIA, A., CONNOLLY, T., COSTELLO, S., KIRKMAN-BROWN, J. C. & PUBLICOVER, S. J. 2010. Techniques for imaging Ca2+ signaling in human sperm. *J Vis Exp*.

NAVARRO, B., KIRICHOK, Y. & CLAPHAM, D. E. 2007. Ksper, a pH-sensitive K+ current that controls sperm membrane potential. *Proc Natl Acad Sci U S A,* 104(18)**,** 7688-7692.

NEILL, J. M. & OLDS-CLARKE, P. 1987. A computer-assisted assay for mouse sperm hyperactivation demonstrates that bicarbonate but not bovine serum albumin is required. *Gamete Res,* 18**,** 121-40.

NG, E. H., AJONUMA, L. C., LAU, E. Y., YEUNG, W. S. & HO, P. C. 2000. Adverse effects of hydrosalpinx fluid on sperm motility and survival. *Hum Reprod,* 15**,** 772-7.

NIELSEN, D. K., JENSEN, A. K., HARBAK, H., CHRISTENSEN, S. C. & SIMONSEN, L. O. 2007. Cell content of phosphatidylinositol (4,5)bisphosphate in Ehrlich mouse ascites tumour cells in response to cell volume perturbations in anisotonic and in isosmotic media. *J Physiol,* 582**,** 1027-36.

NIGGLI, V., SIGEL, E. & CARAFOLI, E. 1982. Inhibition of the purified and reconstituted calcium pump of erythrocytes by micro M levels of DIDS and NAP-taurine. *FEBS Lett,* 138**,** 164-6.

NILIUS, B., EGGERMONT, J., VOETS, T. & DROOGMANS, G. 1996. Volume-activated Cl- channels. *Gen Pharmacol,* 27**,** 1131-40.

NISHIMURA, H., CHO, C., BRANCIFORTE, D. R., MYLES, D. G. & PRIMAKOFF, P. 2001. Analysis of loss of adhesive function in sperm lacking cyritestin or fertilin beta. *Dev Biol,* 233**,** 204-13.

NOBLES, M., HIGGINS, C. F. & SARDINI, A. 2004. Extracellular acidification elicits a chloride current that shares characteristics with ICl(swell). *Am J Physiol Cell Physiol,* 287**,** C1426-35.

O'BRYAN, M. K., SEBIRE, K., MEINHARDT, A., EDGAR, K., KEAH, H. H., HEARN, M. T. & DE KRETSER, D. M. 2001. Tpx-1 is a component of the outer dense fibers and acrosome of rat spermatozoa. *Mol Reprod Dev,* 58**,** 116-25.

O'DRISCOLL, K. E., HATTON, W. J., BURKIN, H. R., LEBLANC, N. & BRITTON, F. C. 2008. Expression, localization, and functional properties of Bestrophin 3 channel isolated from mouse heart. *Am J Physiol Cell Physiol,* 295**,** C1610-24.

O'TOOLE, C. M., ARNOULT, C., DARSZON, A., STEINHARDT, R. A. & FLORMAN, H. M. 2000. Ca(2+) entry through store-operated channels in mouse sperm is initiated by egg ZP3 and drives the acrosome reaction. *Mol Biol Cell,* 11**,** 1571-84.

OAKLEY, L., DOYLE, P. & MACONOCHIE, N. 2008. Lifetime prevalence of infertility and infertility treatment in the UK: results from a population-based survey of reproduction. *Hum Reprod,* 23**,** 447-50.

OIWA, K. & SAKAKIBARA, H. 2005. Recent progress in dynein structure and mechanism. *Curr Opin Cell Biol,* 17**,** 98-103.

OKAMURA, N., TAJIMA, Y., ISHIKAWA, H., YOSHII, S., KOISO, K. & SUGITA, Y. 1986. Lowered levels of bicarbonate in seminal plasma cause the poor sperm motility in human infertile patients. *Fertil Steril,* 45**,** 265-72.

OKO, R. 1998. Occurrence and formation of cytoskeletal proteins in mammalian spermatozoa. *Andrologia,* 30**,** 193-206.

OKO, R., MOUSSAKOVA, L. & CLERMONT, Y. 1990. Regional differences in composition of the perforatorium and outer periacrosomal layer of the rat spermatozoon as revealed by immunocytochemistry. *Am J Anat,* 188**,** 64-73.

OKO, R. J. 1995. Developmental expression and possible role of perinuclear theca proteins in mammalian spermatozoa. *Reprod Fertil Dev,* 7**,** 777-97.

OKUNADE, G., MILLER, M., PYNE, G., SUTLIFF, R., O' CONNOR, K., NEUMANN, J., ANDRIGA, A., MILLER, D., PRASAD, V., DOETSCHMAN, T., PAUL, R. &

SHULL, G. 2004. Targeted ablation of plasma membrane Ca^{2+} -ATPase (PMCA) 1 and 4 indicates a major housekeeping function for PMCA1 and a critical role in hyperactivated sperm motility and male fertility for PMCA4. *J Biol Chem,* 279(32)**,** 33742-33750.

OLIVA, R. 2006. Protamines and male infertility. *Hum Reprod Update,* 12**,** 417-35.

OSMAN, R., ANDRIA, M., JONES, A. & MEIZEL, S. 1989. Steroid induced exocytosis: the human sperm acrosome reaction. *Biochem Biophys Res Commun,* 160**,** 828-833.

PALMER, R. M., REES, D. D., ASHTON, D. S. & MONCADA, S. 1988. L-arginine is the physiological precursor for the formation of nitric oxide in endothelium-dependent relaxation. *Biochem Biophys Res Commun,* 153**,** 1251-6.

PARKER, J. C. 1993. In defense of cell volume? *Am J Physiol,* 265**,** C1191-200.

PEROZO, E. 2006. Gating prokaryotic mechanosensitive channels. *Nat Rev Mol Cell Biol,* 7**,** 109-19.

PETERSEN, C. & SODER, O. 2006. The sertoli cell--a hormonal target and 'super' nurse for germ cells that determines testicular size. *Horm Res,* 66**,** 153-61.

PETERSEN, O. H. 1992. Stimulus-secretion coupling: cytoplasmic calcium signals and the control of ion channels in exocrine acinar cells. *J Physiol,* 448**,** 1-51.

PETRUNKINA, A. M., HARRISON, R. A., TSOLOVA, M., JEBE, E. & TOPFER-PETERSEN, E. 2007. Signalling pathways involved in the control of sperm cell volume. *Reproduction,* 133**,** 61-73.

PETRUNKINA, A. M., JEBE, E. & TOPFER-PETERSEN, E. 2005. Regulatory and necrotic volume increase in boar spermatozoa. *J Cell Physiol,* 204**,** 508-21.

PEZIER, A., GRAUSO, M., ACQUISTAPACE, A., MONSEMPES, C., ROSPARS, J. P. & LUCAS, P. 2010. Calcium activates a chloride conductance likely involved in olfactory receptor neuron repolarization in the moth Spodoptera littoralis. *J Neurosci,* 30**,** 6323-33.

PIPER, A. S. & LARGE, W. A. 2004. Single cGMP-activated Ca(+)-dependent Cl(-) channels in rat mesenteric artery smooth muscle cells. *J Physiol,* 555**,** 397-408.

QI, H., MORAN, M. M., NAVARRO, B., CHONG, J. A., KRAPIVINSKY, G., KRAPIVINSKY, L., KIRICHOK, Y., RAMSEY, I. S., QUILL, T. A. & CLAPHAM, D. E. 2007. All four CatSper ion channel proteins are required for male fertility and sperm cell hyperactivated motility. *Proc Natl Acad Sci USA* 104(4)**,** 1219-1223

REN, D., NAVARRO, B., PEREZ, G., JACKSON, A., HSU, S., SHI, Q., TILLY, J. & CLAPHAM, D. 2001. A sperm ion channel required for sperm motility and male fertility. *Nature* 413**,** 603-609.

ROBSON, L. & HUNTER, M. 1994. Role of cell volume and protein kinase C in regulation of a Cl- conductance in single proximal tubule cells of Rana temporaria. *J Physiol,* 480 (Pt 1)**,** 1-7.

ROCHWERGER, L. & CUASNICU, P. S. 1992. Redistribution of a rat sperm epididymal glycoprotein after in vitro and in vivo capacitation. *Mol Reprod Dev,* 31**,** 34-41.

ROJAS, H., RAMOS, M., BENAIM, G., CAPUTO, C. & DIPOLO, R. 2008. The activity of the Na+/Ca2+ exchanger largely modulates the Ca2+i signal induced by hypo-osmotic stress in rat cerebellar astrocytes. The effect of osmolarity on exchange activity. *J Physiol Sci,* 58**,** 277-9.

ROOSEN-RUNGE, E. C. & HOLSTEIN, A. F. 1978. The human rete testis. *Cell Tissue Res,* 189**,** 409-33.

ROSENBERG, M. F., CALLAGHAN, R., MODOK, S., HIGGINS, C. F. & FORD, R. C. 2004. Three-dimensional structure of P-glycoprotein. The transmembrane regions adopt an asymmetric configuration in the nucleotide-bound state. *J Biol Chem,* 280**,**

2857-2862.

ROSS, P. E. & CAHALAN, M. D. 1995. Ca2+ influx pathways mediated by swelling or stores depletion in mouse thymocytes. *J Gen Physiol,* 106**,** 415-44.

ROSSATO, M., DI VIRGILIO, F., RIZZUTO, R., GALEAZZI, C. & FORESTA, C. 2001. Intracellular calcium store depletion and acrosome reaction in human spermatozoa: role of calcium and plasma membrane potential. *Mol Hum Reprod,* 7**,** 119-128.

RUNFT, L. L., JAFFE, L. A. & MEHLMANN, L. M. 2002. Egg activation at fertilization: where it all begins. *Dev Biol,* 245**,** 237-54.

SANDLE, G. I., PERRY, M. D., MATHIALAHAN, T., LINLEY, J. E., ROBINSON, P., HUNTER, M. & MACLENNAN, K. A. 2007. Altered cryptal expression of luminal potassium (BK) channels in ulcerative colitis. *J Pathol,* 212**,** 66-73.

SAUER, H., RITGEN, J., HESCHELER, J. & WARTENBERG, M. 1998. Hypotonic Ca2+ signaling and volume regulation in proliferating and quiescent cells from multicellular spheroids. *J Cell Physiol,* 175**,** 129-40.

SCHLATT, S. & WEINBAUER, G. 1994. Immunohistochemical localization of proliferating cell nuclear antigen as a tool to study cell proliferation in rodent and primate testes. *Int J Androl***,** 214-222.

SCHLICHTER, L. C. & SAKELLAROPOULOS, G. 1994. Intracellular Ca2+ signaling induced by osmotic shock in human T lymphocytes. *Exp Cell Res,* 215**,** 211-22.

SCHUH, K., CARTWRIGHT, E. J., JANKEVICS, E., BUNDSCHU, K., LIEBERMANN, J., WILLIAMS, J. C., ARMESILLA, A., EMERSON, M., OCEANDY, D., KNOBELOCH, K. P. & NEYSES, L. 2004. Plasma membrane Ca^{2+} ATPase 4 is required for sperm motility and male fertility. *J Biol Chem,* 279(27)**,** 28220-28226.

SCHULTZ, R. M. & KOPF, G. S. 1995. Molecular basis of mammalian egg activation. *Curr Top Dev Biol,* 30**,** 21-62.

SCHWARTZ, D., MAYAUX, M. J., GUIHARD-MOSCATO, M. L., SPIRA, A., JOUANNET, P., CZYGLIK, F. & DAVID, G. 1984. Study of sperm morphologic characteristics in a group of 833 fertile men. *Andrologia,* 16**,** 423-8.

SCHWIEBERT, E. M., BENOS, D. J., EGAN, M. E., STUTTS, M. J. & GUGGINO, W. B. 1999. CFTR is a conductance regulator as well as a chloride channel. *Physiol Rev,* 79**,** 145-166.

SERRANO, H. & GARCIA-SUAREZ, D. 2001. Molecular aspects of mammalian fertilization. *Asian J Androl,* 3**,** 243-9.

SHARPE, R. 1994. *Regulation of Spermatogenesis,* Raven,New York.

SHI, Q. X. & ROLDAN, E. R. 1995. Evidence that a GABAA-like receptor is involved in progesterone-induced acrosomal exocytosis in mouse spermatozoa. *Biol Reprod,* 52(5)**,** 373-381.

SHI, Y.-L. & MA, X.-A. 1998. Ion-channels reconstituted into lipid bilayer from human sperm plasma membrane. *Mol Reprod Dev,* 50**,** 354-360.

SIEGHART, W., FUCHS, K., TRETTER, V., EBERT, V., JECHLINGER, M., HOGER, H. & ADAMIKER, D. 1999. Structure and subunit composition of GABA(A) receptors. *Neurochem Int,* 34(5)**,** 379-385.

SITSAPESAN, R. 1999. Similarities in the effects of DIDS, DBDS and suramin on cardiac ryanodine receptor function. *J Membr Biol,* 168**,** 159-68.

SNOW, J. C., GOLDSTEIN, J. L., SCHMIDT, L. N., LISITZA, P. & LAYDEN, T. J. 1993. Rabbit esophageal cells show regulatory volume decrease: ionic basis and effect of pH. *Gastroenterology,* 105**,** 102-10.

SOLER, C., PEREZ-SANCHEZ, F., SCHULZE, H., BERGMANN, M.,

OBERPENNING, F., YEUNG, C. & COOPER, T. G. 2000. Objective evaluation of the morphology of human epididymal sperm heads. *Int J Androl,* 23**,** 77-84.

STAMBOULIAN, S., KIM, D., SHIN, H. S., RONJAT, M., DE WAARD, M. & ARNOULT, C. 2004. Biophysical and pharmacological characterization of spermatogenic T-type calcium current in mice lacking the CaV3.1 (alpha1G) calcium channel: CaV3.2 (alpha1H) is the main functional calcium channel in wild-type spermatogenic cells. *J Cell Physiol,* 200**,** 116-24.

STAMBOULIAN, S., MOUTIN, M. J., TREVES, S., POCHON, N., GRUNWALD, D., ZORZATO, F., DE WAARD, M., RONJAT, M. & ARNOULT, C. 2005. Junctate, an inositol 1,4,5-triphosphate receptor associated protein, is present in rodent sperm and binds TRPC2 and TRPC5 but not TRPC1 channels. *Dev Biol,* 286**,** 326-37.

STEGER, K., PAULS, K., KLONISCH, T., FRANKE, F. E. & BERGMANN, M. 2000. Expression of protamine-1 and -2 mRNA during human spermiogenesis. *Mol Hum Reprod,* 6**,** 219-25.

STRICKER, S. A. 1999. Comparative biology of calcium signaling during fertilization and egg activation in animals. *Dev Biol,* 211**,** 157-76.

SU, Y. H. & VACQUIER, V. D. 2002. A flagellar K(+)-dependent Na(+)/Ca(2+) exchanger keeps Ca(2+) low in sea urchin spermatozoa. *Proc Natl Acad Sci U S A,* 99**,** 6743-8.

SUAREZ, S. S. 1996. Hyperactivated motility in sperm. *J Androl,* 17**,** 331-5.

SUAREZ, S. S. 2008. Control of hyperactivation in sperm. *Hum Reprod Update,* 14**,** 647-57.

SUAREZ, S. S. & HO, H. C. 2003. Hyperactivated motility in sperm. *Reprod Domest Anim,* 38**,** 119-24.

SUTOVSKY, P. & MANANDHAR, G. 2006. Mammalian spermatogenesis and sperm structure: anatomical and compartmental analysis. *In:* DE JONGE, C. & BARRAT, C. (eds.) *The Sperm Cell.* Cambridge: Cambridge University Press.

SUZUKI, T., FUJINOKI, M., SHIBAHARA, H. & SUZUKI, M. 2010. Regulation of hyperactivation by PPP2 in hamster spermatozoa. *Reproduction,* 139**,** 847-56.

SVECHNIKOV, K., LANDREH, L., WEISSER, J., IZZO, G., COLON, E., SVECHNIKOVA, I. & SODER, O. 2010. Origin, development and regulation of human Leydig cells. *Horm Res Paediatr,* 73**,** 93-101.

TAJIMA, Y. & OKAMURA, N. 1990. The enhancing effects of anion channel blockers on sperm activation by bicarbonate. *Biochim Biophys Acta,* 1034**,** 326-32.

TALBOT, P. 1985. Sperm penetration through oocyte investments in mammals. *Am J Anat,* 174**,** 331-46.

TAO, R., LAU, C. P., TSE, H. F. & LI, G. R. 2008. Regulation of cell proliferation by intermediate-conductance Ca2+-activated potassium and volume-sensitive chloride channels in mouse mesenchymal stem cells. *Am J Physiol Cell Physiol,* 295**,** C1409-16.

TASH, J. & BRACHO, G. 1994. Regulation of sperm motility emerging evidence for a major role for protein phosphatases. *J Androl,* 15**,** 505-509.

TASH, J. & MEANS, A. 1982. Regulation of protein phosphorylation and motility of sperm by cyclic adenosine monophosphate and calcium. *Biol Reprod,* 26**,** 745-763.

TEVES, M. E., GUIDOBALDI, H. A., UNATES, D. R., SANCHEZ, R., MISKA, W. & GIOJALAS, L. C. 2010. Progesterone sperm chemoattraction may be modulated by its corticosteroid-binding globulin carrier protein. *Fertil Steril,* 93**,** 2450-2.

TINEL, H., KINNE-SAFFRAN, E. & KINNE, R. H. 2002. Calcium-induced calcium release participates in cell volume regulation of rabbit TALH cells. *Pflugers Arch,* 443**,** 754-61.

TINEL, H., WEHNER, F. & SAUER, H. 1994. Intracellular Ca2+ release and Ca2+ influx during regulatory volume decrease in IMCD cells. *Am J Physiol,* 267**,** F130-8.

TOSHIMORI, K. & ITO, C. 2003. Formation and organization of the mammalian sperm head. *Arch Histol Cytol,* 66**,** 383-96.

TOSTESON, D. C. & HOFFMAN, J. F. 1960. Regulation of cell volume by active cation transport in high and low potassium sheep red cells. *J Gen Physiol,* 44**,** 169-94.

TOWBIN, H., STAEHELIN, T. & GORDON, J. 1979. Electrophoretic transfer of proteins from polyacrylamide gels to nitrocellulose sheets: procedure and some applications. *Proc Natl Acad Sci U S A,* 76**,** 4350-4.

TRISCHITTA, F., DENARO, M. G. & FAGGIO, C. 2005. Cell volume regulation following hypotonic stress in the intestine of the eel, Anguilla anguilla, is Ca2+-dependent. *Comp Biochem Physiol B Biochem Mol Biol,* 140**,** 359-67.

TURNER, K. O. & MEIZEL, S. 1995. Progesterone-mediated efflux of cytosolic chloride during the human sperm acrosome reaction. *Biochem Biophys Res Commun,* 213(3)**,** 774-780.

TURNER, K. O., SYVANEN, M. & MEIZEL, S. 1997. The human acrosome reaction is highly sensitive to inhibition by cyclodiene insecticides. *J Androl,* 18(6)**,** 571-575.

TURNER, R. M. 2006. Moving to the beat: a review of mammalian sperm motility regulation. *Reprod Fertil Dev,* 18**,** 25-38.

UNWIN, N. 2003. Structure and action of the nicotinic acetylcholine receptor explored by electron microscopy. *FEBS Lett,* 555**,** 91-95.

VAUGHAN-JONES, R. D. & SPITZER, K. W. 2002. Role of bicarbonate in the regulation of intracellular pH in the mammalian ventricular myocyte. *Biochem Cell Biol,* 80**,** 579-96.

VERMA, R. 2001. Sperm quiescence in cauda epididymis: a mini-review. *Asian J Androl,* 3(3)**,** 181-183.

VISCONTI, P. E., BAILEY, J. L., MOORE, G. D., PAN, D., OLDS-CLARKE, P. & KOPF, G. S. 1995a. Capacitation of mouse spermatozoa. I. Correlation between the capacitation state and protein tyrosine phosphorylation. *Development,* 121(4)**,** 1129-1137.

VISCONTI, P. E., GALANTINO-HOMER, H., NING, X., MOORE, G. D., VALENZUELA, J. P., JORGEZ, C. J., ALVAREZ, J. G. & KOPF, G. S. 1999a. Cholesterol efflux-mediated signal transduction in mammalian sperm. beta-cyclodextrins initiate transmembrane signaling leading to an increase in protein tyrosine phosphorylation and capacitation. *J Biol Chem,* 274**,** 3235-42.

VISCONTI, P. E., GALANTINO-HOMER, H., NING, X., MOORE, G. D., VALENZUELA, J. P., JORGEZ, C. J., ALVAREZ, J. G. & KOPF, G. S. 1999b. Cholesterol efflux-mediated signal transduction in mammalian sperm. beta-cyclodextrins initiate transmembrane signaling leading to an increase in protein tyrosine phosphorylation and capacitation. *J Biol Chem,* 274**,** 3235-3242.

VISCONTI, P. E., MOORE, G. D., BAILEY, J. L., LECLERC, P., CONNORS, S. A., PAN, D., OLDS-CLARKE, P. & KOPF, G. S. 1995b. Capacitation of mouse spermatozoa. II. Protein tyrosine phosphorylation and capacitation are regulated by a cAMP-dependent pathway. *Development,* 121(4)**,** 1139-1150.

VISCONTI, P. E., MUSCHIETTI, J. P., FLAWIA, M. M. & TEZON, J. G. 1990. Bicarbonate dependence of cAMP accumulation induced by phorbol esters in hamster spermatozoa. *Biochim Biophys Acta,* 1054**,** 231-6.

VISCONTI, P. E., NING, X., FORNES, M. W., ALVAREZ, J. G., STEIN, P., CONNORS, S. A. & KOPF, G. S. 1999c. Cholesterol efflux-mediated signal transduction in mammalian sperm: cholesterol release signals an increase in protein tyrosine phosphorilation during mouse sperm capacitation. *Dev Biol,* 214(2)**,** 429-443.

VISCONTI, P. E., STEWART-SAVAGE, J., BLASCO, A., BATTAGLIA, L.,

MIRANDA, P., KOPF, G. S. & TEZON, J. G. 1999d. Roles of bicarbonate, cAMP, and protein tyrosine phosphorylation on capacitation and the spontaneous acrosome reaction of hamster sperm. *Biol Reprod,* 61**,** 76-84.

VIVENES, C. Y., PERALTA-ARIAS, R. D., CAMEJO, M. I., GUERRERO, K., FERNANDEZ, V. H., PINERO, S., PROVERBIO, T., PROVERBIO, F. & MARIN, R. 2009. Biochemical identification of dynein-ATPase activity in human sperm. *Z Naturforsch C,* 64**,** 747-53.

WALENSKY, L. & SNYDER, S. 1995. Inositol 1,4,5-trisphosphate receptors selectively localized to the acrosomes of mammalian sperm. *J Cell Biol,* 130**,** 857-869.

WEINBAUER, G., GROMOLL, J., SIMONI, M. & NIESCHLAG, E. 2000. Physiology of Testicular Function. *In:* NIESCHLAG, E. & BEHRE, H. (eds.) *Andrology.* 2nd ed. Berlin: Springer.

WENNEMUTH, G., BABCOCK, D. F. & HILLE, B. 2003. Calcium clearance mechanisms of mouse sperm. *J Gen Physiol,* 122**,** 115-28.

WENNEMUTH, G., WESTENBROEK, R. E., XU, T., HILLE, B. & BABCOCK, D. F. 2000. CaV2.2 and CaV2.3 (N- and R-type) Ca2+ channels in depolarization-evoked entry of Ca2+ into mouse sperm. *J Biol Chem,* 275**,** 21210-7.

WEYAND, I., GODDE, M., FRINGS, S., WEINER, J., MULLER, F., ALTENHOFEN, W., HATT, H. & KAUPP, U. B. 1994. Cloning and functional expression of a cyclic-nucleotide-gated channel from mammalian sperm. *Nature,* 368**,** 859-63.

WHO 1999. *WHO Laboratory Manual for the Examination of Human Semen and Sperm-Cervical Mucus Interaction,* Cambridge, Cambridge University Press.

WIESNER, B., WEINER, J., MIDDENDORFF, R., HAGEN, V., KAUPP, U. B. & WEYAND, I. 1998. Cyclic nucleotide-gated channels on the flagellum control Ca2+ entry into sperm. *J Cell Biol,* 142**,** 473-84.

WILD, S., ROGLIC, G., GREEN, A., SICREE, R. & KING, H. 2004. Global prevalence of diabetes: estimates for the year 2000 and projections for 2030. *Diabetes Care,* 27**,** 1047-53.

WILLIAMS, K. M. & FORD, W. C. 2003. Effects of Ca-ATPase inhibitors on the intracellular calcium activity and motility of human spermatozoa. *Int J Androl,* 26**,** 366-75.

WONG, P., AU, C. & NIGAI, H. 1978. Electrolyte and water transport in rat epididymis, its possible role in sperm maturation *Int J Androl,* Suppl 2**,** 608-28.

WOOD, C. D., NISHIGAKI, T., TATSU, Y., YUMOTO, N., BABA, S. A., WHITAKER, M. & DARSZON, A. 2007. Altering the speract-induced ion permeability changes that generate flagellar Ca2+ spikes regulates their kinetics and sea urchin sperm motility. *Dev Biol,* 306**,** 525-37.

WU, X., YANG, H., ISEROVICH, P., FISCHBARG, J. & REINACH, P. S. 1997. Regulatory volume decrease by SV40-transformed rabbit corneal epithelial cells requires ryanodine-sensitive Ca2+-induced Ca2+ release. *J Membr Biol,* 158**,** 127-36.

WUTTKE, M. S., BUCK, J. & LEVIN, L. R. 2001. Bicarbonate-regulated soluble adenylyl cyclase. *JOP,* 2**,** 154-8.

XIA, J., REIGADA, D., MITCHELL, C. H. & REN, D. 2007. CATSPER channel-mediated Ca^{2+} entry into mouse sperm triggers a tail-to-head propagation. *Biol Reprod,* 77**,** 551-559.

XU, Y., DONG, P. H., ZHANG, Z., AHMMED, G. U. & CHIAMVIMONVAT, N. 2002. Presence of a calcium-activated chloride current in mouse ventricular myocytes. *Am J Physiol Heart Circ Physiol,* 283**,** H302-14.

YANAGIMACHI, R. 1988. Mammalian fertilization. *In:* KNOBIL, E. & NEILL, J. (eds.) *Physiology of Reproduction.* New York: Raven Press.

YANAGIMACHI, R. 1994. *In:* E, K. & NEILL, J. (eds.) *The Physiology of Reproduction.* New York: Raven Press.

YANG, Y. D., CHO, H., KOO, J. Y., TAK, M. H., CHO, Y., SHIM, W. S., PARK, S. P., LEE, J., LEE, B., KIM, B. M., RAOUF, R., SHIN, Y. K. & OH, U. 2008. TMEM16A confers receptor-activated calcium-dependent chloride conductance. *Nature,* 455**,** 1210-5.

YELLOWLEY, C. E., HANCOX, J. C. & DONAHUE, H. J. 2002. Effects of cell swelling on intracellular calcium and membrane currents in bovine articular chondrocytes. *J Cell Biochem,* 86**,** 290-301.

YEUNG, C. H., ANAPOLSKI, M., DEPENBUSCH, M., ZITZMANN, M. & COOPER, T. G. 2003. Human sperm volume regulation. Response to physiological changes in osmolality, channel blockers and potential sperm osmolytes. *Hum Reprod,* 18**,** 1029-36.

YEUNG, C. H., BARFIELD, J. P. & COOPER, T. G. 2005. Chloride channels in physiological volume regulation of human spermatozoa. *Biol Reprod,* 73**,** 1057-63.

YEUNG, C. H., BARFIELD, J. P. & COOPER, T. G. 2006. Physiological volume regulation by spermatozoa. *Mol Cell Endocrinol,* 250**,** 98-105.

YEUNG, C. H., BRETON, S., SETIAWAN, I., XU, Y., LANG, F. & COOPER, T. G. 2004. Increased luminal pH in the epididymis of infertile c-ros knockout mice and the expression of sodium-hydrogen exchangers and vacuolar proton pump H+-ATPase. *Mol Reprod Dev,* 68**,** 159-68.

YEUNG, C. H. & COOPER, T. G. 2001. Effects of the ion-channel blocker quinine on human sperm volume, kinematics and mucus penetration, and the involvement of potassium channels. *Mol Hum Reprod,* 7**,** 819-28.

YEUNG, C. H., COOPER, T. G. & NIESCHLAG, E. 1997. A technique for standardization and quality control of subjective sperm motility assessments in semen analysis. *Fertil Steril,* 67**,** 1156-8.

YEUNG, C. H., OBERLANDER, G. & COOPER, T. G. 1992. Characterization of the motility of maturing rat spermatozoa by computer-aided objective measurement. *J Reprod Fertil,* 96**,** 427-41.

YEUNG, C. H., OBERLANDER, G. & COOPER, T. G. 1994. Maturation of hamster epididymal sperm motility and influence of the thiol status of hamster and rat spermatozoa on their motility patterns. *Mol Reprod Dev,* 38**,** 347-55.

YEUNG, C. H., PEREZ-SANCHEZ, F., SCHROTER, S., KIRCHHOFF, C. & COOPER, T. G. 2001. Changes of the major sperm maturation-associated epididymal protein HE5 (CD52) on human ejaculated spermatozoa during incubation. *Mol Hum Reprod,* 7**,** 617-24.

YEUNG, C. H., SONNENBERG-RIETHMACHER, E. & COOPER, T. G. 1998. Receptor tyrosine kinase c-ros knockout mice as a model for the study of epididymal regulation of sperm function. *J Reprod Fertil Suppl,* 53**,** 137-47.

YEUNG, C. H., SONNENBERG-RIETHMACHER, E. & COOPER, T. G. 1999. Infertile spermatozoa of c-ros tyrosine kinase receptor knockout mice show flagellar angulation and maturational defects in cell volume regulatory mechanisms. *Biol Reprod,* 61**,** 1062-9.

YEUNG, C. H., TUTTELMANN, F., BERGMANN, M., NORDHOFF, V., VORONA, E. & COOPER, T. G. 2009. Coiled sperm from infertile patients: characteristics, associated factors and biological implication. *Hum Reprod,* 24**,** 1288-95.

ZANETTI, N. & MAYORGA, L. S. 2009. Acrosomal swelling and membrane docking are required for hybrid vesicle formation during the human sperm acrosome reaction. *Biol Reprod,* 81**,** 396-405.

ZENG, Y., CLARK, E. N. & FLORMAN, H. M. 1995. Sperm membrane potential: Hyperpolarization during capacitation regulates zona pellucida-dependent acrosomal reaction. *Dev Biol,* 171**,** 554-563.

ZHU, M. H., KIM, T. W., RO, S., YAN, W., WARD, S. M., KOH, S. D. & SANDERS, K. M. 2009. A Ca(2+)-activated Cl(-) conductance in interstitial cells of Cajal linked to slow wave currents and pacemaker activity. *J Physiol,* 587**,** 4905-18.

ZINI, A. & SIGMAN, M. 2009. Are tests of sperm DNA damage clinically useful? Pros and cons. *J Androl,* 30**,** 219-29.

ZUCCARELLO, D., FERLIN, A., CAZZADORE, C., PEPE, A., GAROLLA, A., MORETTI, A., CORDESCHI, G., FRANCAVILLA, S. & FORESTA, C. 2008. Mutations in dynein genes in patients affected by isolated non-syndromic asthenozoospermia. *Hum Reprod,* 23**,** 1957-62.